Electronic Supporting Information

Cobalt(III)-containing penta-dentate "Helmet"-type phthalogens: synthesis, solid-state structures and their thermal and electrochemical characterization

Rasha K. Al-Shewiki,[a] Saddam Weheabby,[b] Nell Uhlig,[a] Marcus Korb,[c] Tom Pester,[d] Stefan Zahn,[e] S. Grecchi,[f] P. R. Mussini,[f] Tobias Rüffer*[a] and Heinrich Lang[a]

[a] *Chemnitz University of Technology, Department of Inorganic Chemistry, Strasse der Nationen 62, 09107, Chemnitz, Germany.*

[b] *Chemnitz University of Technology, Measurement and Sensor Technology, 09126 Chemnitz, Germany.*

[c] *University of Western Australia, School of Molecular Sciences, M310, 6009 Perth WA, Australia.*

[d] *Chemnitz University of Technology, Department of Organic Chemistry, Strasse der Nationen 62, 09111, Chemnitz, Germany.*

[e] *University of Leipzig, Wilhelm Ostwald Institute for Physical and Theoretical Chemistry, Linnestrasse 2, 04103, Leipzig, Germany.*

[f] *University of Milan, Department of Chemistry, Via Golgi 19, 20133 Milano.*

**Corresponding author: tobias.rueffer@chemie.tu-chemnitz.de*

Table of Contents

1. List of Compounds

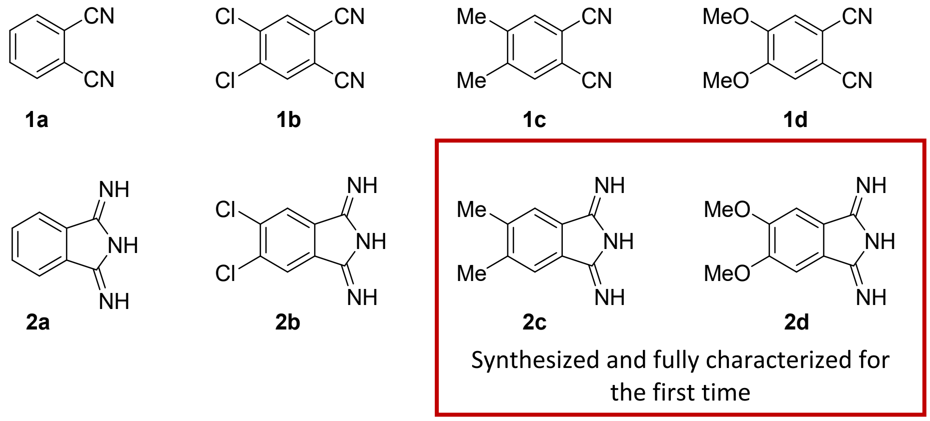

1a **1b** **1c** **1d**

2a **2b** **2c** **2d**

Synthesized and fully characterized for the first time

Figure S1. Structures of starting materials **1a–d** and **2a–d**. Hint: **2d** in form of **2d**·H_2O

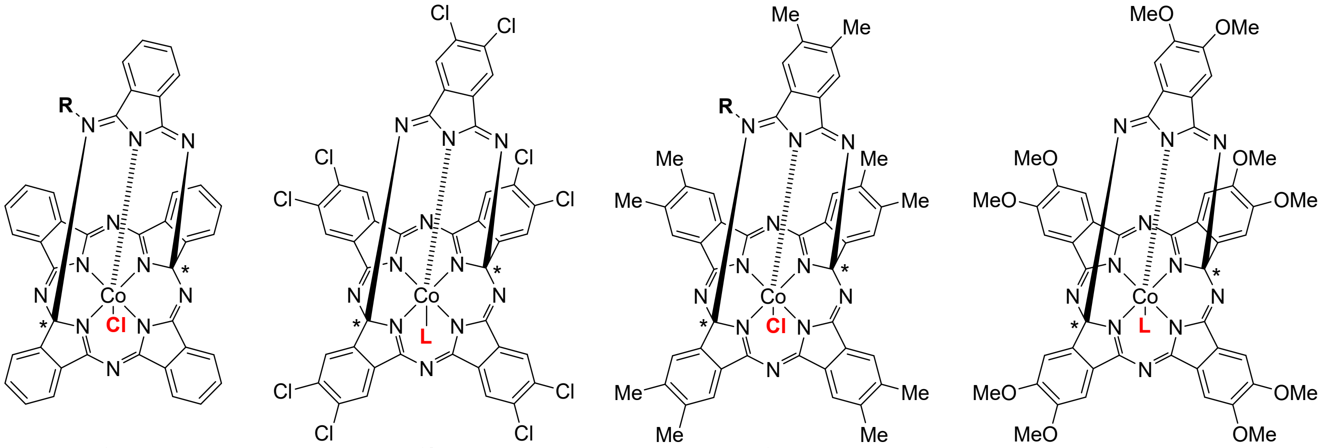

3a
R = H

3b
L = DMF

3c
R = H

3d
L = MeOH

Figure S2. Structures of **3a–d** complexes. Hint: **3a** is in form of **[3a(HCl)(dmf)]·2dmf**, **3b** is in form of **[3b(dmf)]·dmf·H_2O**, **3c** is in form of **[3c(HCl)]·dmf** and **3d** is in form of **[3d(MeOH)]·dmf.** * Indicate asymmetrical carbon atoms.

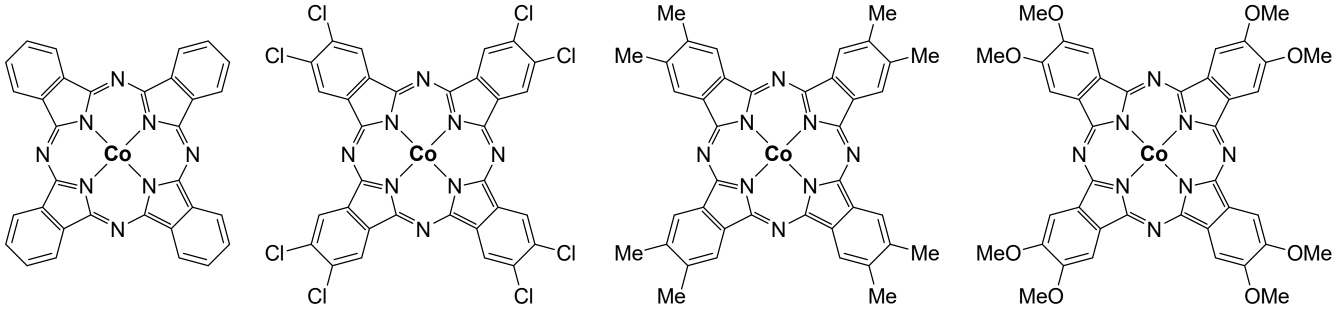

4a **4b** **4c** **4d**

Figure S3. Structures of **4a–d** complexes.

Abbreviation list:

DMAC: dimethylacetamide

DMF: N,N-dimethylformamide

DMF-d_7: heptadeutero-N,N-dimethylformamide

DMSO: dimethylsulfoxide

DMSO-d_6: hexadeutero-dimethylsulfoxide

DPPF: 1,1'-bis(diphenylphosphino)ferrocene

MeOH: methanol

MeCN: acetonitrile

PMHS: polymethylhydrosiloxane

THF: tetrahydrofuran

2. General procedure for the synthesis of starting materials 2a–d

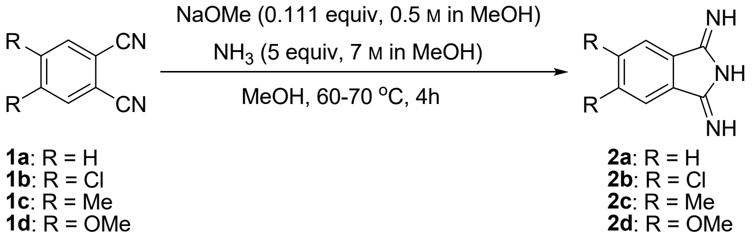

A dried schlenk tube with a magnetic stirrer was charged with the corresponding phthalonitrile **1a–d** (1 equiv) and 40 mL dry MeOH. Notice: **1c** and **1d** were synthesized as described in Sections 2.1.3.3 and 2.1.3.5, respectively. Then NaOMe (0.111 equiv, 0.5 M in MeOH) and NH_3 (5 equiv, 7 M in MeOH) were added in one portion at ambient temperature. Afterwards, the system was fully closed and the reaction mixture was heated to 60-70 °C for 4 h under solvothermal-like conditions. After cooling down, all the volatiles were removed under reduced pressure, and the residue was used without further purification unless specified.

2.1 Detailed description of starting materials 2a–d; Synthesis

2.1.1 1,3-diiminoisoindoline 2a

2a was prepared according to the general procedure from phthalonitrile **1a** (1.00 g, 7.80 mmol) in 40 mL dry MeOH, NaOMe (1.70 mL, 0.5 M in MeOH, 0.867 mmol, 0.111 equiv) and NH_3 (5.60 mL, 7 M in MeOH, 39.0 mmol, 5 equiv), and was further purified by recrystallization from MeOH.

Light green solid; Yield: 1.11 g (98% based on **1a**). **^{1}H NMR** (500.3 MHz, DMSO-d_6): δ 8.52 (br, s, 3H, H$^{1,1',1''}$), 7.82 (m, 2H, H$^{4,4'}$), 7.55 (m, 2H, H$^{5,5'}$) ppm. **^{13}C{^{1}H} NMR** (125 MHz, DMSO-d_6): δ 169.95 (C$^{2,2'}$), 137.02 (C$^{3,3'}$), 130.19 (C$^{5,5'}$), 120.98 (C$^{4,4'}$) ppm. **HRMS** (ESI-TOF, positive mode): *m/z* Calcd for $C_8H_7N_3$ [M+H]$^+$: 146.0713; found: 146.0719. **FT-IR** (KBr): 3280 (m), 3255 (m), 2977 (s), 1696 (m), 1642 (m), 1602 (m), 1538 (s), 1468 (w), 1442 (m), 1311 (m), 1262 (s), 1176 (w), 1158 (s), 1137 (s), 1081 (w), 1066 (m), 1013 (w), 987 (w), 950 (w), 879 (m), 818 (w), 774 (m), 745 (w), 707 (w). 694 (m), 663 (w), 631 (w), 546 (m) cm^{-1}. **Anal. Calcd** for $C_8H_7N_3$ (145.16 g mol^{-1}): C, 66.19; H, 4.86; N, 28.95%, **Found**: C, 66.11; H, 4.85; N, 28.93%. MP = 196 ^{0}C.

2.1.2 5,6-dichloro-1,3-diiminoisoindoline 2b

2b was prepared according to the general procedure from 4,5-dichlorophthalonitrile **1b** (1.00 g, 5.08 mmol) in 40 mL dry MeOH, NaOMe (1.10 mL, 0.5 M in MeOH, 0.564 mmol, 0.111 equiv) and NH_3 (3.60 mL, 7 M in MeOH, 25.4 mmol, 5 equiv). Used without further purification.

Light green solid; Yield: 1.06 g (97% based on **1b**). **^{1}H NMR** (500.3 MHz, DMSO-d_6): δ 8.71 (br, s, 3H, H$^{1,1',1''}$), 8.08 (s, 2H, H$^{4,4'}$) ppm. **^{13}C{^{1}H} NMR** (125 MHz, DMSO-d_6): δ 168.70 (C$^{2,2'}$), 137.42 (C$^{5,5'}$), 132.83 (C$^{3,3'}$), 122.74 (C$^{4,4'}$) ppm. **HRMS** (ESI-TOF, positive mode): *m/z* Calcd for $C_8H_5Cl_2N_3$ [M+H]$^+$: 213.9933; found: 213.9950. **FT-IR** (KBr): 3270 (w), 2920 (s), 1722 (m), 1643 (m), 1593 (m), 1549 (s), 1459 (m), 1435 (m), 1421 (w), 1389 (s), 1301 (s), 1282 (s), 1222 (m), 1181 (m), 1142 (s), 1112 (w), 1079 (m), 912 (w), 897 (w), 887 (w), 870 (s), 797 (w), 769 (w), 711 (w), 686 (w), 674 (m), 644 (w), 604 (w), 525 (w) cm^{-1}. **Anal. Calcd** for $C_8H_5Cl_2N_3$ (214.05 g mol^{-1}): C, 44.89; H, 2.35; N, 19.63%, **Found**: C, 44.82; H, 2.33; N, 19.59%. MP = 252–253 ^{0}C (dec).

2.1.3 5,6-dimethyl-1,3-diiminoisoindoline and 5,6-dimethoxy-1,3-diiminoisoindoline 2c and 2d

To prepare **2c** and **2d** their corresponding 4,5-disubstituted phthalonitriles (**1c** and **1d**) were synthesized according to a modified procedure[1–3]and shown in the following scheme:

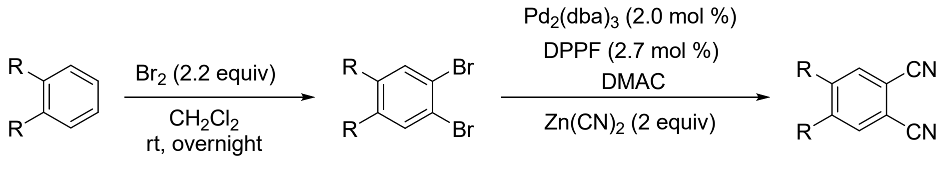

R = Me
R = OMe

1c: R = Me
1d: R = OMe

2.1.3.1 4,5-dimethylphthalonitrile 1c

For the synthesis of **1c** the starting compound 1,2-dibromo-4,5-dimethylbenzene was required, which was synthesized as described next.

2.1.3.2 1,2-bibromo-4,5-dimethylbenzene[1]

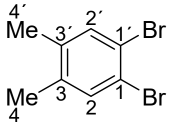

Bromine (25 mL, 0.485 mol, 2.34 equiv) was added dropwise to a round-bottom flask containing 1,2-dimethylbenzene (25 mL, 22 g, 0.207 mol, 1 equiv) in the course of 5 h at 0–5 ^{0}C. The reaction mixture was next allowed to warm to ambient temperature and it was stirred at that temperature overnight. Afterwards, chloroform ($CHCl_3$) (100 mL) was added and the reaction mixture was transferred into a separatory funnel and washed thoroughly with $Na_2S_2O_4$ 2 M solution (2 × 50 mL) and water (5 × 50 mL). Organic phase was then dried over Na_2SO_4, and all the volatiles were removed with a rotary evaporator. The crude product was then recrystallized from MeOH. The obtained white crystals of 1,2-dibromo-4,5-dimethylbenzene was used without further purification.

White solid; Yield: 56.57 g (91% based on 1,2-dimethylbenzene). **^{1}H NMR** (500.3 MHz, $CDCl_3$): δ 7.37 (s, 2H, $H^{2,2´}$), 2.18 (s, 6H, $H^{4,4´}$) ppm. **^{13}C{^{1}H} NMR** (125.8, $CDCl_3$): δ 137.48 ($C^{3,3´}$), 134.36 ($C^{2,2´}$), 121.26 ($C^{1,1´}$), 19.19 ($C^{4,4´}$) ppm. **FT-IR** (KBr): 3037 (w), 2975 (w), 2947 (w), 2918 (w), 2852 (w), 2732 (w), 1738 (w), 1535 (w), 1472 (s), 1440 (s), 1373 (m), 1341 (m), 1257 (w), 1156 (s), 1116 (s), 1019 (m), 995 (w), 891 (s), 873 (s), 809 (w), 643 (m), 562 (w) cm^{-1}.

2.1.3.3 4,5-dimethylphthalonitrile 1c[2]

To a solution of 1,2-dibromo-4,5-dimethylbenzene (2.00 g, 7.58 mmol) in dimethylacetamide (DMAC) (16 mL), polymethylhydrosiloxane (PMHS) (0.200 g) was added in one portion at ambient temperature. Afterwards, the reaction mixture was heated to 110 ^{0}C, and tris(dibenzylideneacetone)dipalladium ($Pd_2(dba)_3$) (0.152 g, 0.166 mmol) and 1,1’-bis(diphenylphosphino)ferrocene (DPPF) (0.114 g, 0.260 mmol) were added in one portion. Then $Zn(CN)_2$ (1.78 g, 15.16 mmol) was added in 4–5 portions within 30 min and the reaction mixture was stirred at that temperature for 3 h. After cooling to ambient temperature, the reaction mixture was diluted with ethyl acetate (EtOAc) (40 mL) and filtered. Filtrate was then transferred into a separatory funnel and washed thoroughly with water (3 × 40 mL). Organic phase was then dried over $MgSO_4$. After that all the volatiles were removed with a rotary evaporator and the crude product was purified by column chromatography on silica gel (n-hexane-CH_2Cl_2 6:4 (*v*/*v*)) to afford the desired 4,5-dimethylphthalonitrile **1c**.

White solid; Yield: 1.03 g (87% based on 1,2-dibromo-4,5-dimethylbenzene). **^{1}H NMR** (500.3 MHz, DMSO-d$_6$): δ 7.95 (s, 2H, $H^{3,3'}$), 2.34 (s, 6H, $H^{5,5'}$) ppm. **^{13}C{^{1}H} NMR** (125 MHz, DMSO-d$_6$): δ 144.14 ($C^{4,4'}$), 134.31 ($C^{3,3'}$), 116.08 ($C^{1,1'}$), 111.57 ($C^{2,2'}$), 19.28 ($C^{5,5'}$) ppm. **FT-IR** (KBr): 3108 (w), 3038 (w), 2986 (w), 2959 (w), 2927 (w), 2770 (w), 2229 (s), 1805 (w), 1599 (s), 1553 (m), 1496 (s), 1451 (m), 1382 (m), 1294 (w), 1276 (w), 1257 (m), 1193 (w), 1019 (m), 899 (m), 668 (w), 535 (s) cm^{-1}.

2.1.3.4 5,6-dimethyl-1,3-diiminoisoindoline 2c

2c was prepared according to the general procedure with slight modifications: To a suspension of 4,5-dimethylphthalonitrile (1.00 g, 6.40 mmol) in 40 mL dry MeOH, NaOMe (1.40 mL, 0.5 M in MeOH, 0.711 mmol, 0.111 equiv) and NH_3 (4.60 mL, 7 M in MeOH, 32.0 mmol, 5 equiv) were added in one portion at ambient temperature. Afterwards, the system was fully closed and the reaction mixture was heated to 68 ^oC for 4 h under solvothermal-like condition. Upon heating all the solid material was fully dissolved. However, after stirring for 2 h at 68 ^oC an insoluble blue-green precipitate was formed. Afterwards, the resulting mixture had been cooled, the precipitate was collected by filtration, washed with cold MeOH (4 × 40 mL), then was dried *in vacuo* to give 5,6-dimethyl-1,3-diiminoisoindoline (**2c**) which was used without further purification.

Light blue-green solid; Yield: 1.01 g (91% based on **1c**). **^{1}H NMR** (500.3 MHz, DMSO-d$_6$): δ 8.37 (br, s, 3H, $H^{1,1',1''}$), 7.57 (s, 2H, $H^{4,4'}$), 2.31 (s, 6H, $H^{6,6'}$) ppm. **HRMS** (ESI-TOF, positive mode): *m/z* Calcd for $C_{10}H_{11}N_3$ $[M+H]^+$: 174.1026; found: 174.1023. **FT-IR** (KBr): 3261 (w), 3088 (w), 3015 (w), 2950 (s), 1719 (w), 1639 (m), 1599 (w), 1545 (s), 1448 (m), 1433 (w), 1412 (m), 1368 (w), 1320 (w), 1294 (s), 1244 (m), 1132 (s), 1077 (m), 1021 (w), 994 (w), 900 (w), 876 (s), 796 (w), 717 (w), 673 (w), 612 (w), 528 (w) cm^{-1}. **Anal. Calcd** for $C_{10}H_{11}N_3$ (173.21 g mol^{-1}): C, 69.34; H, 6.40; N, 24.26%, **Found**: C, 69.30; H, 6.39; N, 24.32%. MP = 279–280 ^oC.

2.1.3.5 4,5-dimethoxyphthalonitrile 1d

For the synthesis of **1d** the starting compound 1,2-dibromo-4,5-dimethoxybenzene was required, which was synthesized as described next.

2.1.3.6 ***1,2-Dibromo-4,5-dimethoxybenzene***[3]

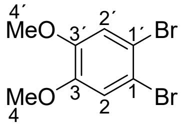

To a solution of 1,2-dimethoxybenzene (25 g, 0.181 mol) in CH_2Cl_2 (50 mL), a solution of bromine (20.5 mL, 0.400 mol) in CH_2Cl_2 (50 mL) was added dropwise within 5 h at 0–5 ^oC. The reaction mixture was next allowed to warm to ambient temperature and it was stirred at that temperature overnight. Afterwards, CH_2Cl_2 (100 mL) was added and the reaction mixture was transferred into a separatory funnel and washed thoroughly with $Na_2S_2O_4$ 2 M solution (2 × 50 mL) and water (5 × 50 mL). Organic phase was then dried over Na_2SO_4, and all the volatiles were removed with a rotary evaporator. The white powdered solid of 1,2-dibromo-4,5-dimethoxybenzene was used without further purification.

White solid; Yield: 51.41 g (96% based on 1,2-dimethoxybenzene). **^{1}H NMR** (500.3 MHz, DMSO-d_6): δ 7.26 (s, 2H, $H^{2,2'}$), 3.77 (s, 6H, $H^{4,4'}$) ppm. **^{13}C{^{1}H} NMR** (125 MHz, DMSO-d_6): δ 148.95 ($C^{3,3'}$), 116.19 ($C^{2,2'}$), 113.78 ($C^{1,1'}$), 56.05 ($C^{4,4'}$) ppm. **FT-IR** (KBr): 3104 (w), 3079 (w), 3053 (w), 3010 (m), 2962 (w), 2930 (w), 2903 (w), 2839 (m), 2579 (w), 1681 (w), 1585 (m), 1571 (w), 1497 (s), 1458 (s), 1435 (s), 1351 (s), 1329 (m), 1260 (w), 1249 (s), 1181 (s), 1119 (w), 1027 (s), 885(m), 852 (s), 834 (w), 784 (m), 710 (w), 668(w), 649 (m), 538 (w) cm^{-1}.

2.1.3.7 ***4,5-dimethoxyphthalonitrile 1d***[2]

To a solution of 1,2-dibromo-4,5-dimethoxybenzene (2.00 g, 6.76 mmol) in dimethylacetamide (16 mL), polymethylhydrosiloxane (PMHS) (0.200 g) was added in one portion at ambient temperature. Afterwards, the reaction mixture was heated to 120 ^oC, and $Pd_2(dba)_3$ (0.135 g) and DPPF (0.102 g) were added in a single portions. Then $Zn(CN)_2$ (1.586, 13.50 mmol) was added in 4-5 portions within 30 min and the reaction mixture was stirred at that temperature for 3 h. After cooling to ambient temperature, the reaction mixture was diluted with EtOAc (40 mL) and filtered. The filtrate was then transferred into a separatory funnel and washed thoroughly with water (3 × 40 mL). Organic phase was then dried over $MgSO_4$, and all the volatiles were removed with a rotary evaporator and the crude product was purified by column chromatography on silica gel (n-hexane-CH_2Cl_2 7:3 (*v*/*v*)) to afford the desired 4,5-dimethoxyphthalonitrile **1d**.

White solid; Yield: 1.12 g (88% based on 1,2-dibromo-4,5-dimethoxybenzene). **^{1}H NMR** (500.3 MHz, DMSO-d$_6$): δ 7.69 (s, 2H, H$^{3,3'}$), 3.90 (s, 6H, H$^{5,5'}$) ppm. **^{13}C{^{1}H} NMR** (125 MHz, DMSO-d$_6$): δ 152.38 (C$^{4,4'}$), 116.28 (C$^{3,3'}$), 115.94 (C$^{1,1'}$), 107.46 (C$^{2,2'}$), 56.63 (C$^{5,5'}$) ppm. **FT-IR** (KBr): 3128, 3068, 2974, 2228, 1592, 1564, 1520, 1463, 1446, 1395, 1359, 1293, 1235, 1197, 1149, 1092, 1017, 978, 881, 829, 536 cm^{-1}.

2.1.3.8 5,6-dimethoxy-1,3-diiminoisoindoline 2d·H$_2$O

2d was prepared according to the general procedure with slight modifications: To a suspension of 4,5-dimethoxylphthalonitrile (1.00 g, 5.31 mmol) in 40 mL dry MeOH, NaOMe (1.20 mL, 0.5 M in MeOH, 0.589 mmol, 0.111 equiv) and NH$_3$ (3.80 mL, 7 M in MeOH, 26.6 mmol, 5 equiv) were added in one portion at ambient temperature. Afterwards, the system was fully closed and the reaction mixture was heated to 68 °C for 4 h under solvothermal-like condition. Upon heating all solid material are fully dissolved, then after cooling down to ambient temperature, the solvent was removed under reduced pressure and the crude product was then dissolved in CH$_2$Cl$_2$ (40 mL) and transferred into a separatory funnel and washed thoroughly with water (2 × 30 mL). Organic phase was then dried over Na$_2$SO$_4$, and all the volatiles were removed with a rotary evaporator. The yellow solid was shown by all analytical methods applied to be the water adduct of 5,6-dimethoxy-1,3-diiminoisoindoline (**2d·H$_2$O**). This material was used without further purification.

Yellow solid; Yield: 1.06 g (97% based on **1d**). **^{1}H NMR** (500.3 MHz, DMSO-d$_6$): δ 8.41 (br, 3H, H$^{1,1',1''}$), 7.47 (s, 2H, H$^{4,4'}$), 3.84 (s, 6H, H$^{6,6'}$) ppm. **^{13}C{^{1}H} NMR** (125 MHz, DMSO-d$_6$): δ 169.20 (C$^{2,2'}$), 151.14 (C$^{5,5'}$), 128.86 (C$^{3,3'}$), 104.56 (C$^{4,4'}$), 55.87 (C$^{6,6'}$) ppm. **HRMS** (ESI-TOF, positive mode): *m/z* Calcd for $C_{10}H_{11}N_3O_2$ [M+H]$^+$: 206.0914; found: 206.0924. **FT-IR** (KBr): 3433 (s), 3258, 3090, 2970, 2834, 1690 (m), 1638 (m), 1551 (s), 1496 (w), 1462 (w), 1419 (m), 1346 (w), 1289 (s), 1214 (m), 1190 (w), 1135 (m), 1045 (s), 968 (w), 912 (w), 871 (m), 830 (w), 730 (w), 663 (w), 545 (w) cm^{-1}. **Anal. Calcd** for $C_{10}H_{11}N_3O_2 \cdot H_2O$ (223.23 g mol^{-1}): C, 53.80; H, 5.87; N, 18.82%, **Found**: C, 53.81; H, 5.89; N, 18.80%. MP = 280–281 °C (dec).

2.2 Characterization of the starting materials 2a–d

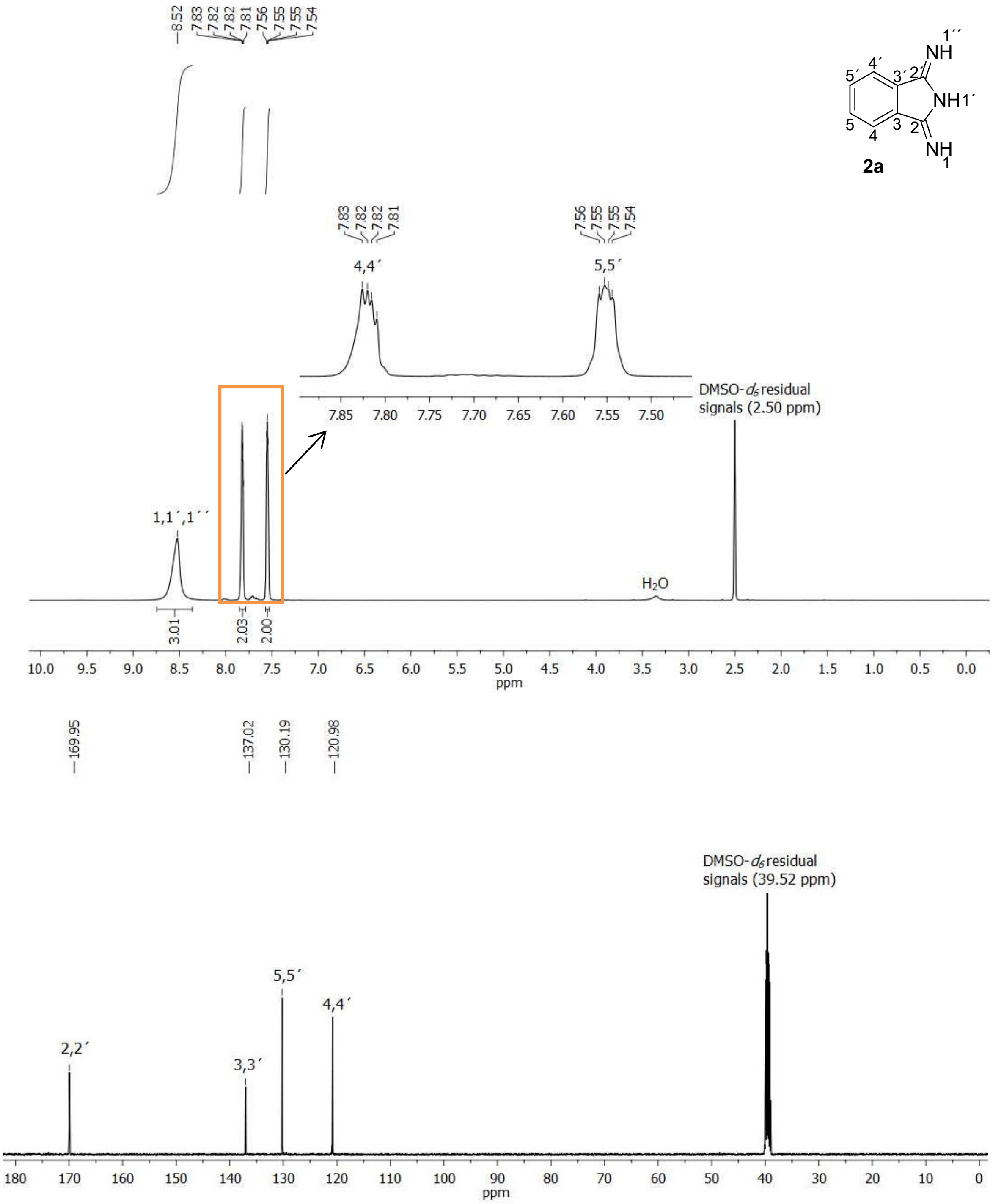

Figure S4. ^{1}H (above) and ^{13}C{^{1}H} NMR (below) spectra of **2a** in DMSO-d$_6$.

Acquisition Parameter

Source Type	ESI	Ion Polarity	Positive	Set Nebulizer	0.3 Bar
Focus	Not active	Set Capillary	4500 V	Set Dry Heater	180 °C
Scan Begin	50 m/z	Set End Plate Offset	-500 V	Set Dry Gas	4.0 l/min
Scan End	3000 m/z	Set Collision Cell RF	150.0 Vpp	Set Divert Valve	Source

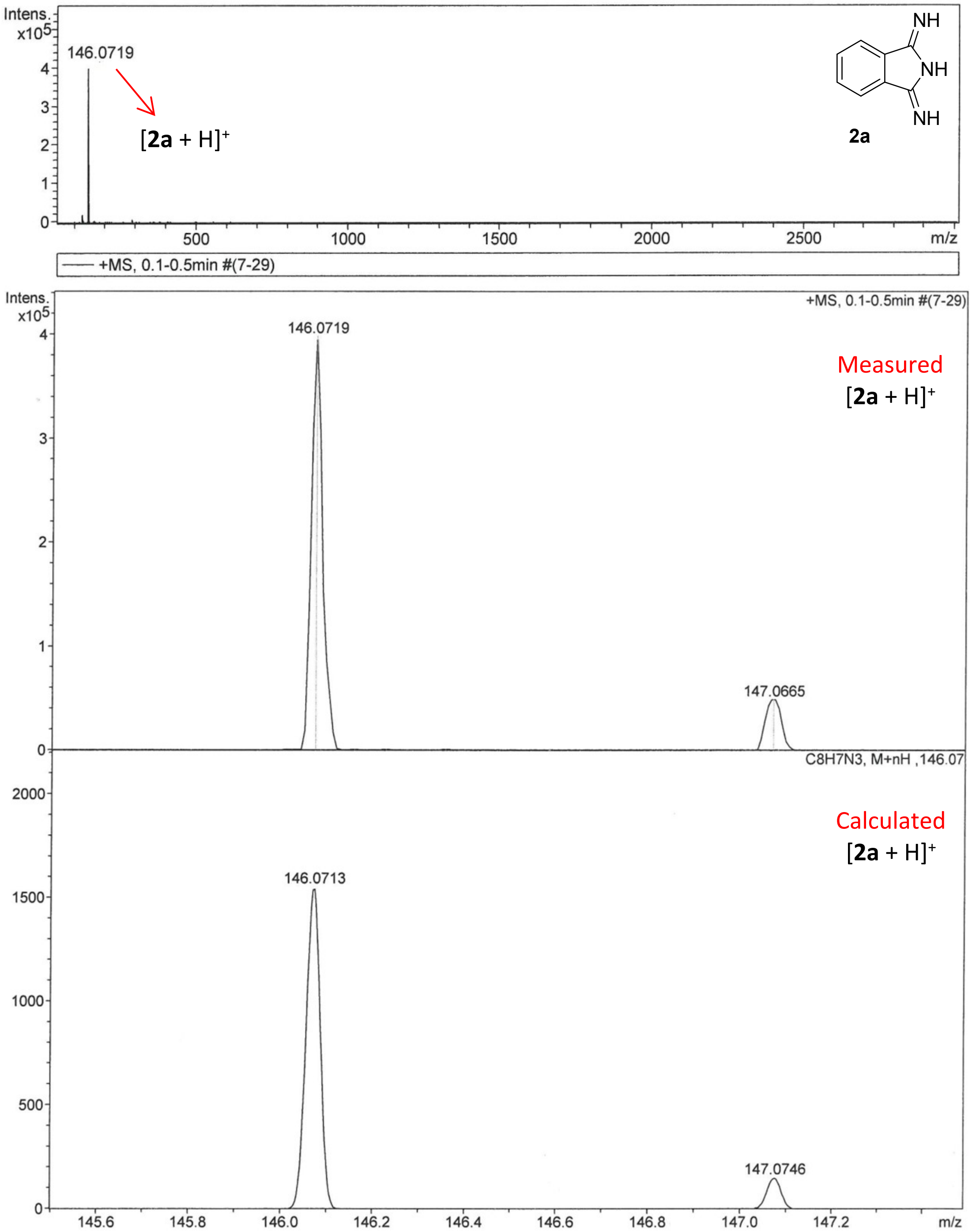

Figure S5. HRMS (ESI-TOF) of **2a** (measured in MeOH/MeCN). The spectrum on top is the experimentally obtained spectrum. The mol peak is shown below in an enlarged view with its calculated isotope distribution patterns.

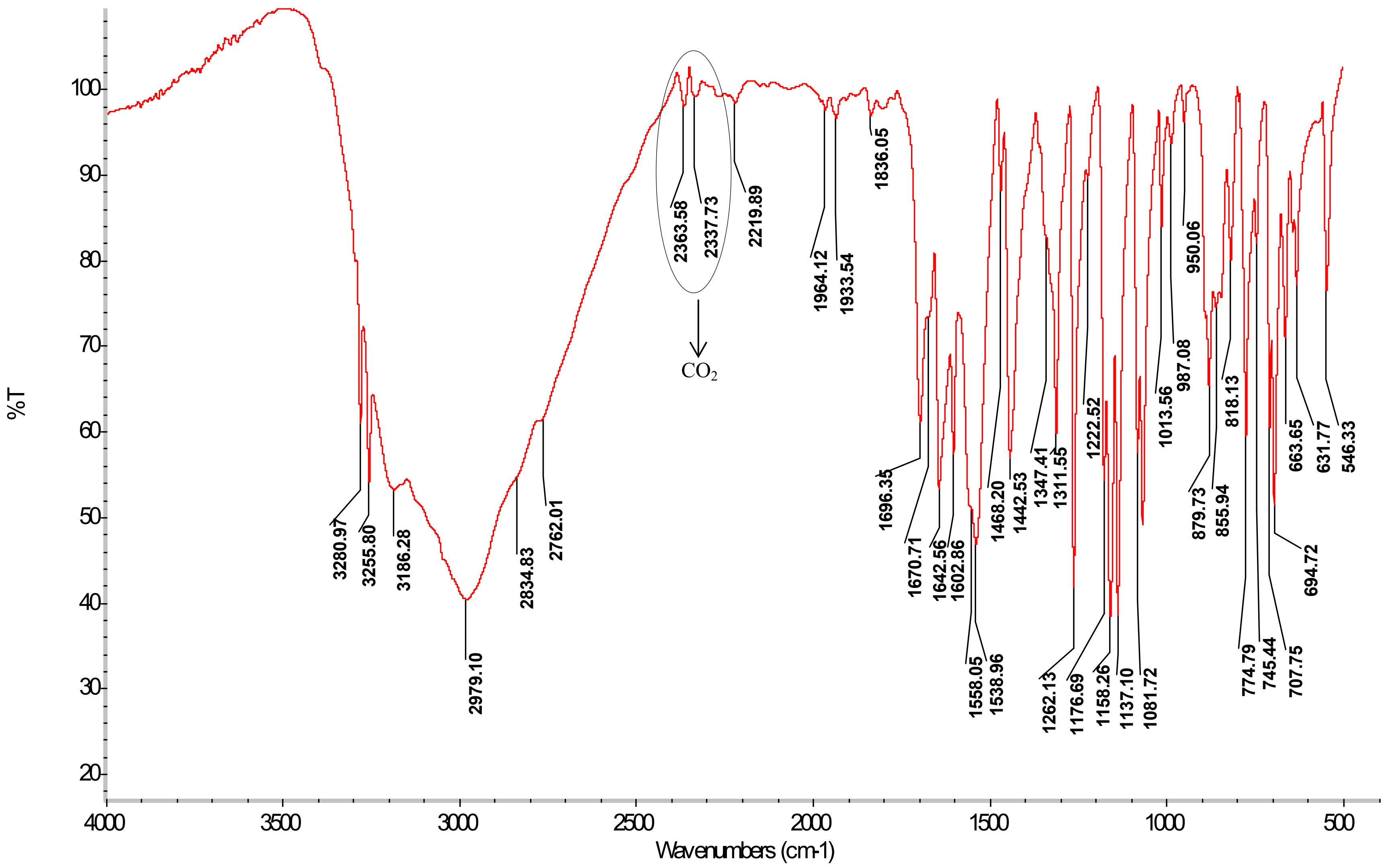

Figure S6. FT-IR spectrum (KBr) of **2a**.

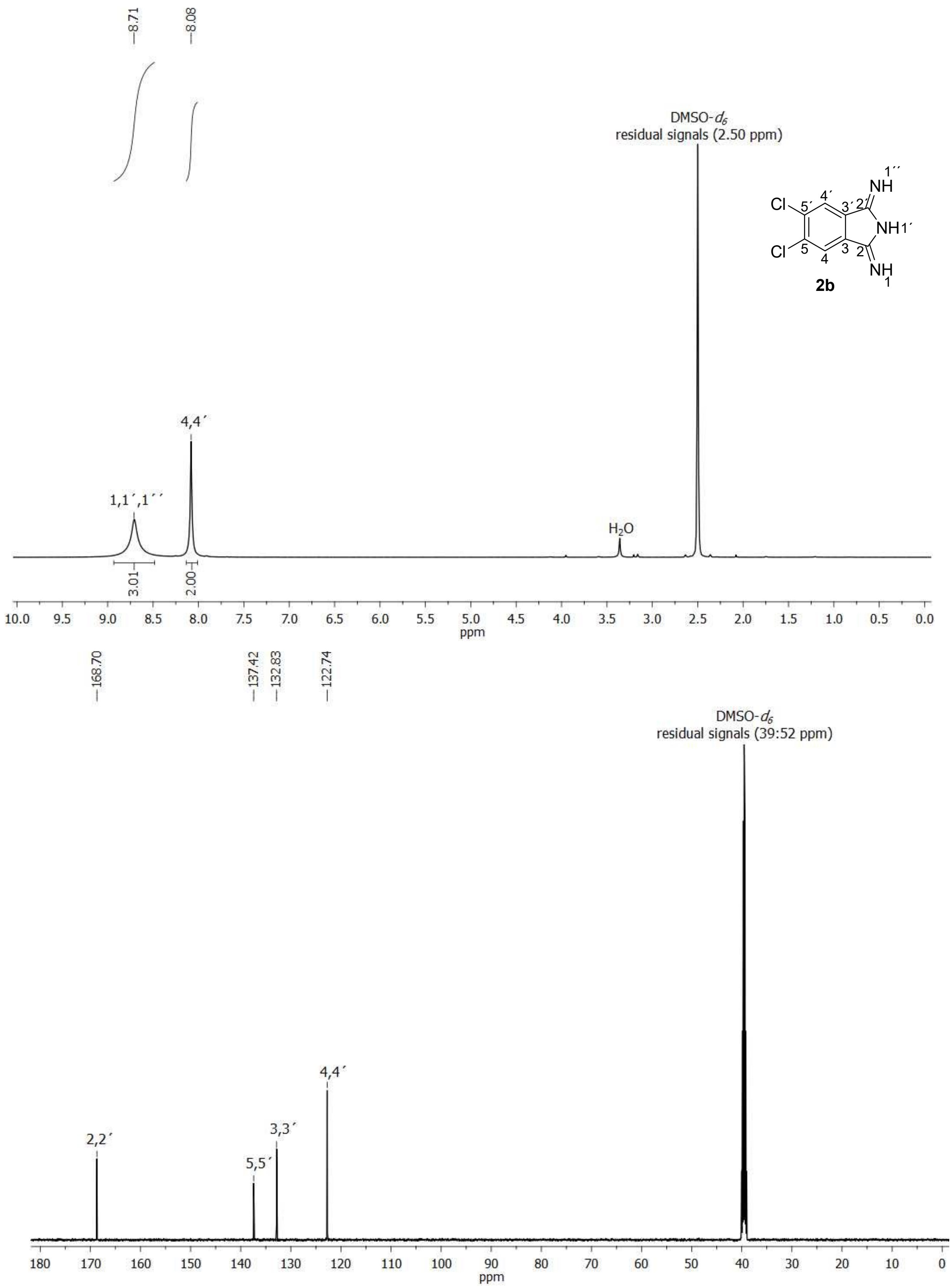

Figure S7. ^{1}H (above) and ^{13}C{^{1}H} NMR (below) spectra of **2b** in DMSO-d$_6$.

Acquisition Parameter

Source Type	ESI	Ion Polarity	Positive	Set Nebulizer	0.3 Bar
Focus	Not active	Set Capillary	4500 V	Set Dry Heater	180 °C
Scan Begin	50 m/z	Set End Plate Offset	-500 V	Set Dry Gas	4.0 l/min
Scan End	3000 m/z	Set Collision Cell RF	150.0 Vpp	Set Divert Valve	Source

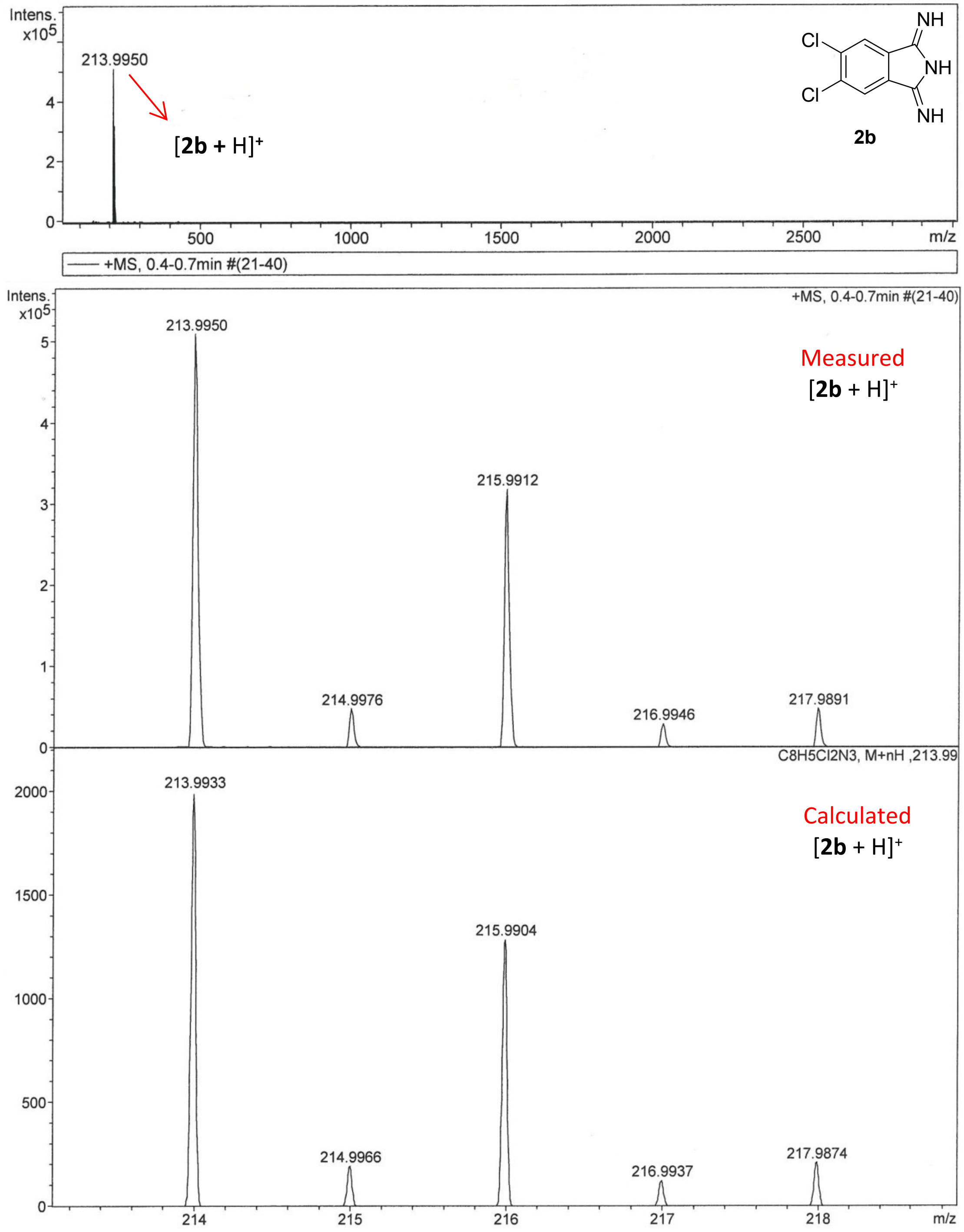

Figure S8. HRMS (ESI-TOF) of **2b** (measured in DMSO/MeCN). The spectrum on top is the experimentally obtained spectrum. The mol peak is shown below in an enlarged view with its calculated isotope distribution patterns.

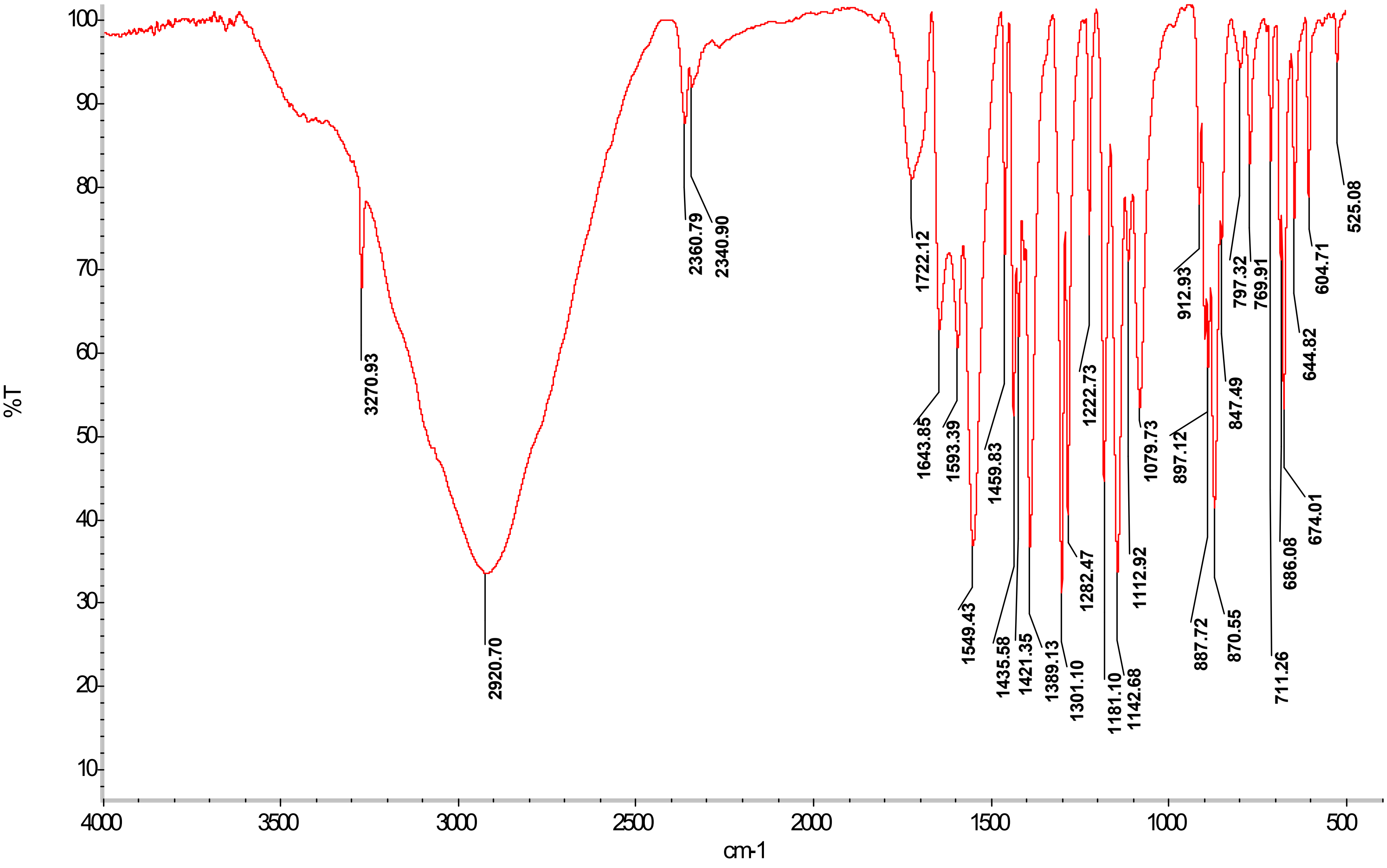

Figure S9. FT-IR spectrum (KBr) of **2b**.

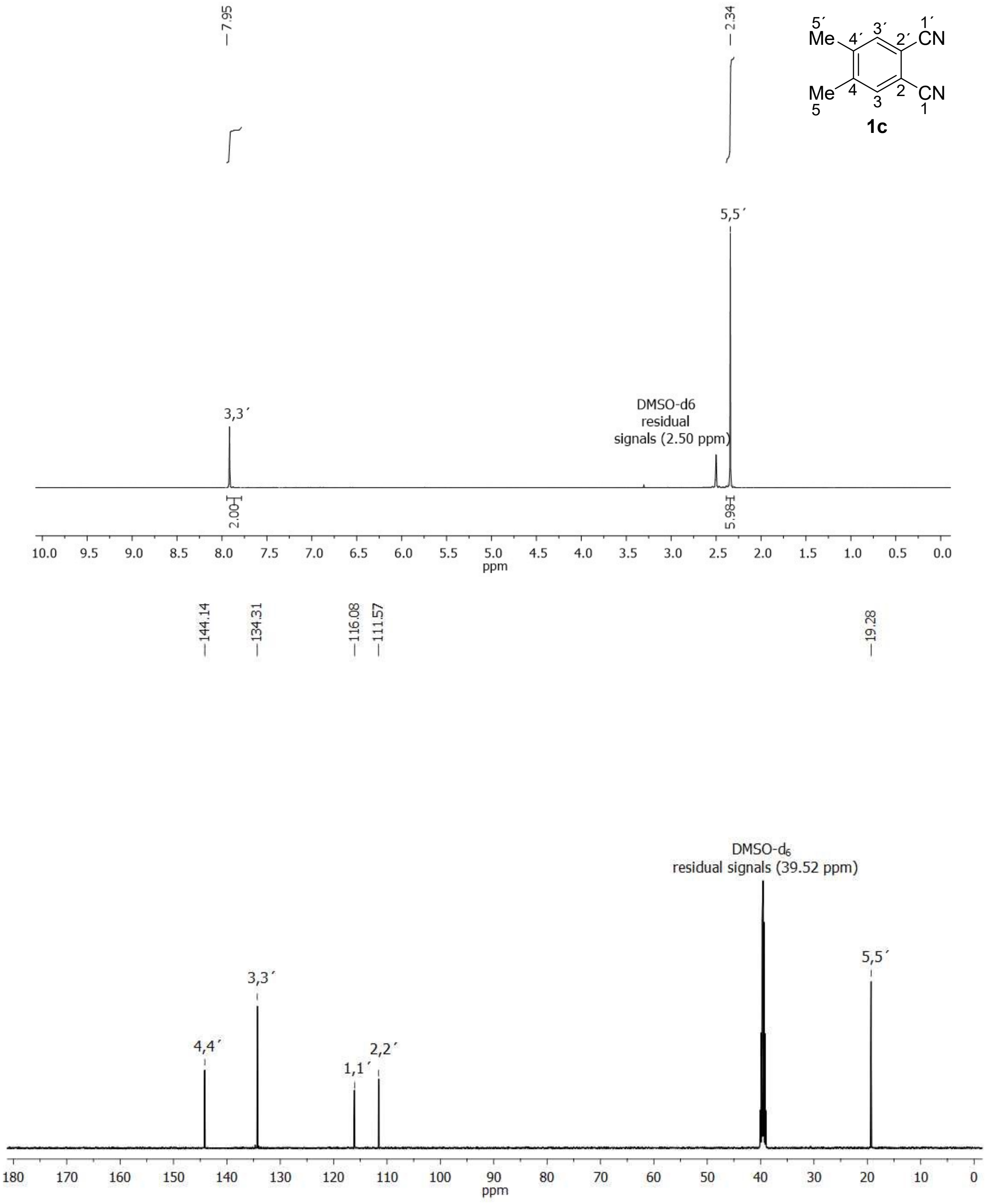

Figure S10. ^{1}H (above) and ^{13}C{^{1}H} NMR (below) spectra of **1c** in DMSO-d$_6$.

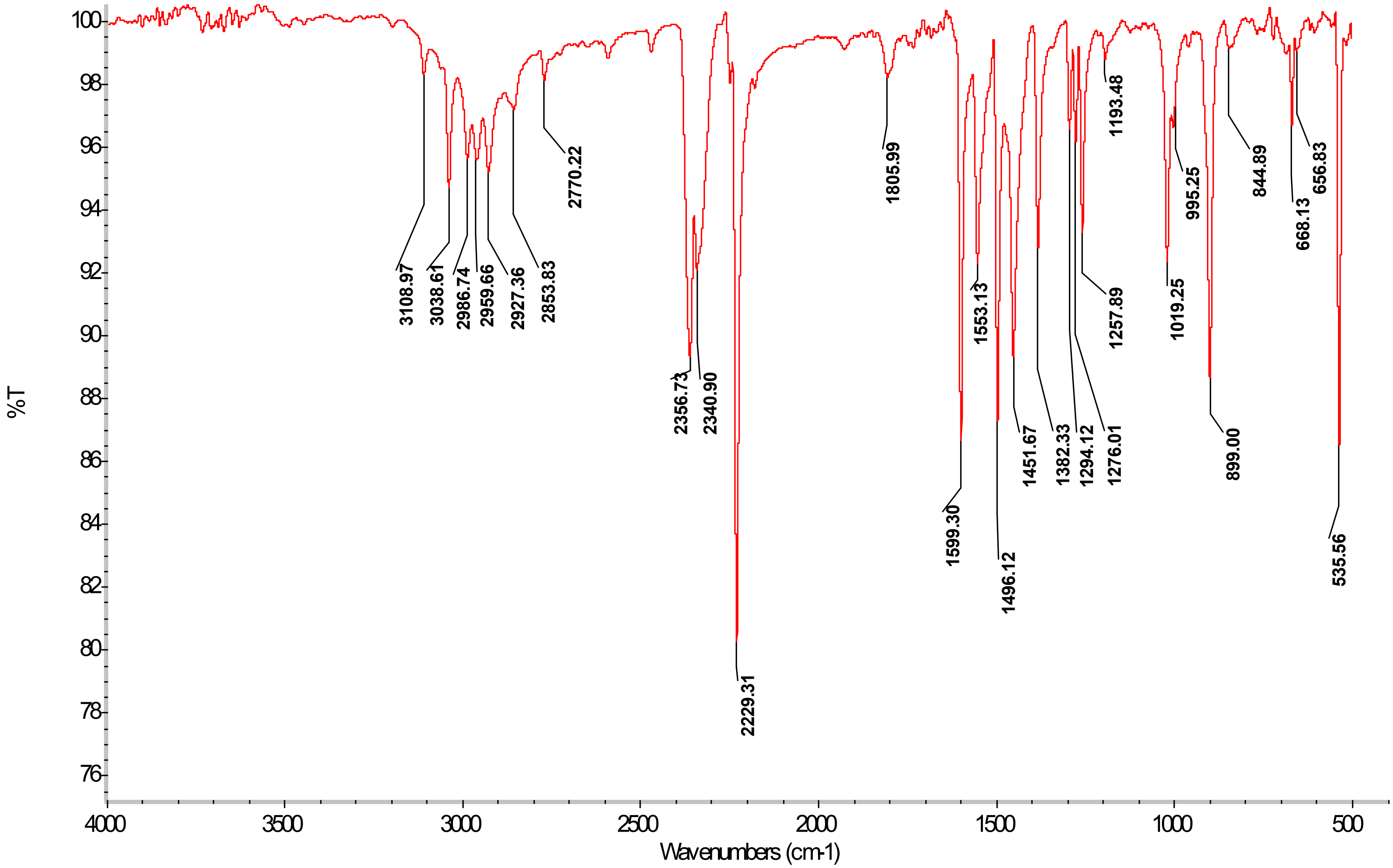

Figure S11. FT-IR spectrum (KBr) of **1c**.

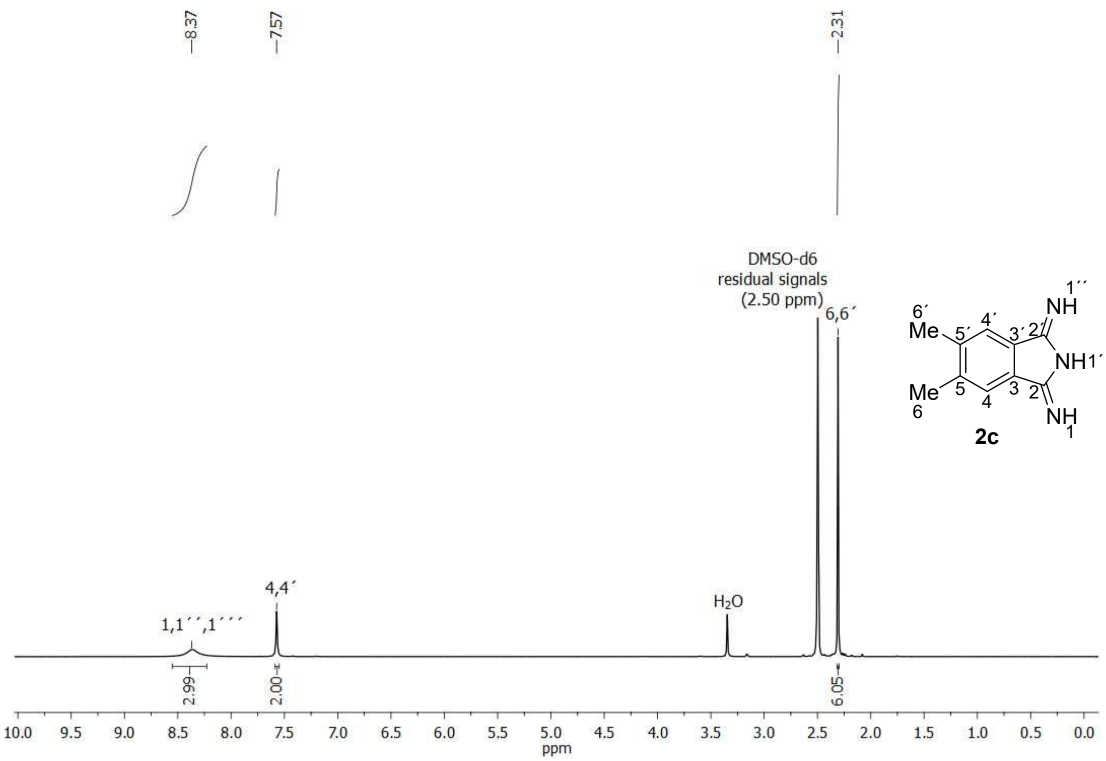

Figure S12. ^1H NMR spectrum of **2c** in DMSO-d_6. The solubility of **2c** in DMSO-d_6 or the other NMR solvents is too insufficient to allow the recording of a meaningful $^{13}C\{^1H\}$ NMR spectrum.

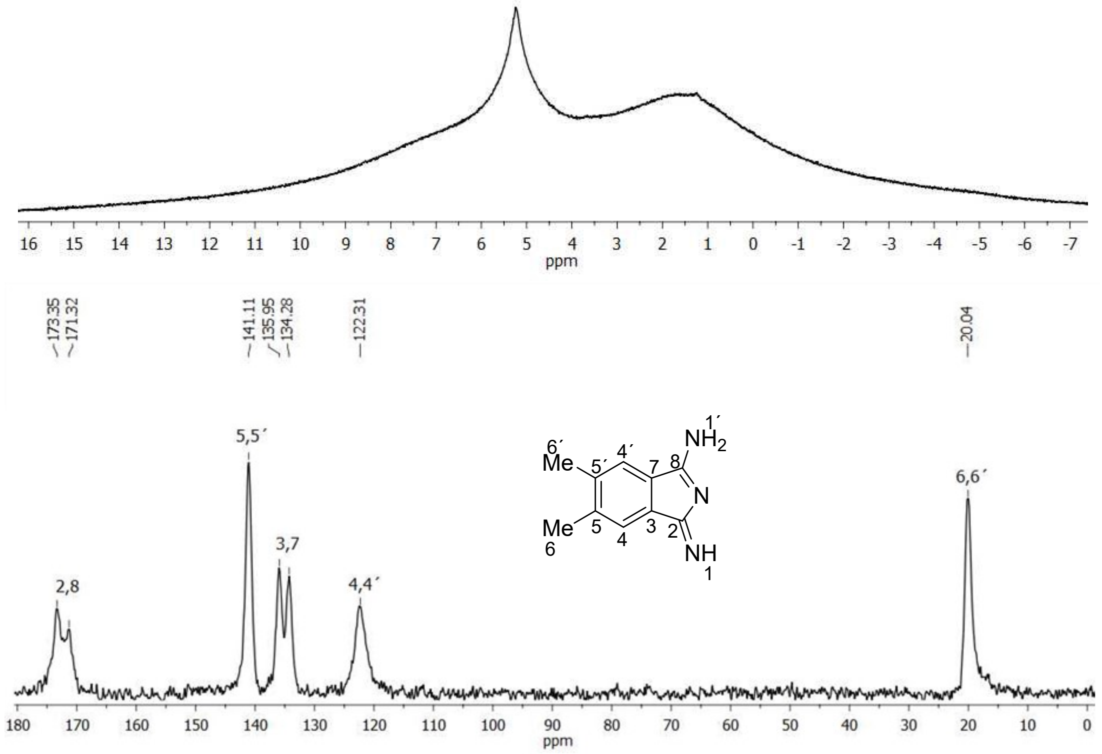

Figure S13. ^1H-MAS-CP NMR (above) and $^{13}C\{^1H\}$-MAS-CP NMR (below) spectra of **2c**.

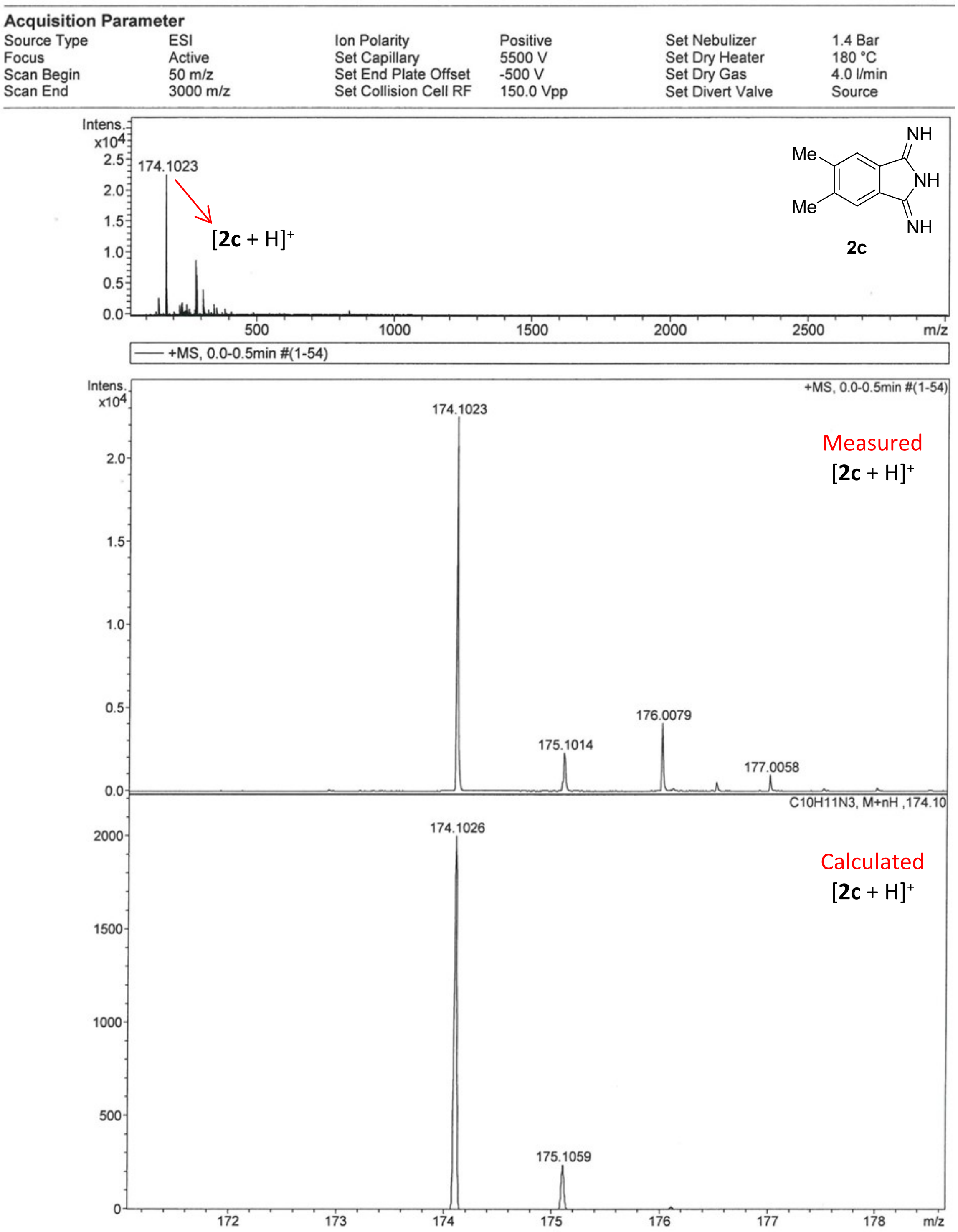

Acquisition Parameter

Source Type	ESI	Ion Polarity	Positive	Set Nebulizer	1.4 Bar
Focus	Active	Set Capillary	5500 V	Set Dry Heater	180 °C
Scan Begin	50 m/z	Set End Plate Offset	-500 V	Set Dry Gas	4.0 l/min
Scan End	3000 m/z	Set Collision Cell RF	150.0 Vpp	Set Divert Valve	Source

Figure S14. HRMS (ESI-TOF) of **2c** (measured in DMSO/CH_3CN). The spectrum on top is the experimental obtained spectrum. The indicated ion peaks are shown underneath with their calculated isotope distribution patterns, starting from the lowest assigned *m*/z value to the highest. The other cations of low *m*/*z* values is due to contaminants which typically appear in such measurements as described in the literature.[4,5] Notice: The poor solubility of **2c** is indicated further by the intensity of the [**2c**+H]$^+$ peak, which is one magnitude lower compared to the other here reported 1,3-diimininoisoindolines.

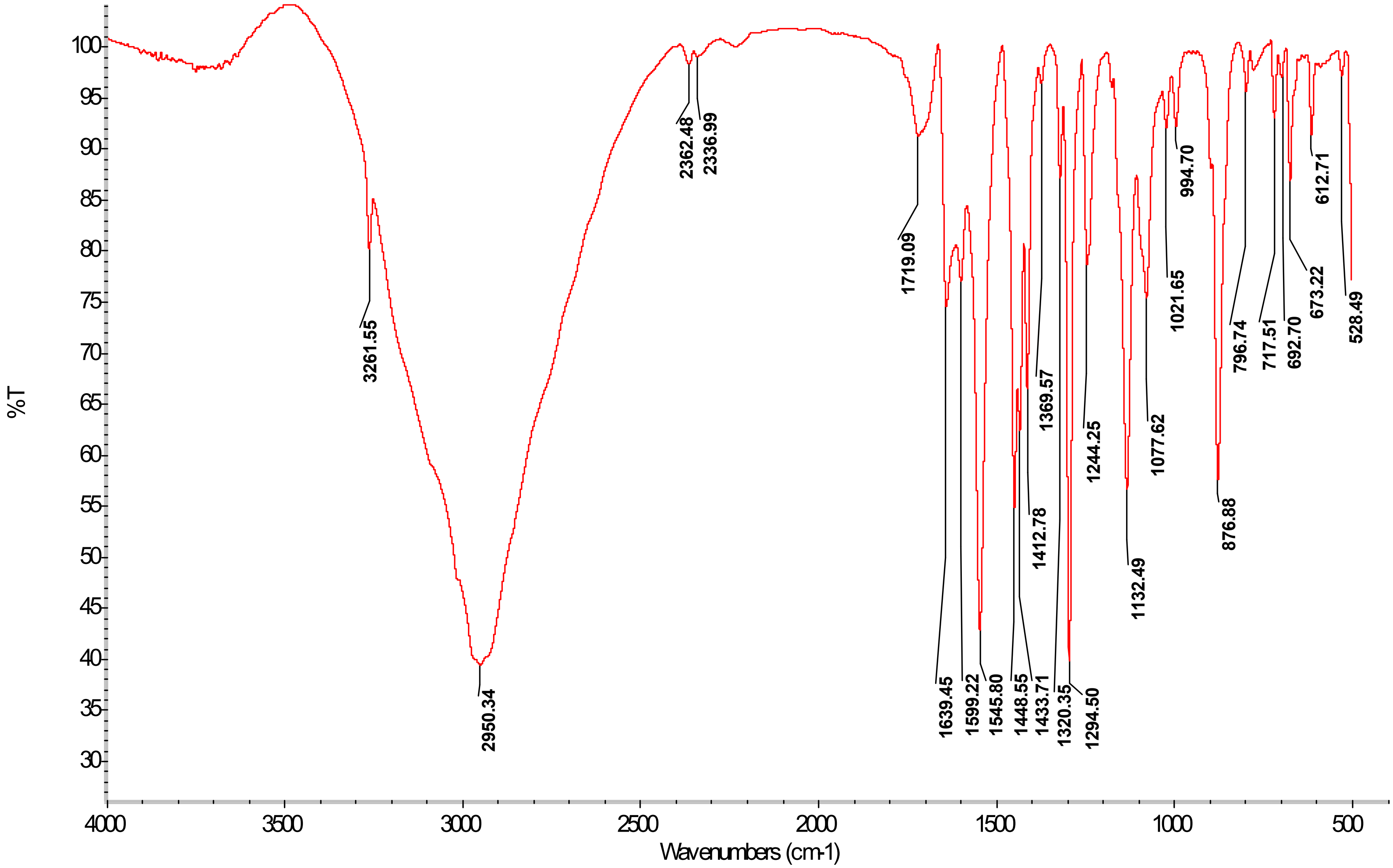

Figure S15. FT-IR spectrum (KBr) of **2c**.

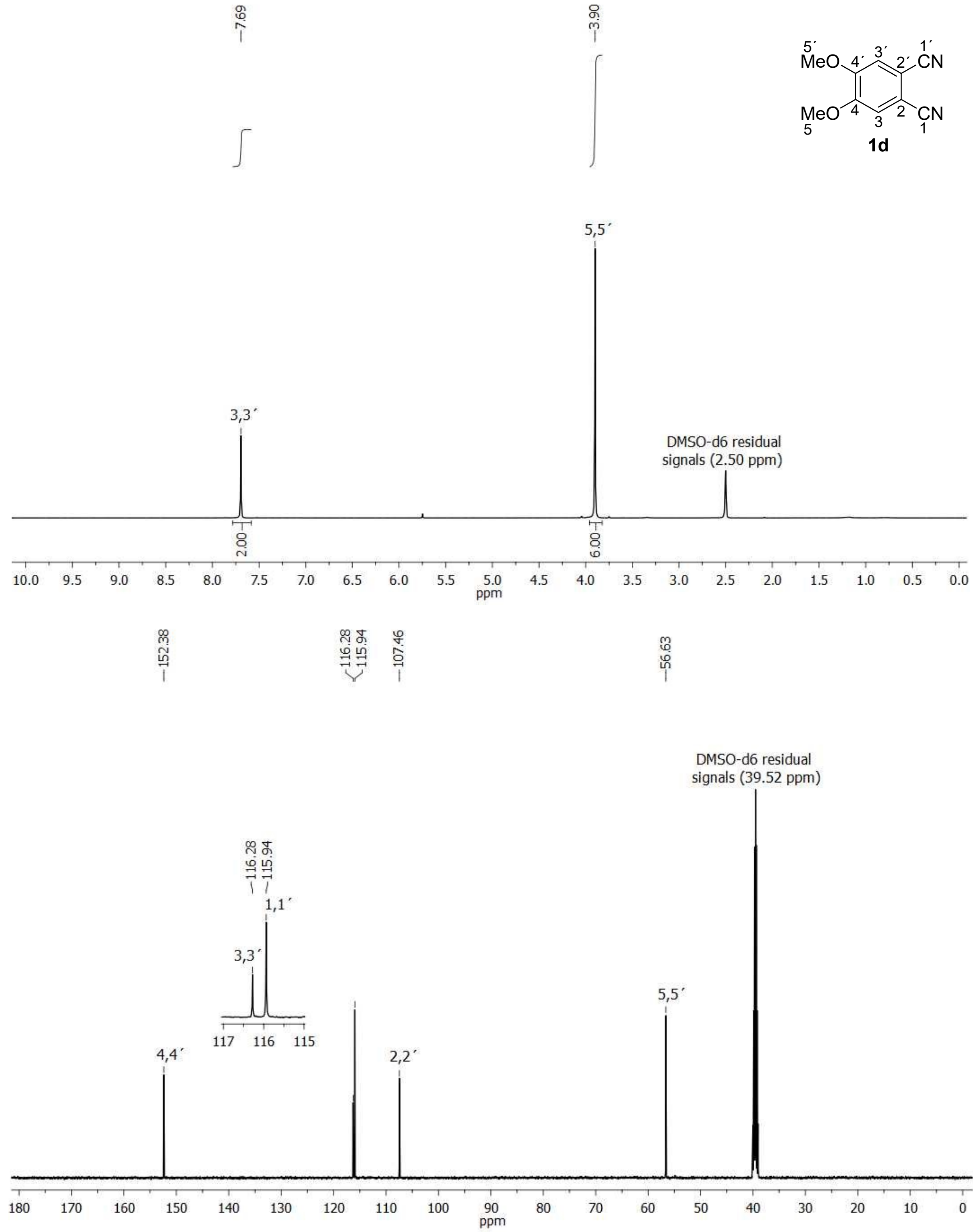

Figure S16. ^{1}H (above) and ^{13}C{^{1}H} NMR (below) spectra of **1d** in DMSO-d$_6$.

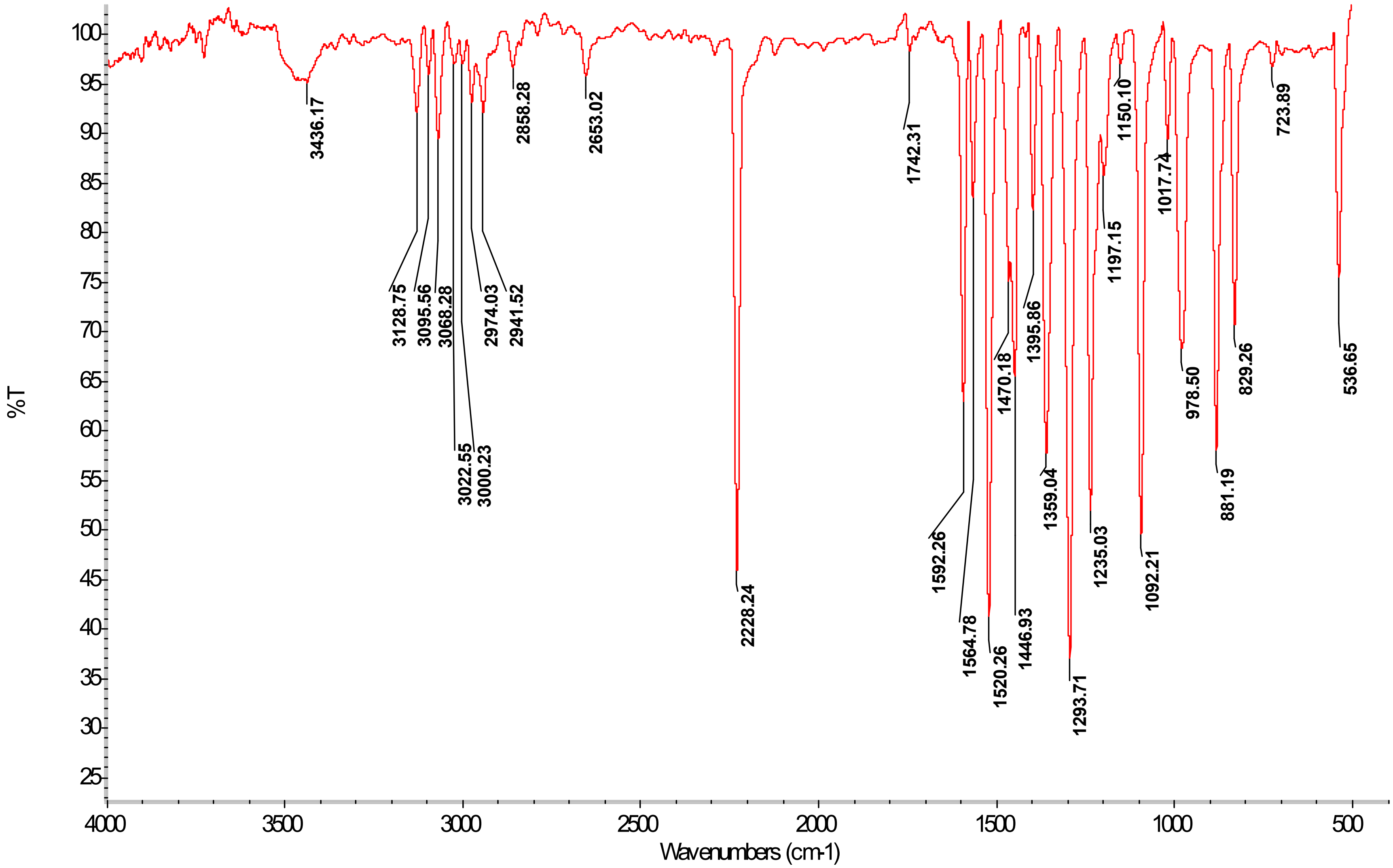

Figure S17. FT-IR spectrum (KBr) of **1d**.

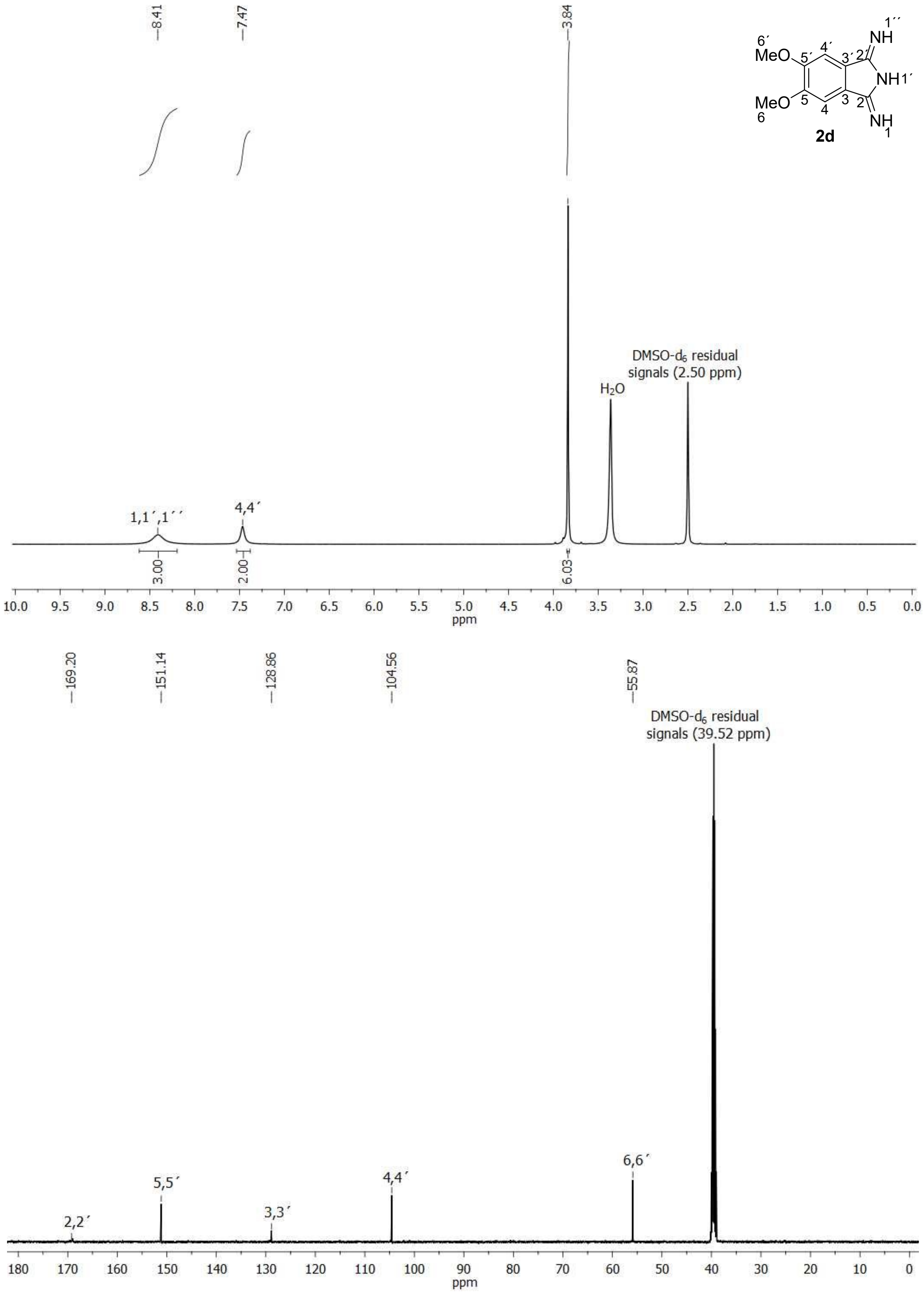

Figure S18. ^{1}H (above) and ^{13}C{^{1}H} NMR (below) spectra of **2d·H$_2$O** in DMSO-d$_6$.

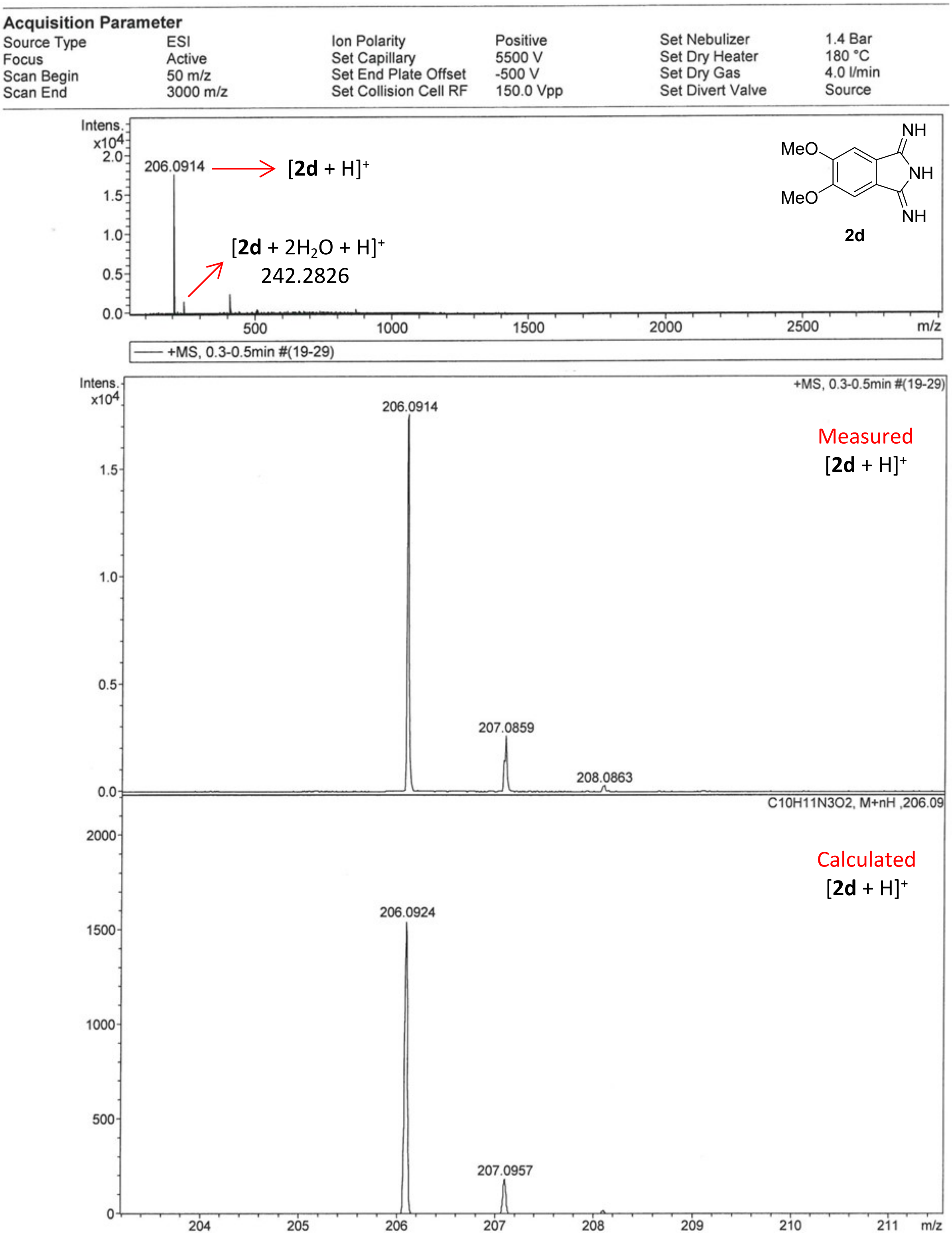

Acquisition Parameter

Source Type	ESI	Ion Polarity	Positive	Set Nebulizer	1.4 Bar
Focus	Active	Set Capillary	5500 V	Set Dry Heater	180 °C
Scan Begin	50 m/z	Set End Plate Offset	-500 V	Set Dry Gas	4.0 l/min
Scan End	3000 m/z	Set Collision Cell RF	150.0 Vpp	Set Divert Valve	Source

Figure S19. HRMS (ESI-TOF) of **2d·H$_2$O** (measured in CH_2Cl_2/CH_3CN). The spectrum on top is the experimental obtained spectrum. The spectrum on top is the experimentally obtained spectrum. The mol peak is shown below in an enlarged view with its calculated isotope distribution patterns. Notice: In the solvent mixture used is sufficiently soluble for characterization, but not as high as **2a–b** (cf. the intensities and comments made for **2c**).

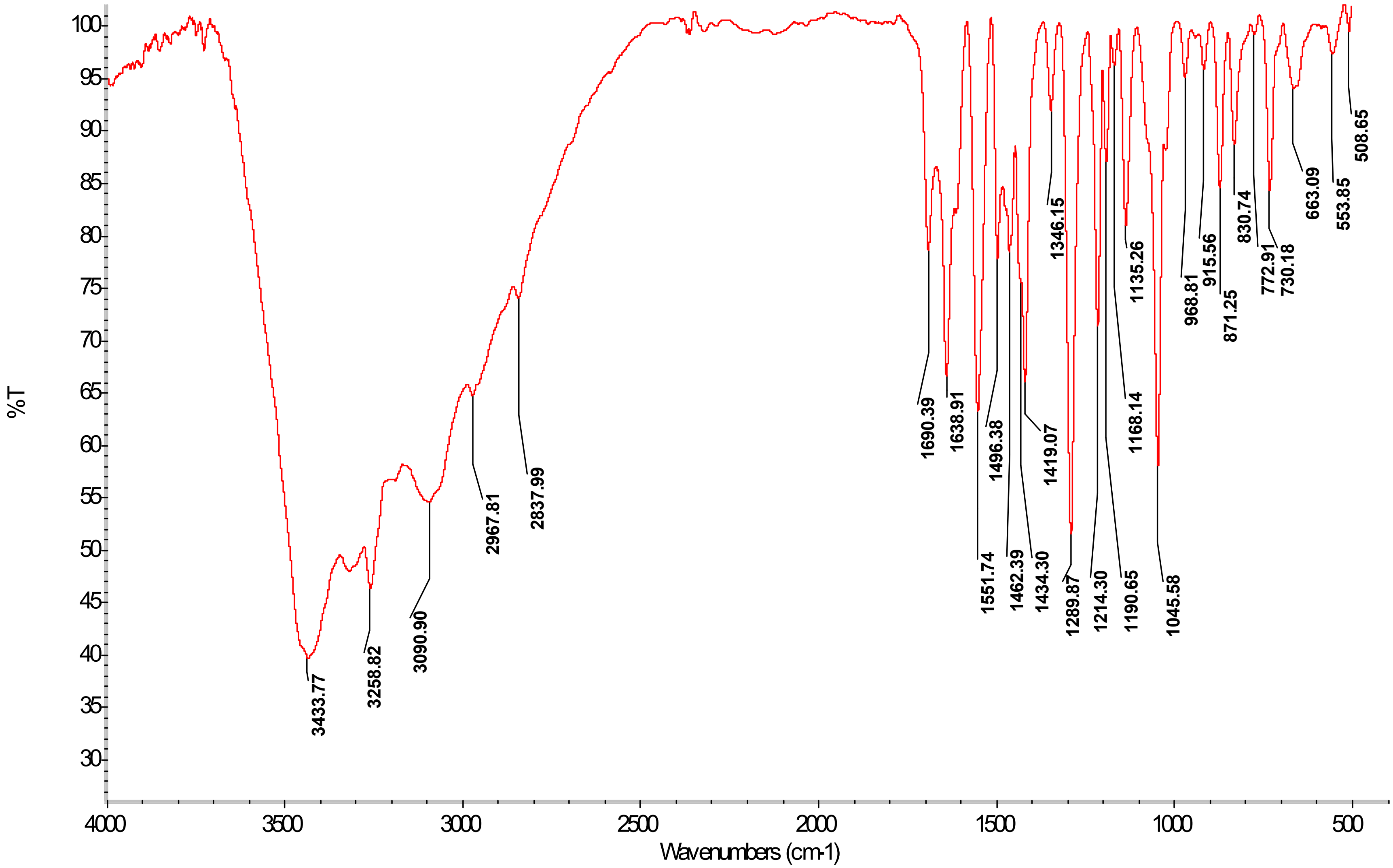

Figure S20. FT-IR spectrum (KBr) of **2d·H$_2$O**.

2.3 Thermogravimetric analysis (TGA) measurements of 2a–d

The thermal stability of the starting materials **2a–d** were investigated by using a Mettler Toledo TGA/DSC 11600 system with a MX1 balance. Before collecting the data, the starting materials were dried under vacuum to remove the solvents residues. The heating scan was from 40–500 ^{0}C under Argon (Ar), the heating rates were 10 K/min.

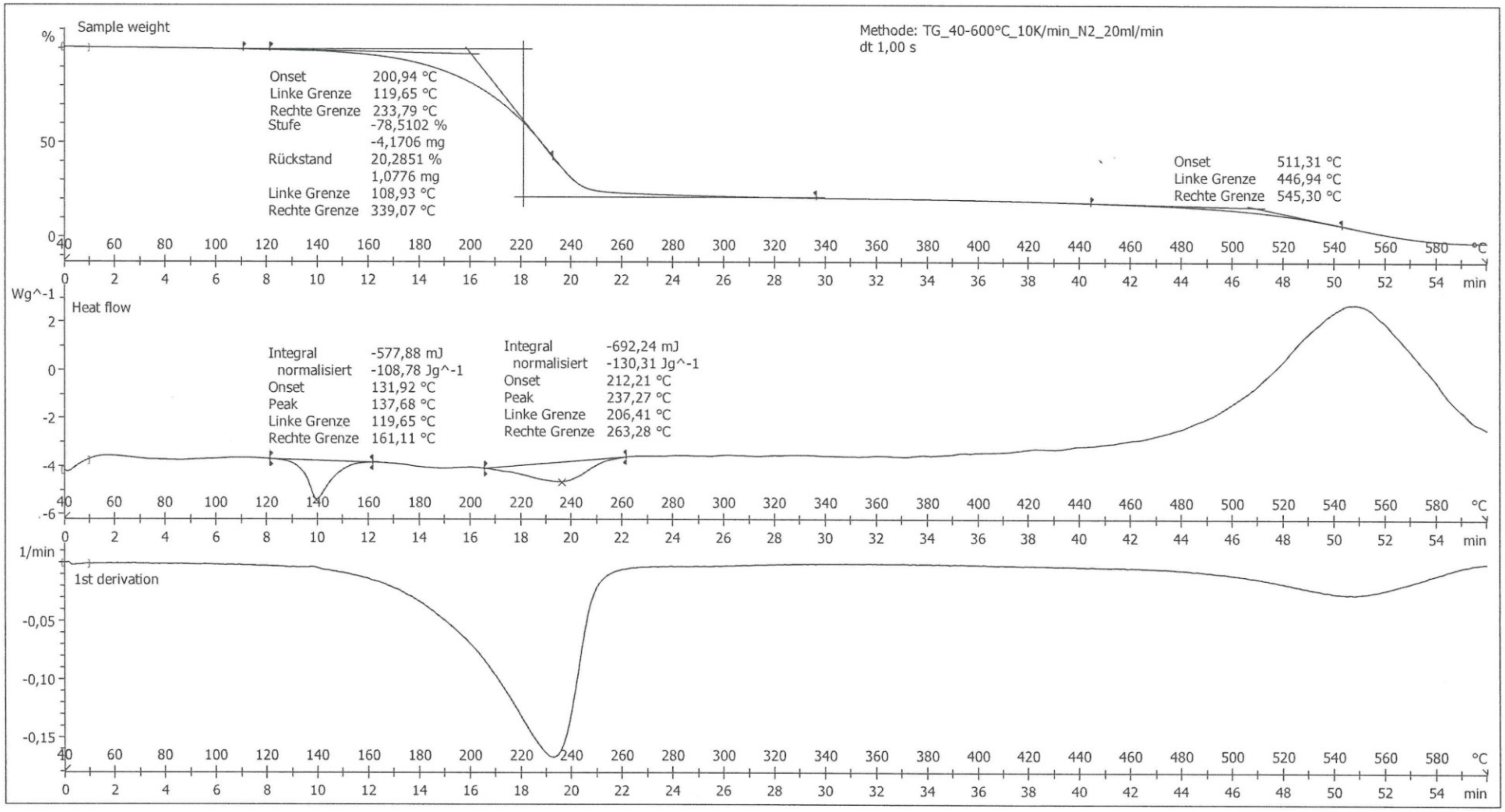

Figure S21. TGA (top), DSC (middle) and TGA´ (below) traces of **2a**.

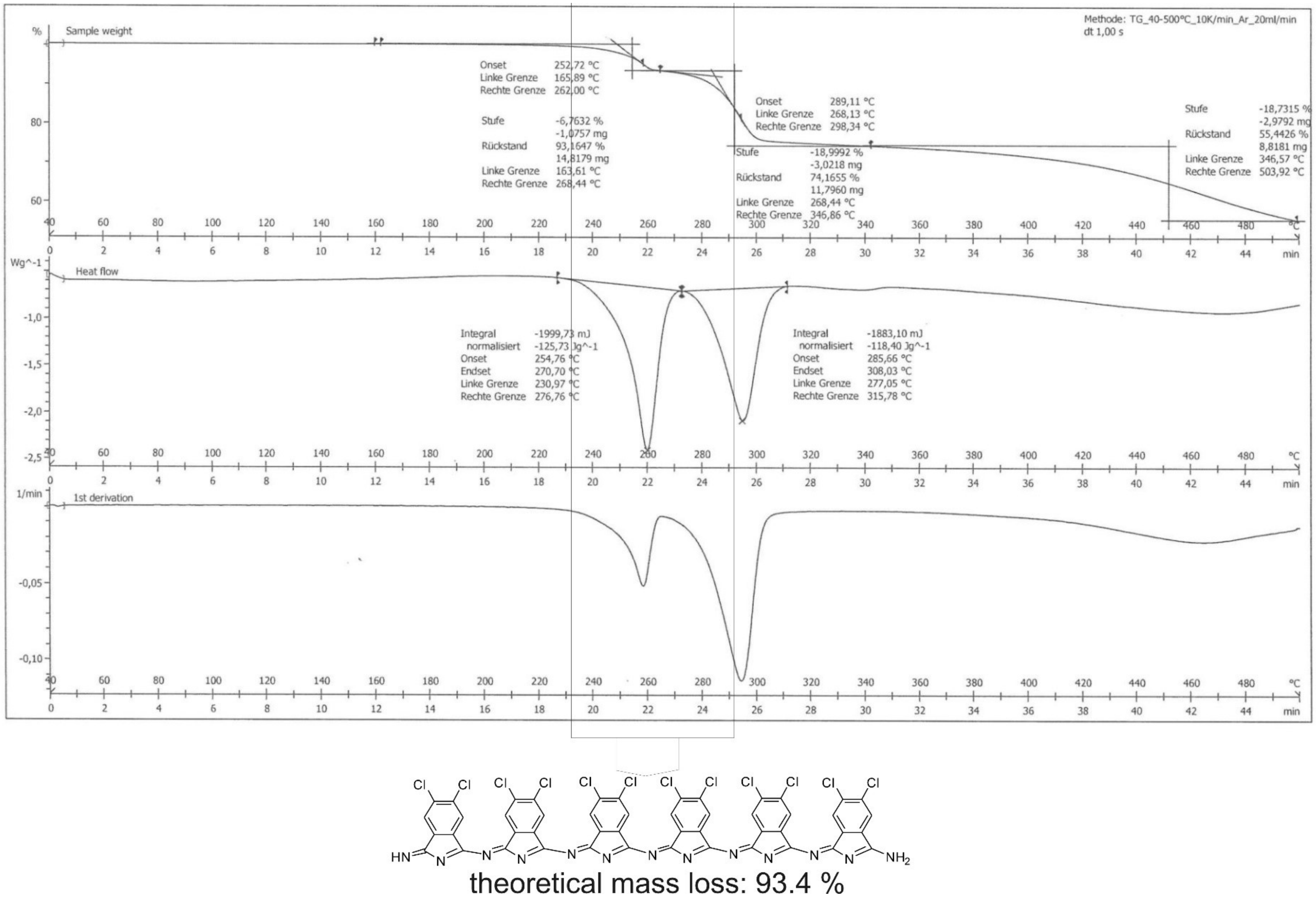

Figure S22. TGA (top), DSC (middle) and TGA´ (below) traces of **2b**.

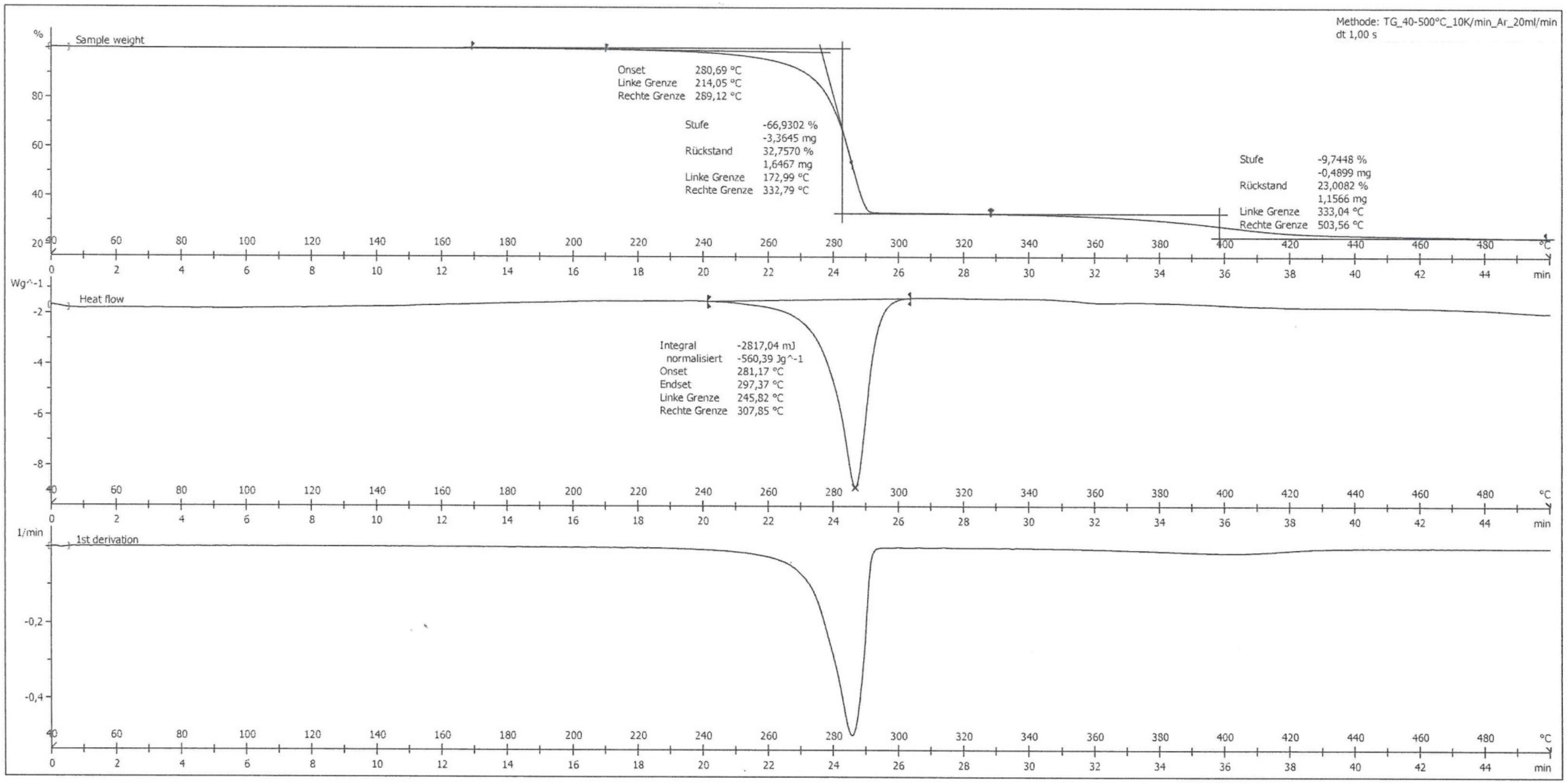

Figure S23. TGA (top), DSC (middle) and TGA´ (below) traces of **2c**.

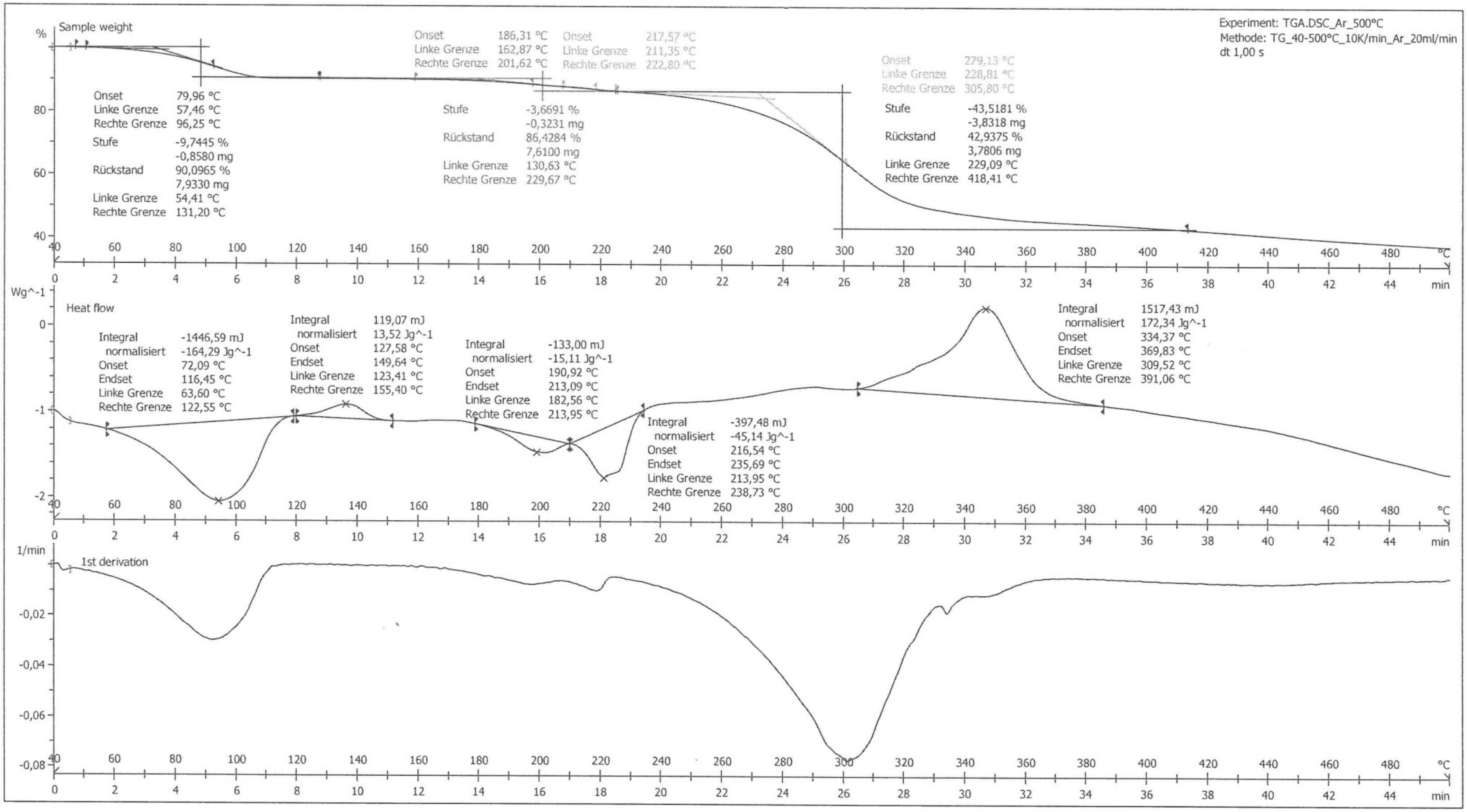

Figure S24. TGA (top), DSC (middle) and TGA´ (below) traces of **2d·H$_2$O**.

3. General procedure for the synthesis of 3a–d and 4a–d

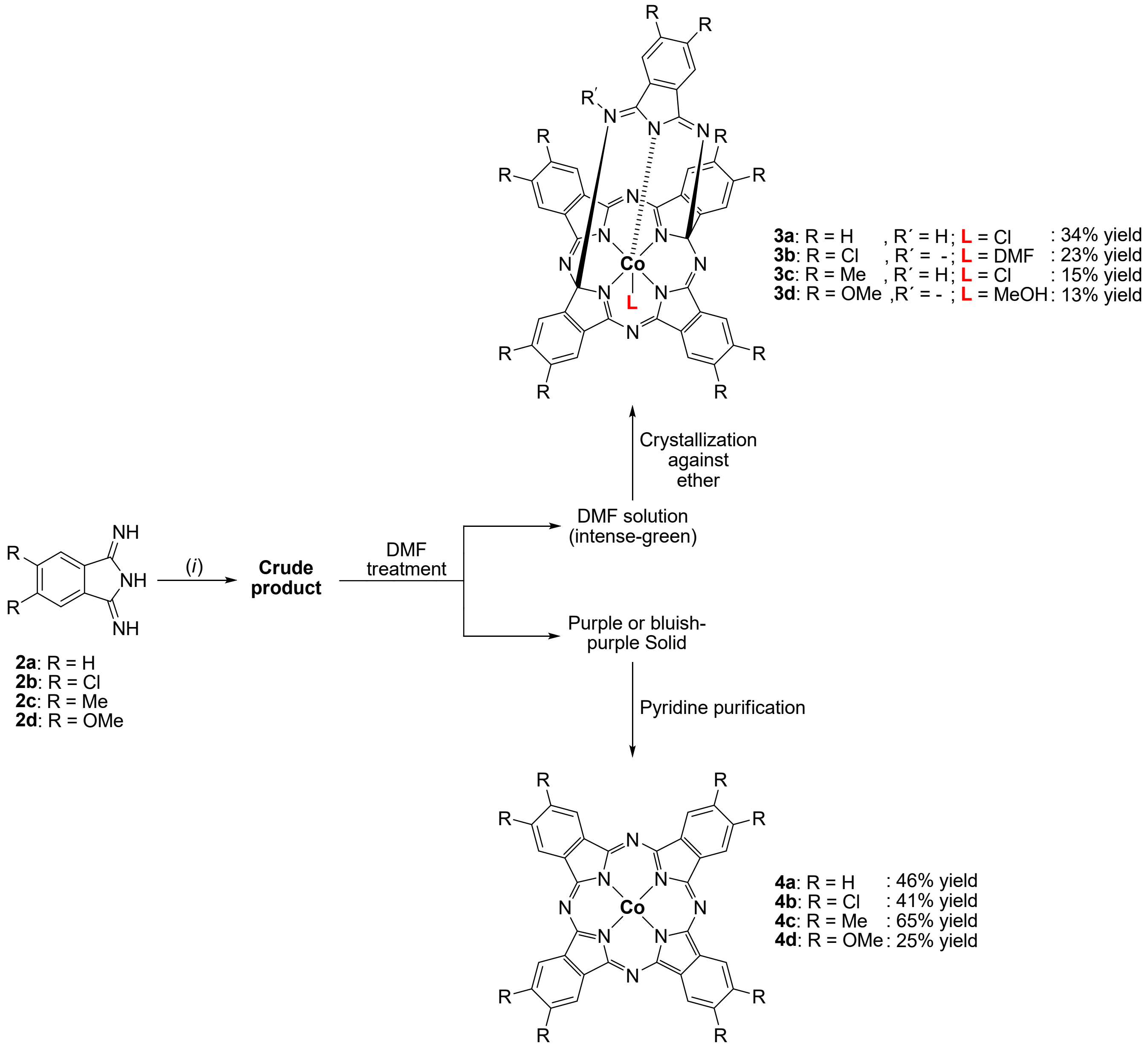

Scheme S1. Synthesis and separation of **3a**–**d** and **4a**–**d** (*i*) $CoCl_2 \cdot 6H_2O$, 1,2,4-trichlorobenzene, Δ (heating in time and temperature intervals); <u>hint</u>: heating was continued until the NH_3 liberation ceased.

4. Detailed descriptions for the synthesis and characterization of 3a–d

4.1 Synthesis of 3a–d

<u>Comment:</u> We focus next on the descriptions of **3a–d**. The descriptions of the Co(II)phthalocyanines **4a–d**, which were obtained along with the isolation of **3a–d**, are reported below in Section 6.

Synthesis of 3a (in form of [3a(HCl)(dmf)]·2dmf)

3a was prepared according to the general procedure from 1,3-diiminoisoindoline **2a** (2.50 g, 17.2 mmol, 5 equiv) in 1,2,4-trichlorobenzene (150 mL), and $CoCl_2·6H_2O$ (0.8195 g, 3.44 mmol, 1 equiv).

Remark: Upon reaching 120 ^oC the NH_3 development started and continued for about 5 days after heating to 210 ^oC.

Dark red crystals; Yield: 0.8882 g (34%, based on $CoCl_2·6H_2O$). **^{1}H NMR** (500.3 MHz, DMF-d_7): δ 8.54 (d, 2H), 8.1 (d, 2H), 8.01-8.05 (m, 7H), 7.91-7.94 (td, 2H), 7.77-7.84 (m, 2H), 7.68-7.74 (m, 4H), 7.51-7.52 (dd, 2H) ppm. **HRMS** (ESI-TOF, positive mode): *m/z* Calcd for $C_{40}H_{21}CoN_{11}$ $[M-HCl-3dmf+H]^+$: 714.1308; found: 714.1440. **FT-IR** (KBr): 3414 (br), 3053 (w), 2924 (w), 2853 (w), 1664 (s), 1626 (m), 1569 (s), 1533 (s), 1474 (s), 1447 (s), 1395 (s), 1387, 1326 (m), 1289 (m), 1257 (w),1226 (m), 1194 (m), 1168(w), 1147 (w), 1125 (m), 1097 (m), 1078 (w), 1058 (w), 1032 (m), 1012 (w), 992 (w), 942 (w), 924 (w), 881 (w), 779 (m), 755 (w), 730 (s), 703 (w), 654 (w), 596 (w), 511 (w) cm^{-1}. **Anal. Calcd** for $C_{49}H_{42}ClCoN_{14}O_3$ (**[3a(HCl)(dmf)]·2dmf)**, 968.26 g mol^{-1}): C, 60.71; H, 4.37; N, 20.23%. **Found**: C, 60.47; H, 4.08; N, 19.91%. **UV/Vis** (CH_2Cl_2, 25 ^oC): λ_{max}, nm (ε, M^{-1} cm^{-1}): 232 (89125), 247 (91201), 315 (34674), 385 (7762), 458 (3388). **FTIR (out of the crystals after column chromatography 3a·**MeOH**)**: 3414 (br), 3059 (w), 1652 (s), 1626 (m), 1613 (w), 1560 (s), 1535 (s), 1472 (s), 1450 (s), 1397 (s), 1322 (m), 1297 (m), 1212 (m), 1177 (w), 1163 (w), 1146 (w), 1125 (m), 1098 (m), 1079 (w), 1030 (m), 1013 (m), 971 (w), 956 (w), 926 (w), 881 (w), 847 (w), 808 (w), 777 (m), 754 (w), 730 (vs), 697 (m), 682 (w), 654 (w), 601 (w), 514 (w) cm^{-1}. **^{1}H NMR** (500.3 MHz, CD_2Cl_2): δ 7.21 (2H, $H^{20,20'}$), 7.51 (2H, $H^{19,19'}$), 7.56 (2H, $H^{12,12'}$), 7.60 (2H, $H^{13,13'}$), 7.62 (2H, $H^{5,5'}$) , 7.80 (2H, $H^{4,4'}$) , 7.99 (2H, $H^{11,11'}$), 8.03 (2H, $H^{14,14'}$), 8.04 (2H, $H^{6,6'}$) , 8.49 (2H, $H^{3,3'}$) ppm, **^{13}C{^{1}H} NMR** (125 MHz, CD_2Cl_2): δ 92.10 ($C^{1,1'}$), 120.11 ($C^{19,19'}$), 121.75 ($C^{11,11'}$), 121.95 ($C^{14,14'}$), 122.26 ($C^{6,6'}$), 124.36 ($C^{3,3'}$), 129.27 ($C^{5,5'}$), 129.53 ($C^{20,20'}$), 131.14 ($C^{12,12'}$), 131.69 ($C^{4,4'}$), 131.73 ($C^{13,13'}$), 134.85 ($C^{2,2'}$), 139.04 ($C^{15,15'}$), 139.75 ($C^{10,10'}$), 141.46 ($C^{18,18'}$), 155.48 ($C^{7,7'}$), 157.86 ($C^{17,17'}$), 161.12 ($C^{16,16'}$), 166.35 ($C^{8,8'}$), 167.20 ($C^{9,9'}$) ppm.

Synthesis of 3b (in form of [3b(dmf)]·dmf·H_2O)

3b was prepared according to the general procedure from 5,6-dichloro-1,3-diiminoisoindoline **2b** (2.50 g, 11.7 mmol, 5 equiv) in 1,2,4-trichlorobenzene (150 mL), and $CoCl_2·6H_2O$ (0.5558 g, 2.34 mmol, 1 equiv).

Remark: Upon reaching 100 ^oC the NH_3 development started and continued for about 4 days after heating to 210 ^oC. Next it was cooled to room temperature and filtrated. Surprisingly and exclusively observed for **3b** the initially optically transparent and dark green filtrate was kept for about 5 days and by time an orange precipitate was formed, which was filtered off. This material was subjected to a column chromatography (on silica gel, dichloromethane as eluent) to get analytically pure **3b**. Orange solid; Yield: 0.2997 g, (11%, based on $CoCl_2 \cdot 6H_2O$). A second fraction of **3b** was isolated as described in the general procedure.

Orange crystals; Yield: 0.3201 g (12%, based on $CoCl_2 \cdot 6H_2O$). **^{1}H NMR** (500.3 MHz, CD_2Cl_2): δ 7.61 (s, 2H), 8.01 (s, 2H), 8.07 (s, 2H), 8.11 (s, 2H), 8.52 (s, 2H) ppm. **HRMS** (ESI-TOF, positive mode): *m/z* Calcd for $C_{40}H_{11}Cl_{10}CoN_{11}$ [M-2dmf-H_2O+H]$^+$: 1057.7358; found: 1057.7344. **FT-IR** (KBr): 3094 (w), 3069 (w), 2960 (w), 2923 (w), 1711 (w), 1651 (m), 1568 (s), 1534 (s), 1474 (m), 1440 (m), 1393 (s), 1373 (s), 1324 (w), 1299 (w), 1258 (w), 1226 (m), 1202 (m), 1167 (w), 1143 (w), 1095 (m), 1041 (m), 1015 (m), 972 (w), 946 (w), 927 (w), 894 (m), 862 (w), 808 (m), 782 (m), 739 (w), 713 (w), 658 (m), 565 (w), 528 (w), 505 (w) cm^{-1}. **Anal. Calcd** for $C_{46}H_{26}Cl_{10}CoN_{13}O_3$ (**[3b(dmf)]·dmf·H_2O**, 1222.25 g mol^{-1}): C, 45.20; H, 2.14; N, 14.90%. **Found**: C, 45.53; H, 2.19; N, 14.89%. Notice: Most likely due to the required grinding prior to measurement the material caught water from the aerobic environment. **UV/Vis** (CH_2Cl_2, 25 °C): λ_{max}, nm (ε, M^{-1} cm^{-1}): 243 (87096), 262 (104713), 318 (34674), 398 (6761), 475 (2884).

Synthesis of 3c **(in form of [3c(HCl)]·dmf)**

3c was prepared according to the general procedure from 5,6-dimethyl-1,3-diiminoisoindoline (2.00 g, 11.5 mmol, 5 equiv) in 1,2,4-trichlorobenzene (150 mL), and $CoCl_2 \cdot 6H_2O$ (0.5495 g, 2.31 mmol, 1 equiv).

Remark: Upon reaching 140 ^{o}C the NH_3 development started and continued for about 3 days after heating to 210 ^{o}C.

Orange-red crystals; Yield: 0.3011 g (14.6 %, based on $CoCl_2 \cdot 6H_2O$). **HRMS** (ESI-TOF, positive mode): *m/z* Calcd for $C_{50}H_{41}CoN_{11}$ [M-HCl-dmf+H]$^+$: 854.2873; found: 854.2917 (in DMF/CH_3CN/HCOOH). **FT-IR** (KBr): 3413 (br), 2970 (w), 2942 (w), 2919 (w), 2861 (w), 1660 (m), 1625 (s), 1568 (s), 1532 (s), 1483 (m), 1453 (s), 1418 (m)1392 (w), 1381 (s), 1318 (m), 1253 (m), 1234 (w), 1208 (w), 1191 (m), 1171 (m), 1149 (s), 1118 (w), 1103 (m), 1048 (w), 1004 (m), 966 (w), 886 (m), 843 (w), 807 (w), 793 (w), 762 (w), 748 (w), 736 (w), 720 (w), 666 (w), 601 (w), 552 (w) cm^{-1}. **Anal. Calcd** for $C_{53}H_{48}ClCoN_{12}O$ (**[3c(HCl)]·dmf**, 962.31 g mol^{-1}): C, 66.07; H, 5.02; N, 17.45%. **Found**: C, 65.92; H, 4.98; N, 16.98%. Neither ^{1}H nor ^{13}C{1H} NMR spectra could be recorded due to the very poor solubility of **3c** in common solvents.

Synthesis of 3d **(in form of [3d(MeOH)]·dmf)**

3d was prepared according to the general procedure from 5,6-dimethoxy-1,3-diiminoisoindoline (2.50 g, 12.2 mmol, 5 equiv) in 1,2,4-trichlorobenzene (150 mL), and $CoCl_2 \cdot 6H_2O$ (0.5798 g, 2.44 mmol, 1 equiv).

Remark: Upon reaching 100 °C the NH_3 development started and continued for about 4 days after heating to 210 °C. In contrast to **3a–c** the crystals of **3d**, obtained according to the general procedure, were never suitable for single crystal X-ray crystallographic studies but were microcrystalline materials only.

Orange crystals; Yield: 0.3321 g (13%, based on $CoCl_2 \cdot 6H_2O$). **HRMS** (ESI-TOF, positive mode): *m/z* Calcd for $C_{50}H_{41}CoN_{11}O_{10}$ [M-MeOH-dmf+H]$^+$: 1014.2364; found: 1014.2383. **FT-IR** (KBr): 2934 (m), 2842 (w), 1771 (w), 1748 (w), 1723 (m), 1660 (m), 1604 (w), 1559 (s), 1532 (s), 1496 (m), 1476 (s), 1456 (s), 1423 (w), 1386 (s), 1346 (m), 1298 (s), 1283 (s), 1217 (m), 1202 (w), 1181 (w), 1154 (m), 1109 (w), 1070 (s), 1029 (m), 1007 (w), 996 (w), 978 (w), 872(w), 847 (w), 818 (m), 786 (w), 765 (w), 745 (w), 711 (w), 664 (w), 642 (w), 602 (w), 573 (w), 512 (w) cm^{-1}. **Anal. Calcd** for $C_{54}H_{51}CoN_{12}O_{12}$ (1118.31 g mol^{-1}): C, 57.96; H, 4.59; N, 15.02%. **Found**: C, 57.39; H, 4.43; N, 14.91%. Neither ^1H nor $^{13}C\{^1H\}$ NMR spectra could be recorded due to insolubility of **3d** in NMR solvents. **UV/Vis** (CH_2Cl_2, 25 °C): λ_{max}, nm (ε, M^{-1} cm^{-1}): 251 (52480), 272 (67608), 323 (26915), 384 (15135).

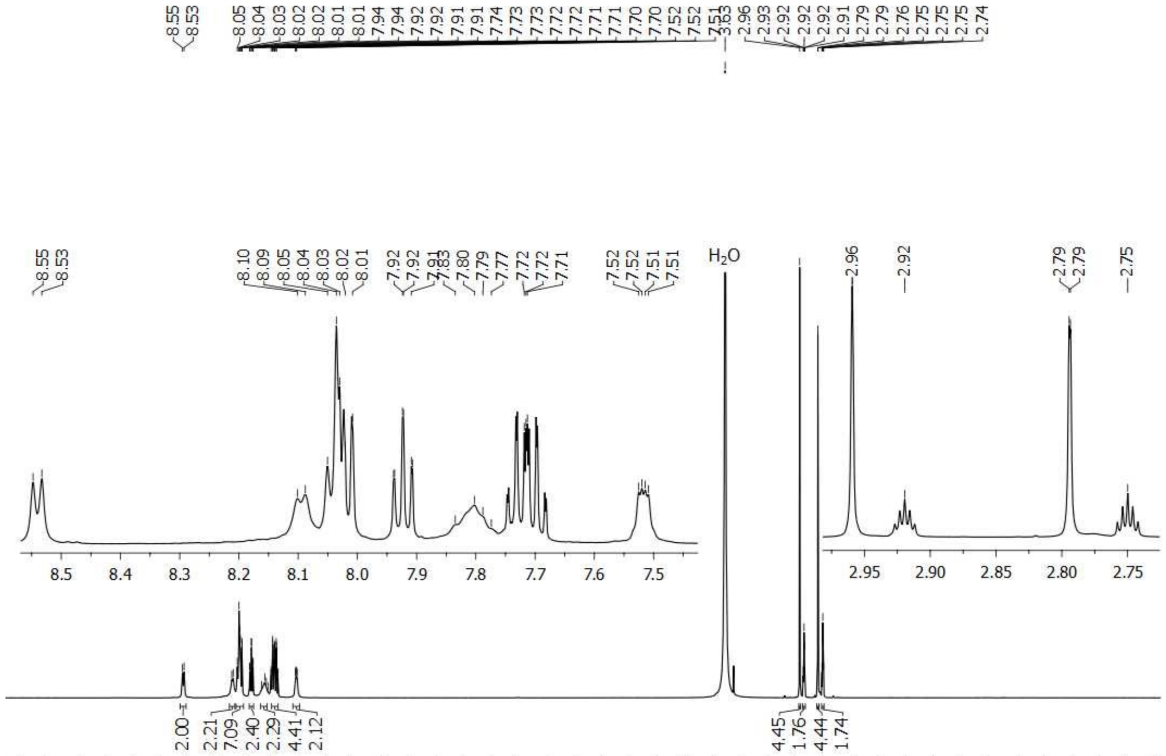

Figure S25. ^1H NMR spectrum of **3a** in DMF-d_7. DMF-d_7 residual signals (multiplicity): 2.75 (5), 2.92 (5) and 8.03 (1) ppm, while 2.79, 2.96 and 8.04 ppm are the ^1H NMR signals of DMF (crystallization solvent).[6]

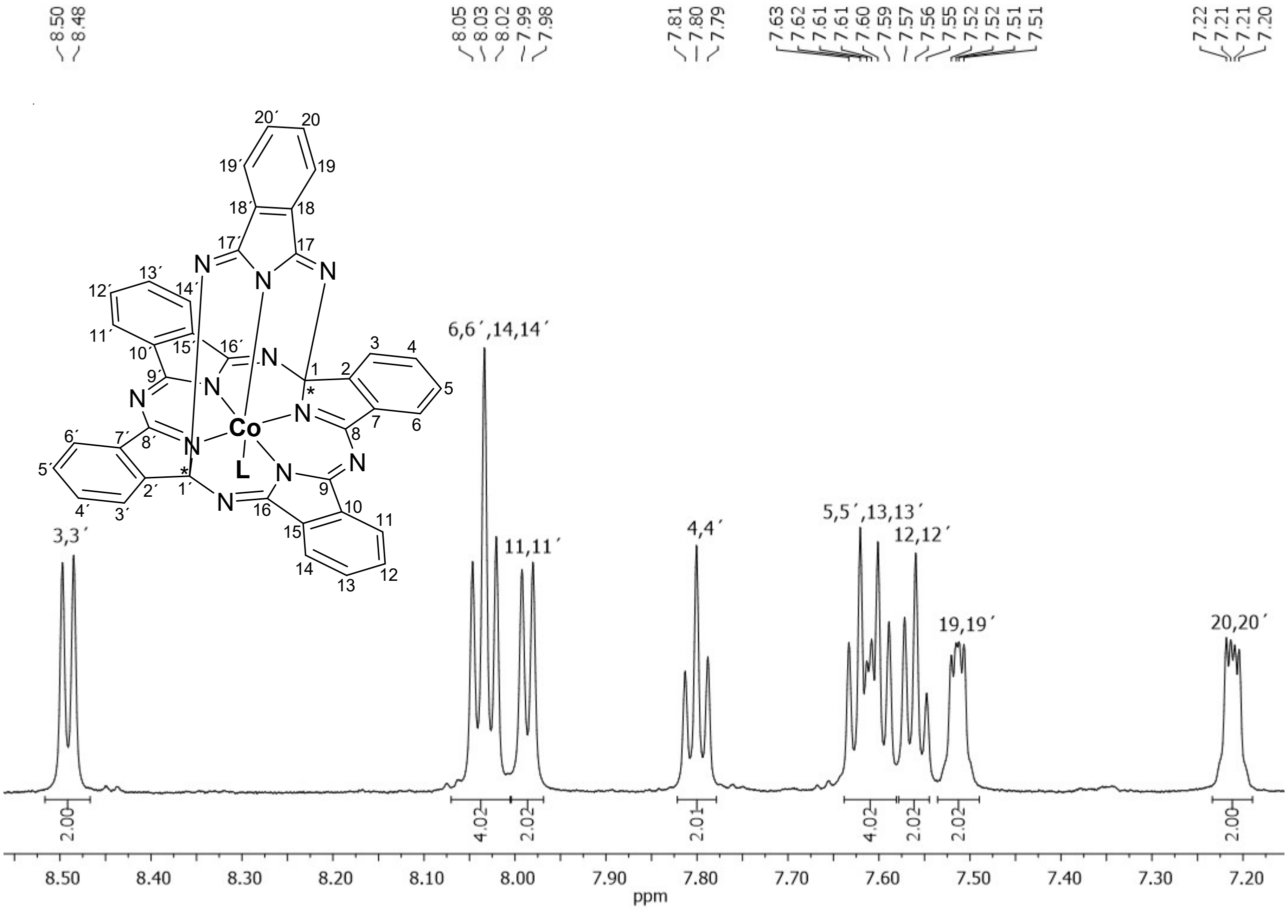
8.50
8.48
8.05
8.03
8.02
7.99
7.98
7.81
7.80
7.79
7.63
7.62
7.61
7.61
7.60
7.59
7.57
7.56
7.55
7.52
7.52
7.51
7.51
7.22
7.21
7.21
7.20
Co
L
3,3´
6,6´,14,14´
11,11´
4,4´
5,5´,13,13´
12,12´
19,19´
20,20´
2.00
4.02
2.02
2.01
4.02
2.02
2.02
2.00
8.50
8.40
8.30
8.20
8.10
8.00
7.90
7.80
7.70
7.60
7.50
7.40
7.30
7.20
ppm

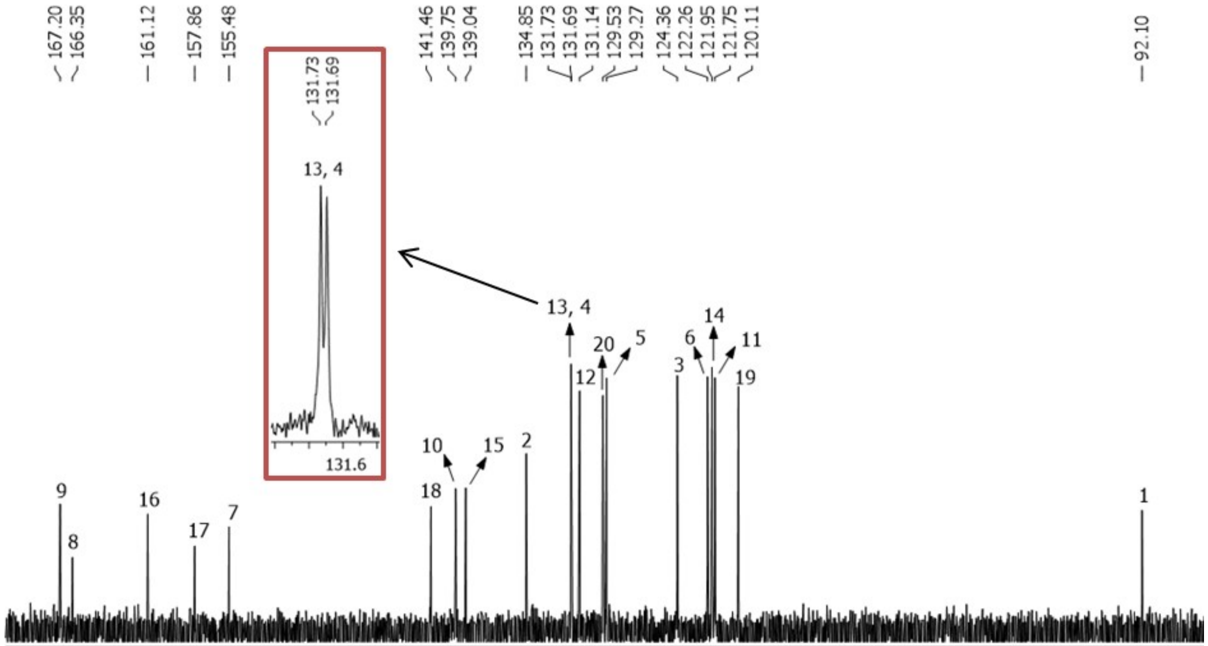
167.20
166.35
161.12
157.86
155.48
141.46
139.75
139.04
134.85
131.73
131.69
131.14
129.53
129.27
124.36
122.26
121.95
121.75
120.11
92.10
131.73
131.69
13, 4
131.6
13, 4
14
20
5
6
11
12
3
19
10
15
2
18
9
8
16
17
7
1
170
165
160
155
150
145
140
135
130
125
120
115
110
105
100
95
90
ppm

Figure S26. Top: ^{1}H NMR spectrum of **3a**·MeOH in CD_2Cl_2, and bottom: ^{13}C{H}NMR spectrum of **3a**·MeOH in CD_2Cl_2 at rt.

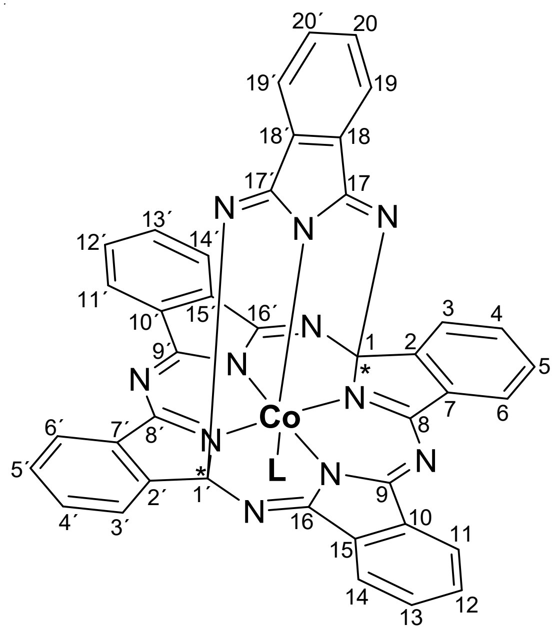

Table S1: ^{1}H and ^{13}C{1H} NMR data of **3a**

^{1}H NMR

	$H^{3,3´}$	$H^{4,4´}$	$H^{5,5´}$	$H^{6,6´}$	$H^{11,11´}$	$H^{12,12´}$	$H^{13,13´}$	$H^{14,14´}$	$H^{19,19´}$	$H^{20,20´}$
δ:	8.49	7.80	7.62	8.04	7.99	7.56	7.60	8.03	7.51	7.21
	(d, 2H)	(m, 2H)	(2H)	(2H)	(d, 2H)	(td, 2H)	(2H)	(2H)	(m, 2H)	(m, 2H)

^{13}C NMR

	C1	**C2**	**C3**	**C4**	**C5**	**C6**	**C7**	**C8**	**C9**	**C10**	**C11**	**C12**	**C13**	**C14**	**C15**	**C16**	**C17**	**C18**
δ:	92.10	134.85	124.36	131.7	129.27	122.26	155.48	166.35	167.20	139.75	121.75	131.14	131.7	121.95	139.04	161.12	157.86	141.46

	C19	**C20**
δ:	120.11	129.53

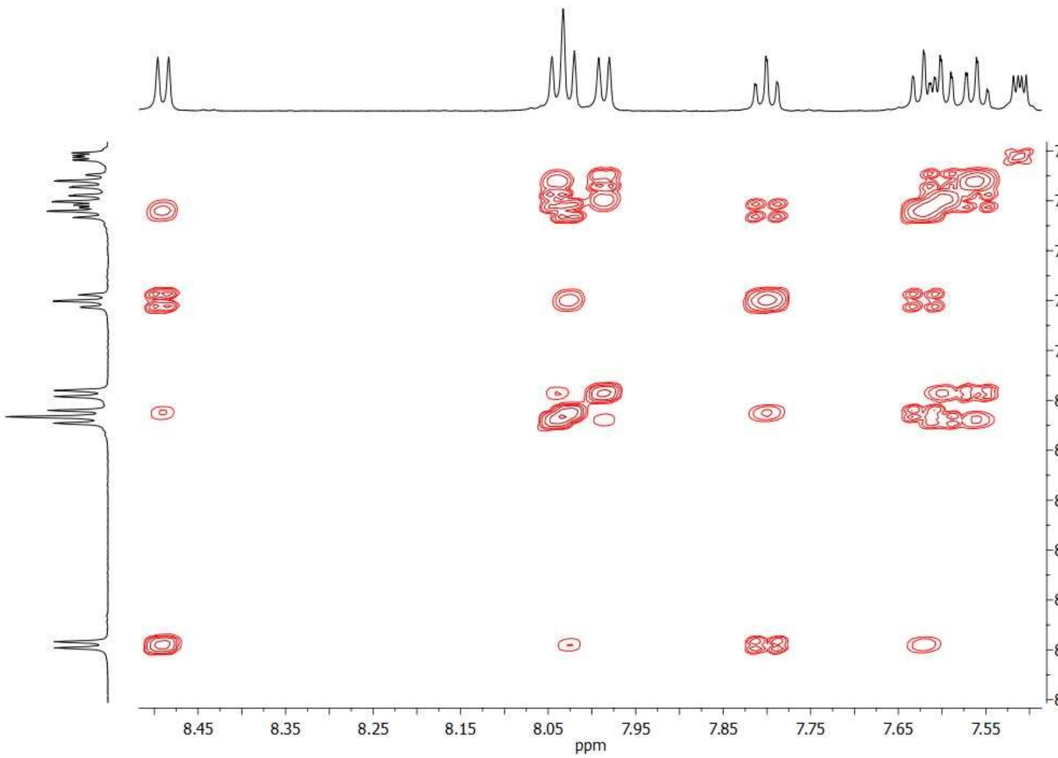

Figure S27. The 2D homonuclear ^1H-^1H COSY NMR spectrum of complex **3a** in CD_2Cl_2 at ambient temperature.

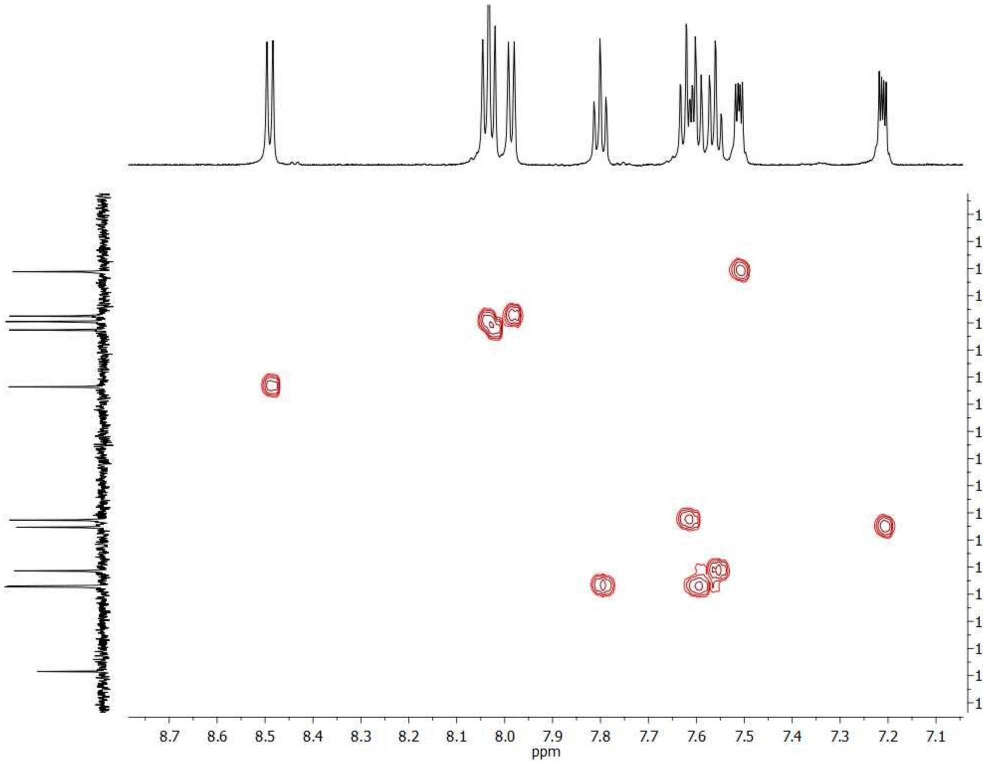

Figure S28. The 2D heteronuclear ^1H-^{13}C HSQC NMR spectrum of complex **3a** in CD_2Cl_2 at ambient temperature.

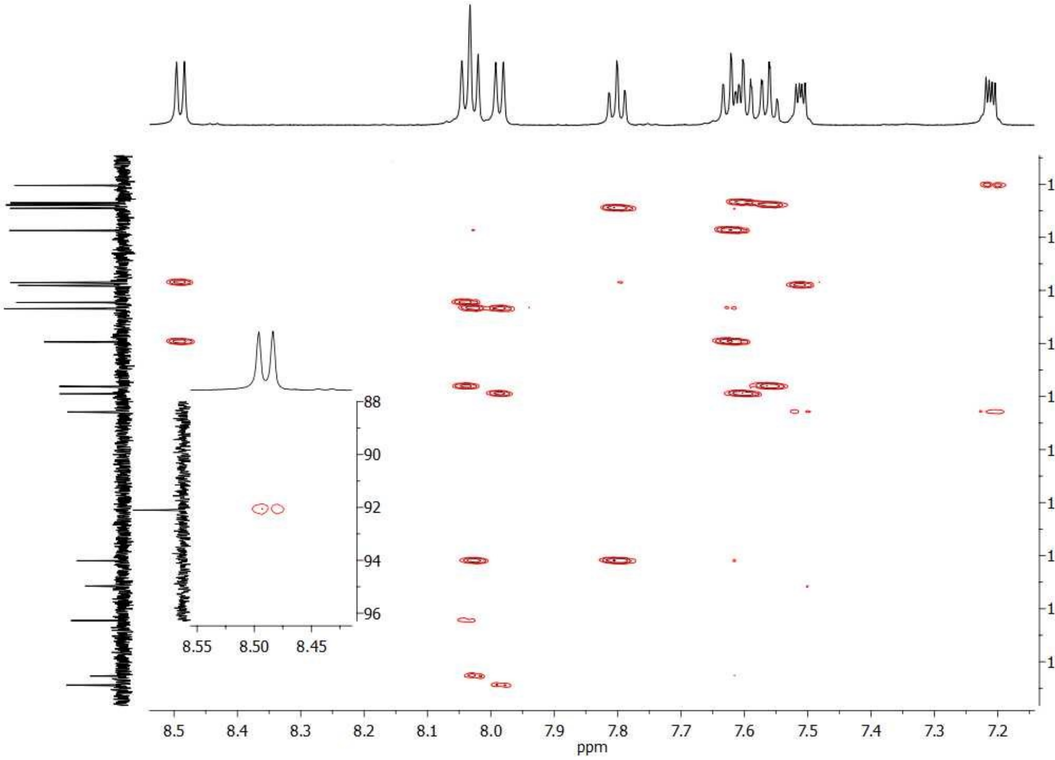

Figure S29. The 2D heteronuclear ^1H-^{13}C HMBC spectrum of complex **3a** in CD_2Cl_2 at ambient temperature.

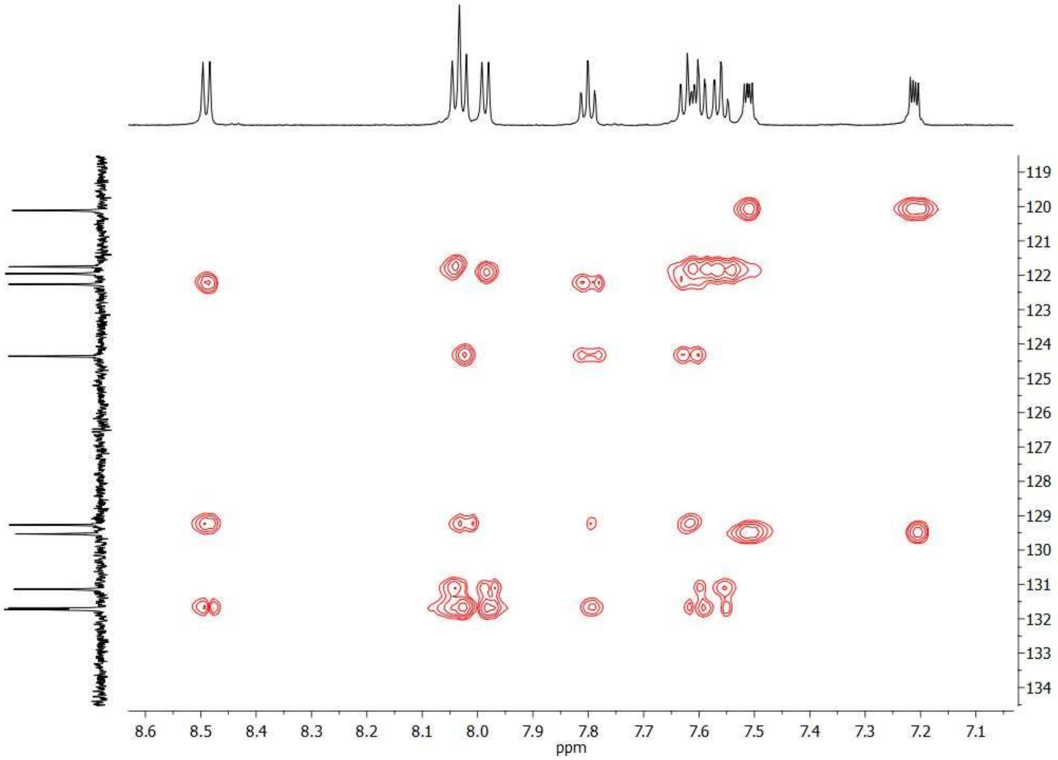

Figure S30. The 2D heteronuclear ^1H-^{13}C HSQC-TOCSY spectrum of complex **3a** in CD_2Cl_2 at ambient temperature.

Acquisition Parameter

Source Type	ESI	Ion Polarity	Positive	Set Nebulizer	0.4 Bar
Focus	Active	Set Capillary	4500 V	Set Dry Heater	190 °C
Scan Begin	50 m/z	Set End Plate Offset	-500 V	Set Dry Gas	4.0 l/min
Scan End	3000 m/z	Set Collision Cell RF	600.0 Vpp	Set Divert Valve	Source

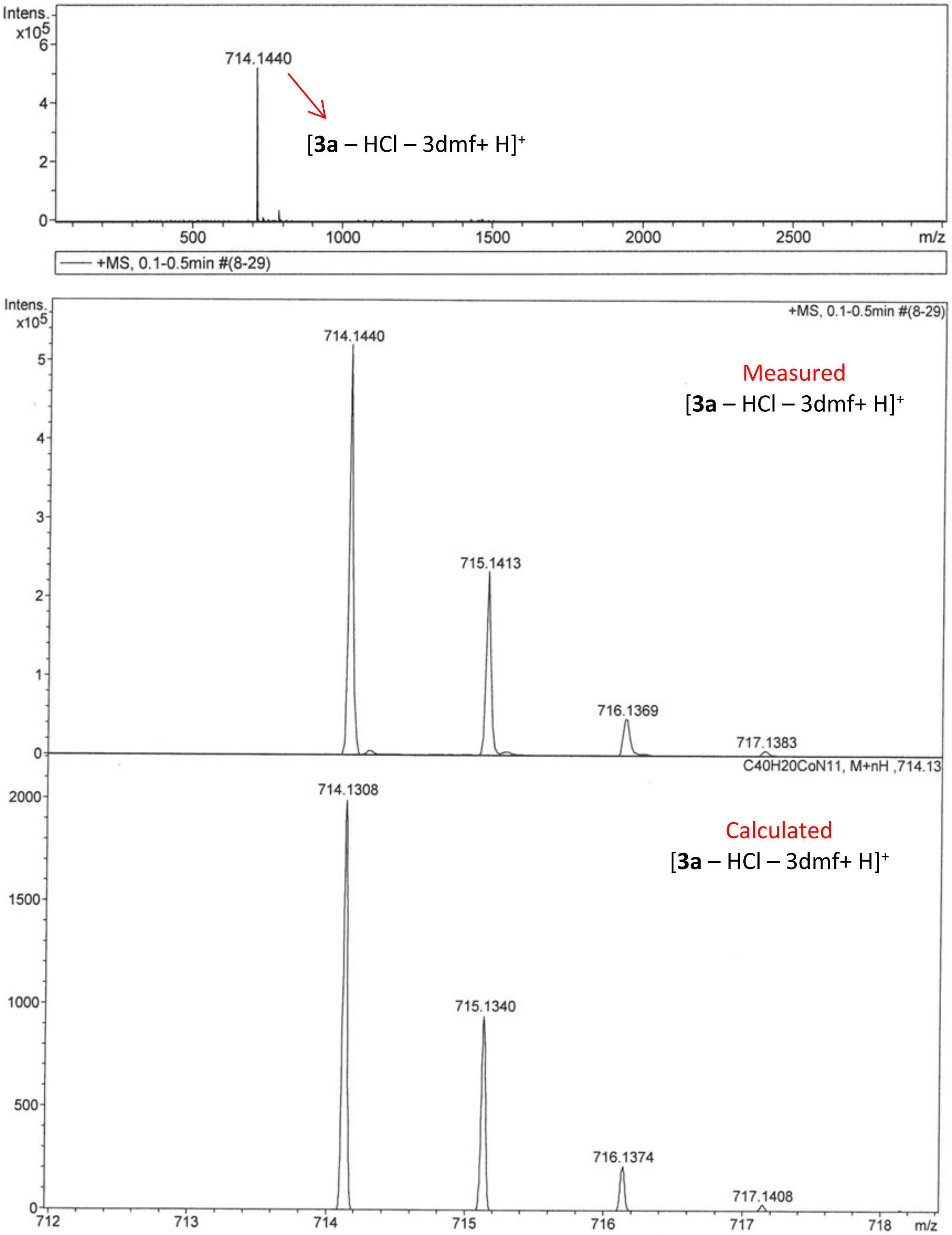

Figure S31. HRMS (ESI-TOF) of **3a** (measured in DMF/CH_3CN). The spectrum on top is the experimental obtained spectrum. The indicated ion peaks are shown underneath with their calculated isotope distribution patterns, starting from the lowest *m*/z value to the highest.

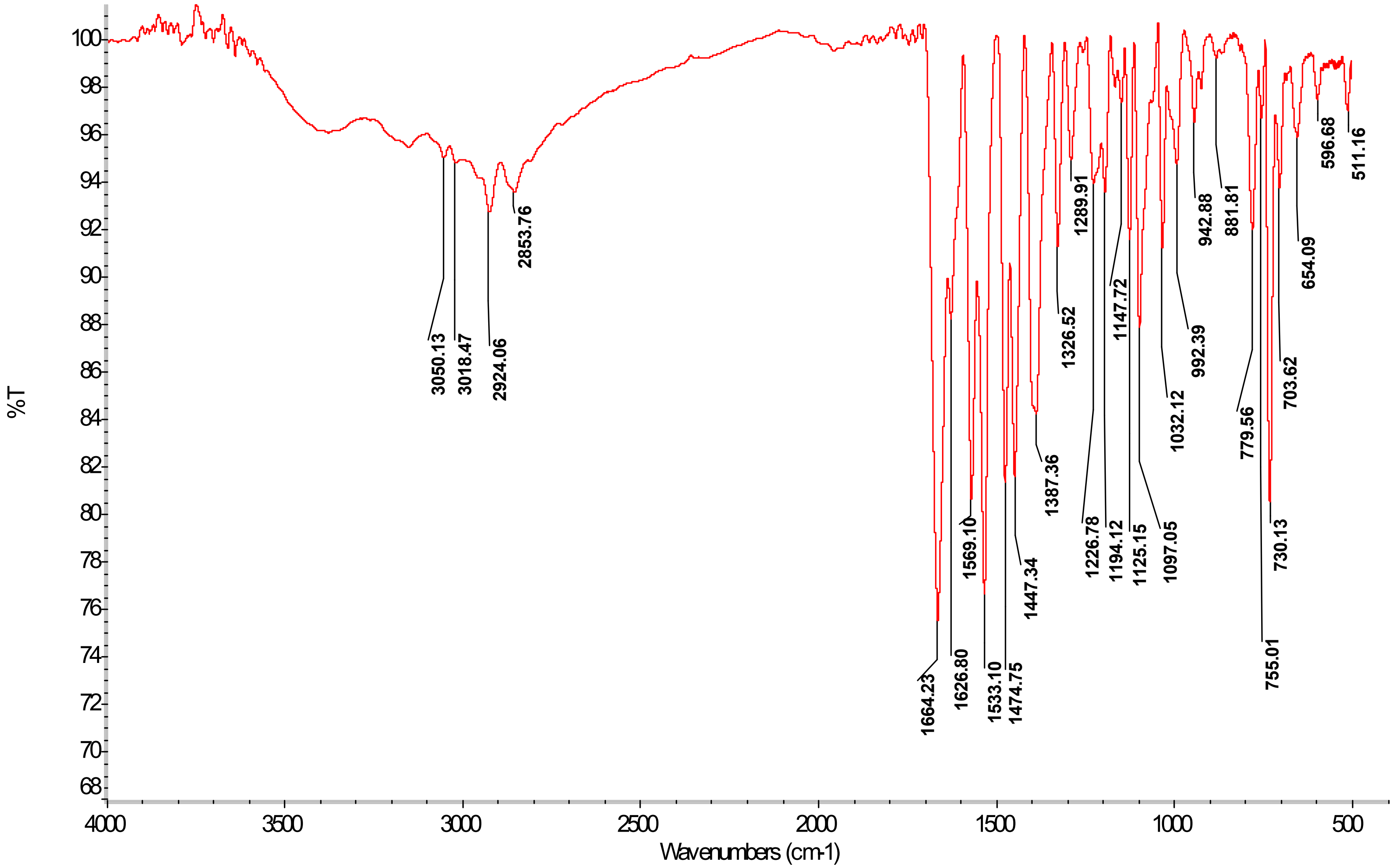

Figure S32. FT-IR spectrum (KBr) of **3a** crystals.

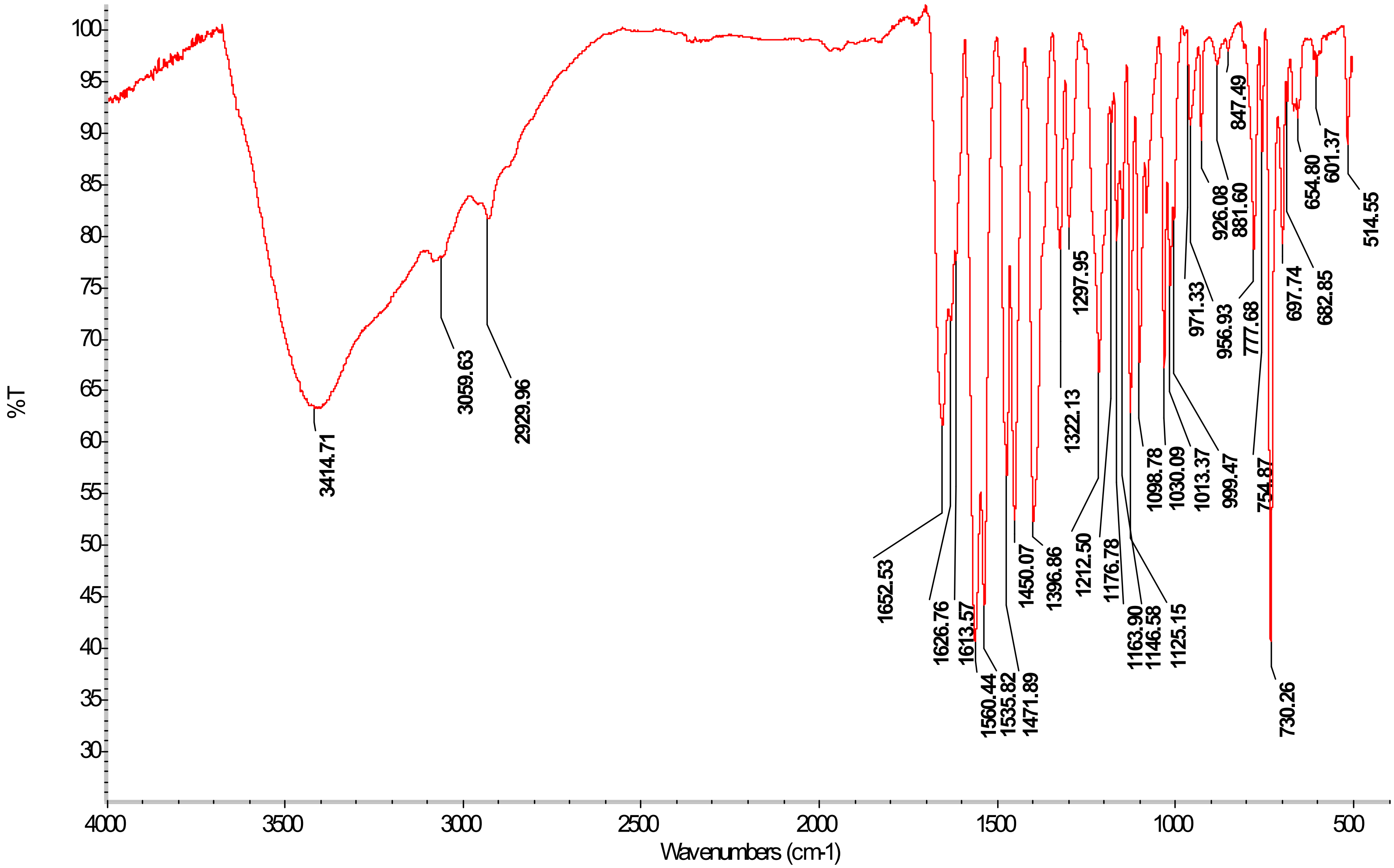

Figure S33. FT-IR spectrum (KBr) of **3a**·MeOH after column chromatography.

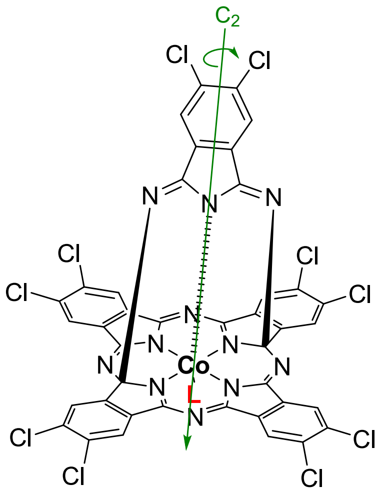

	^{1}H-NMR				
δ	7.61	8.01	8.07	8.11	8.52
	(s, 2H)	(s, 2H)	(s, 2H)	(s, 2H)	(s, 6H)

The multiplicity refers to the virtual appearance of separately groups of ^{1}H NMR resonances.

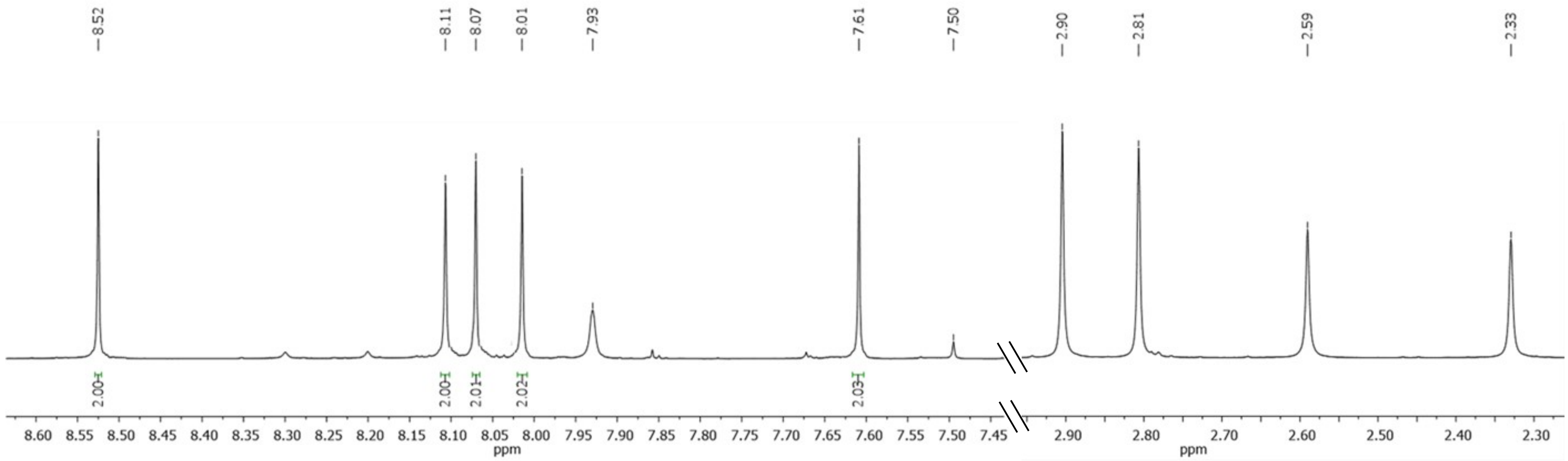

Figure S34. ^{1}H NMR spectra of **3b** in CD_2Cl_2. 2.81, 2.90 and 7.93 ppm are the ^{1}H NMR signals of DMF (crystallization solvent) in CD_2Cl_2. While ^{1}H NMR signals at 2.33, 2.59 and 7.50 ppm are for coordinating DMF.

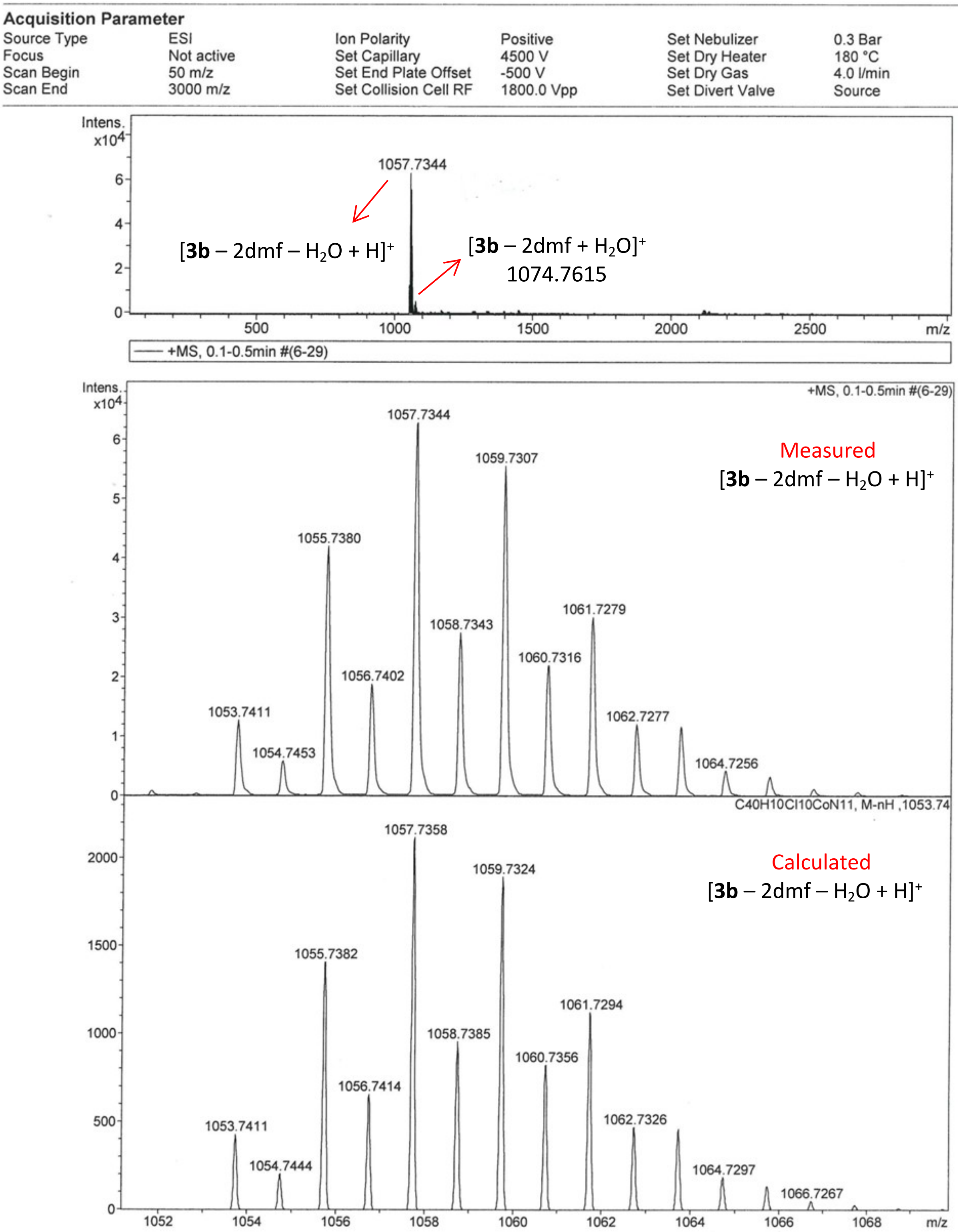

Acquisition Parameter

Source Type	ESI	Ion Polarity	Positive	Set Nebulizer	0.3 Bar
Focus	Not active	Set Capillary	4500 V	Set Dry Heater	180 °C
Scan Begin	50 m/z	Set End Plate Offset	-500 V	Set Dry Gas	4.0 l/min
Scan End	3000 m/z	Set Collision Cell RF	1800.0 Vpp	Set Divert Valve	Source

Figure S35. HRMS (ESI-TOF) of **3b** (measured in CH_2Cl_2/CH_3CN). The spectrum on top is the experimental obtained spectrum. The indicated ion peaks are shown underneath with their calculated isotope distribution patterns, starting from the lowest *m*/z value to the highest.

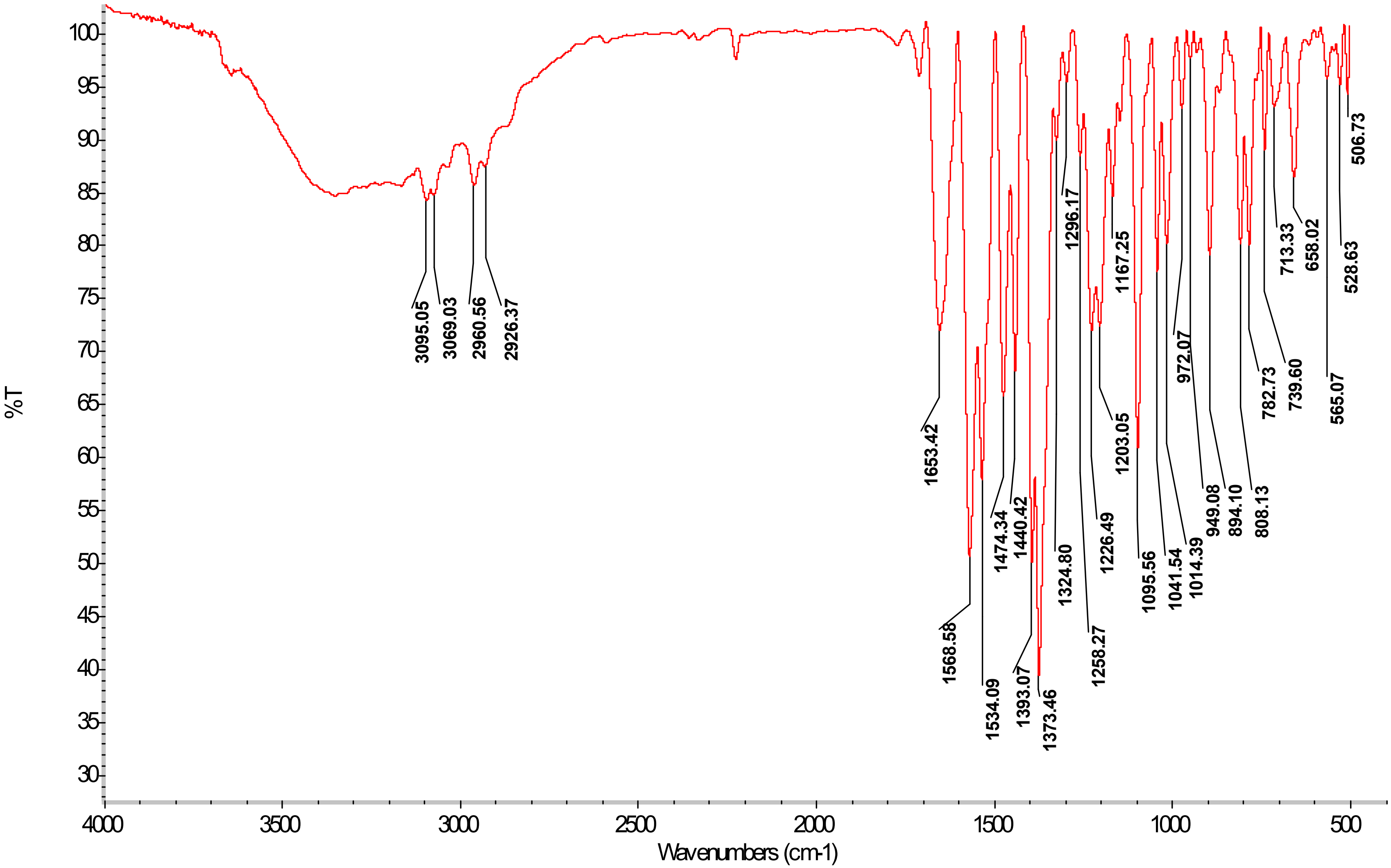

Figure S36. FT-IR spectrum (KBr) of **3b**.

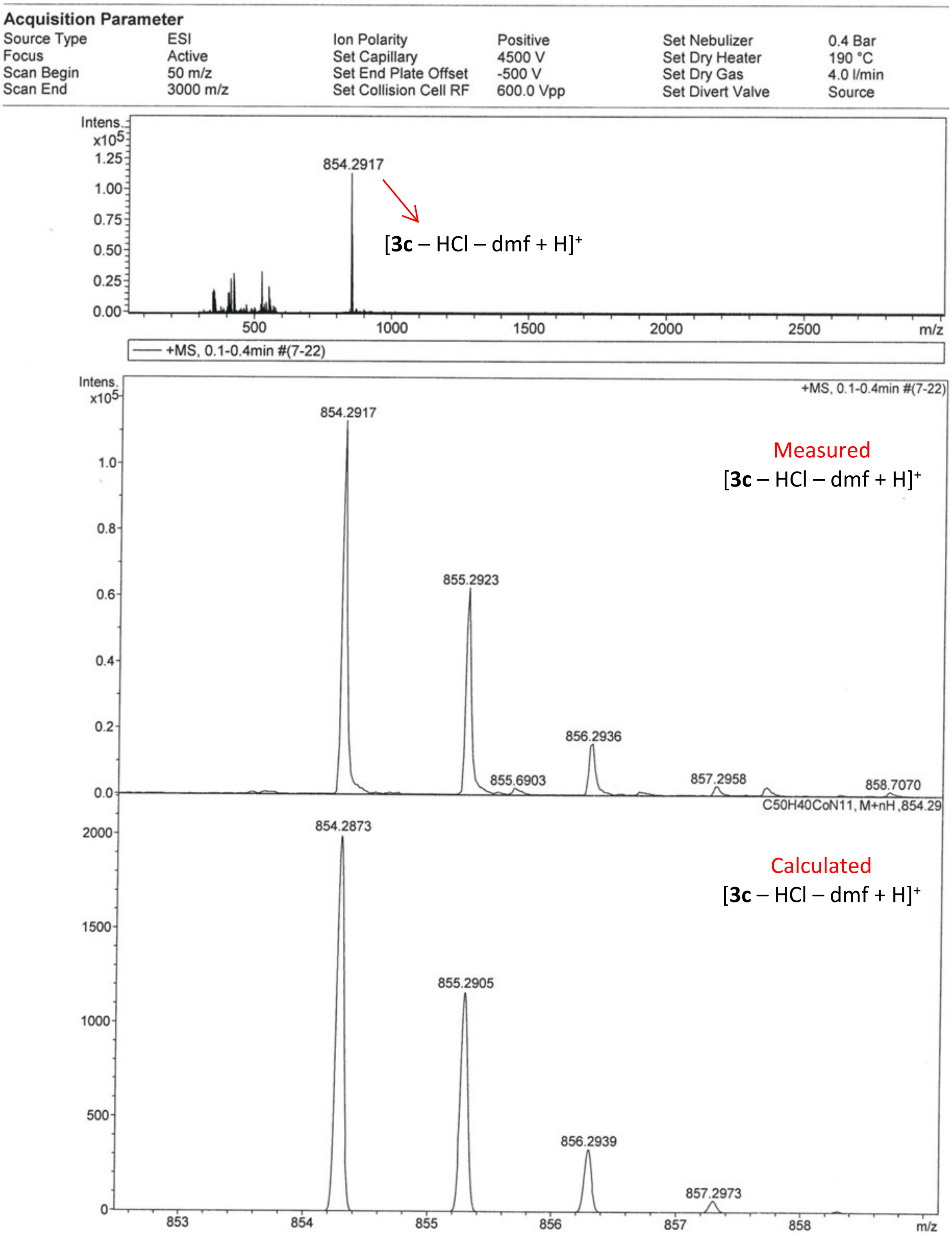

Acquisition Parameter

Source Type	ESI	Ion Polarity	Positive	Set Nebulizer	0.4 Bar
Focus	Active	Set Capillary	4500 V	Set Dry Heater	190 °C
Scan Begin	50 m/z	Set End Plate Offset	-500 V	Set Dry Gas	4.0 l/min
Scan End	3000 m/z	Set Collision Cell RF	600.0 Vpp	Set Divert Valve	Source

Figure S37. HRMS (ESI-TOF) of **3c** (measured in DMF/CH_3CN/HCOOH). The spectrum on top is the experimental obtained spectrum. The indicated ion peaks are shown underneath with their calculated isotope distribution patterns, starting from the lowest *m*/*z* value to the highest. The other cations of low *m*/*z* values is due to contaminants which typically appear in such measurements as described in the literature.[4,5]

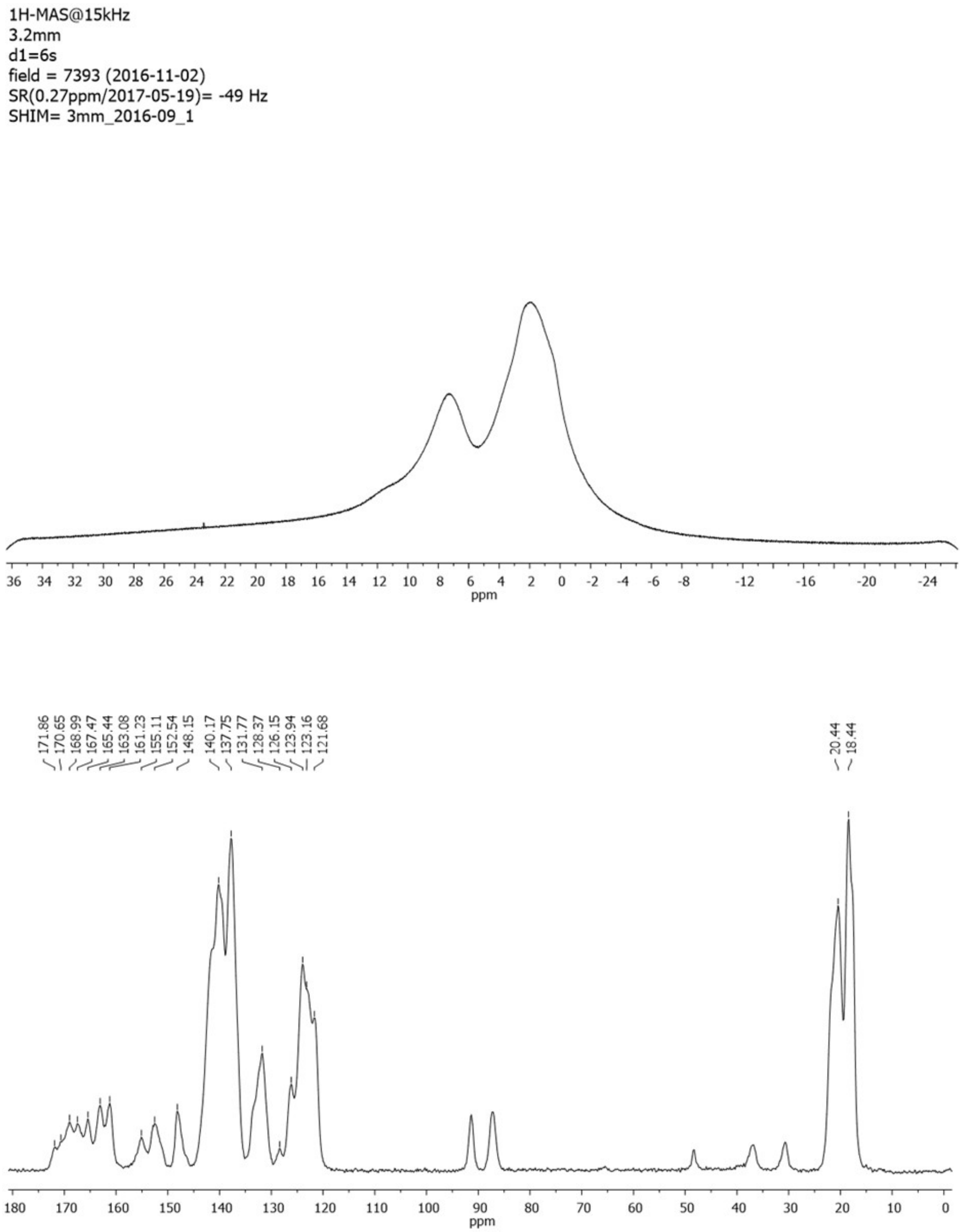
1H-MAS@15kHz
3.2mm
d1=6s
field = 7393 (2016-11-02)
SR(0.27ppm/2017-05-19)= -49 Hz
SHIM= 3mm_2016-09_1

Figure S38. ^{1}H-MAS-CP NMR (above) and ^{13}C{^{1}H}-MAS-CP NMR spectra (below) of **3c**.

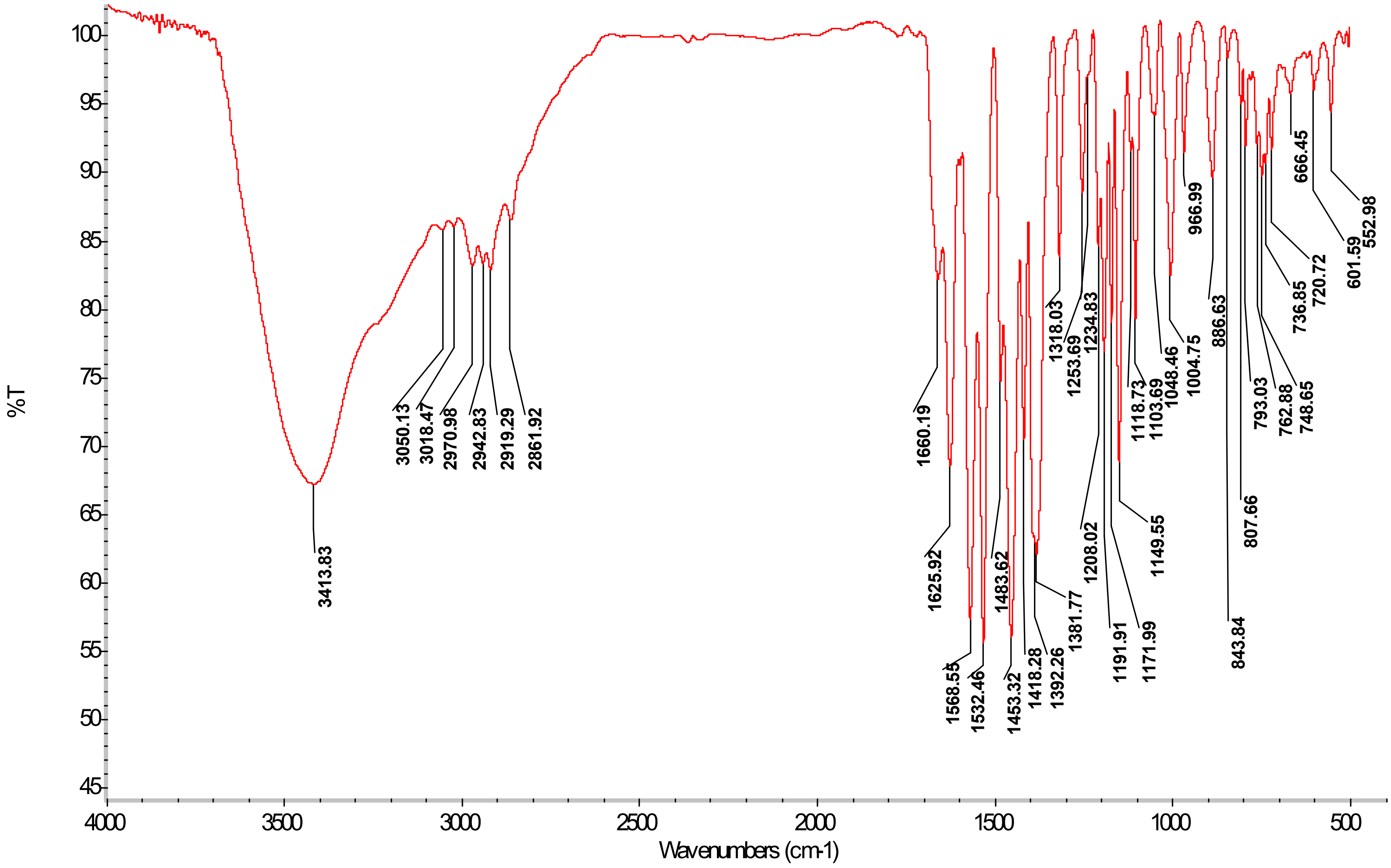

Figure S39. FT-IR spectrum (KBr) of **3c**.

Acquisition Parameter

Source Type	ESI	Ion Polarity	Positive	Set Nebulizer	0.3 Bar
Focus	Not active	Set Capillary	4500 V	Set Dry Heater	180 °C
Scan Begin	50 m/z	Set End Plate Offset	-500 V	Set Dry Gas	4.0 l/min
Scan End	3000 m/z	Set Collision Cell RF	1800.0 Vpp	Set Divert Valve	Source

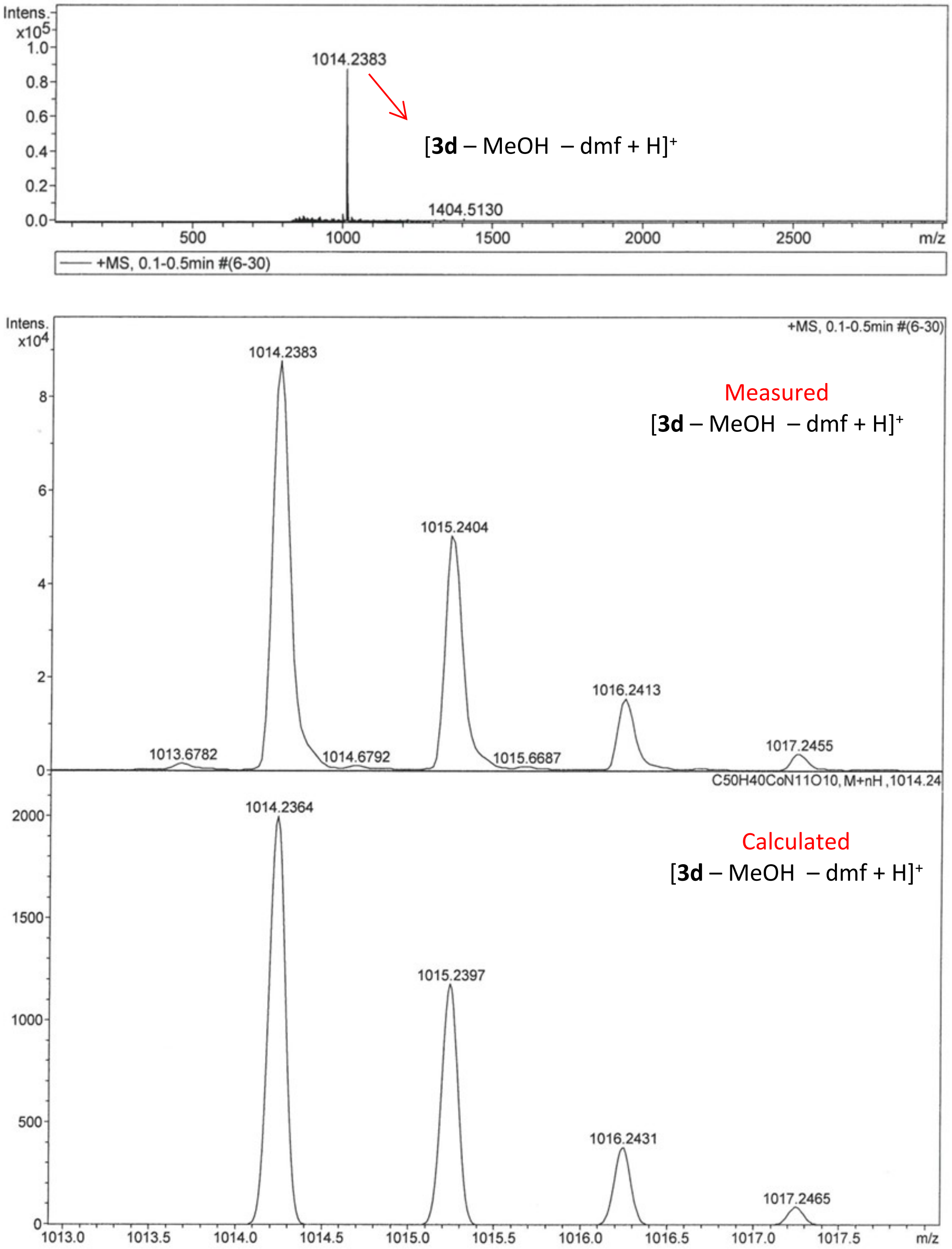

Figure S40. HRMS (ESI-TOF) of **3d** (measured in $CH_2Cl_2/CH_3CN/HCOOH$). The spectrum on top is the experimental obtained spectrum. The indicated ion peaks are shown underneath with their calculated isotope distribution patterns, starting from the assigned *m*/z value to the highest.

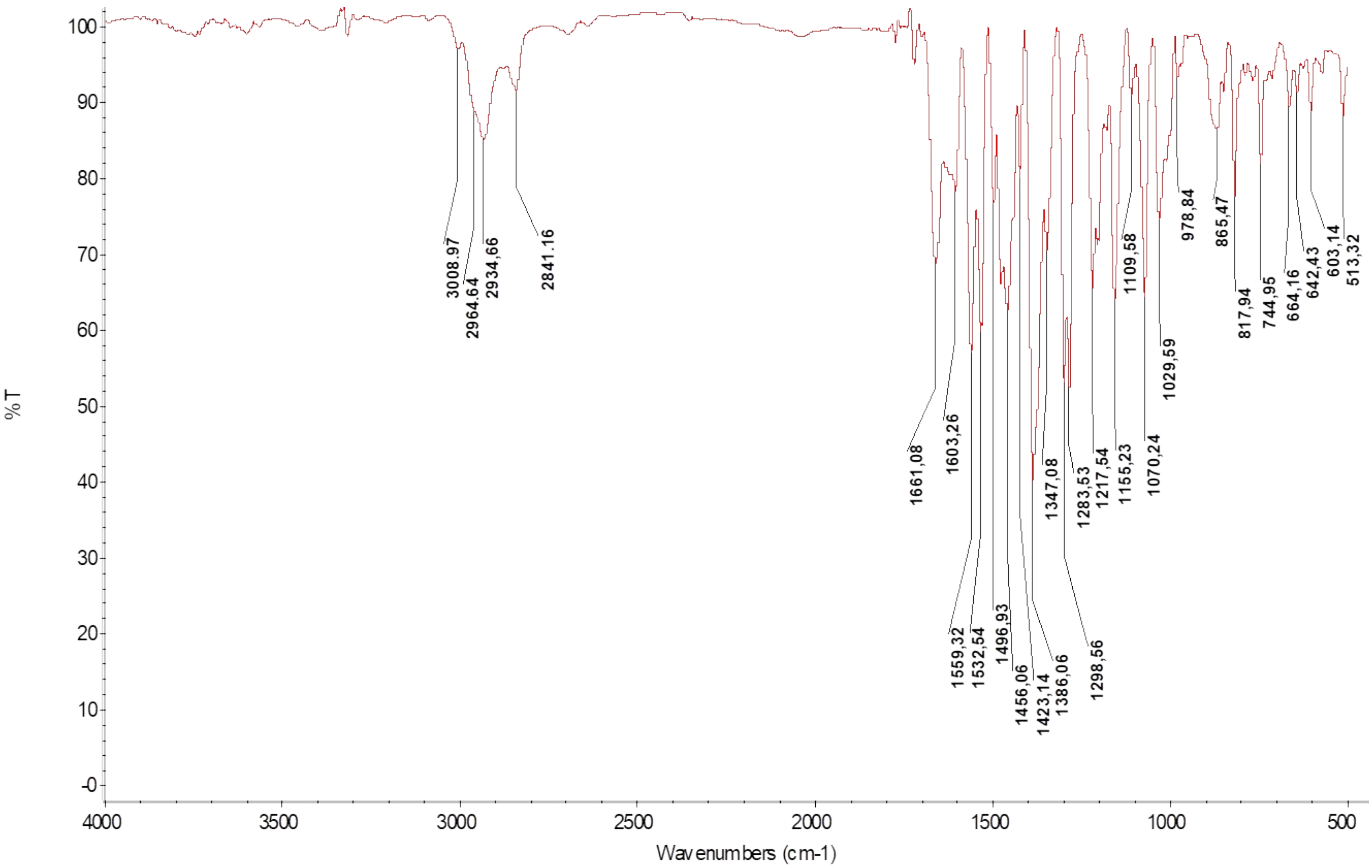

Figure S41 FT-IR spectrum (KBr) of **3d**.

Table S2. Some vibration frequencies (cm^{-1}) in IR spectra of **3a–d**.*

3a	3b	3c	3d	Assignment
3053 3015	3094 3069 3034	3050 3018	3088 3008	sp^2 C-H stretching (aromatic)
2955 2924 2853	2960 2923	2970 2942 2919 2862	2964 2934 2841	Symmetric and asymmetric sp^3 C-H stretching (alkyl)
1664	1652	1660	1661	ν(C=O)
1607	1615	1598	1603	ν(C=C), skeletal vibration
1533	1534	1532	1533	ν(–N=), vibrations of nitrogen bridging atoms
1474	1474	1483	1475	ν(isoindole), vibrations of the pyrrole and benzene residues
1447	1440	1453	1438	The same
1326	1320	1318	1346	ν(pyrrole)
1289	1299	1283	1283	In-plane bending vibrations of $C_{arom.}$-H
779	782	777	786	C-H out-of-plane bending
755	761	748	745	C-H out-of-plane deformation (in Pc skeleton)
730	739	736	726	C-H out-of-plane bending

4.2 Thermogravimetric analysis (TGA) measurements of 3a–d

The thermal stability of the **3a–d** were investigated by using a Mettler Toledo TGA/DSC 11600 system with a MX1 balance. Before collecting the data, the starting materials were dried under vacuum to remove the solvents residues. The heating scan was from 40-800 ^{o}C under Argon (Ar), the heating rates were 10 K.

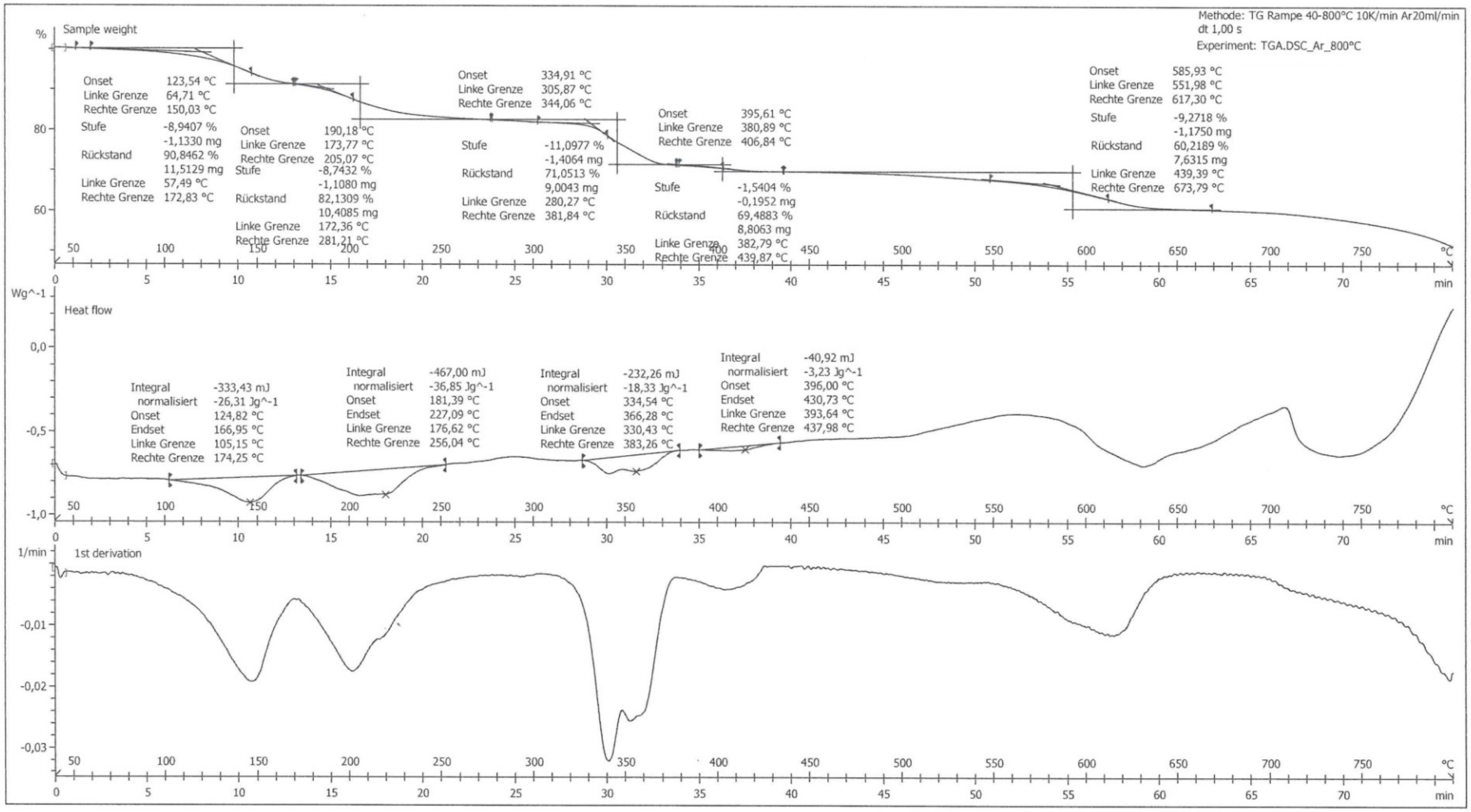

Figure S42. TGA (top), DSC (middle) and TGA´ (below) traces of **3a**.

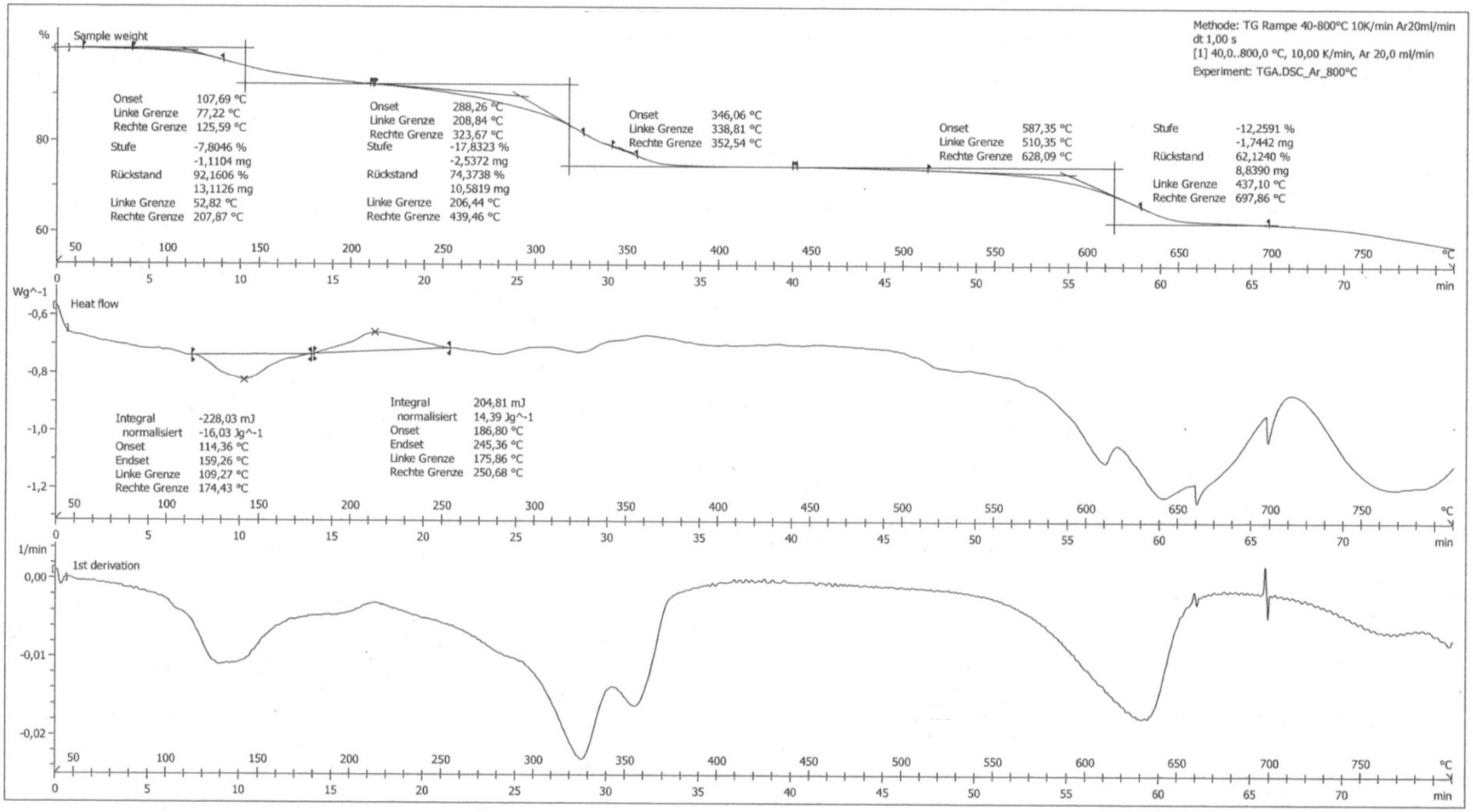

Figure S43. TGA (top), DSC (middle) and TGA´ (below) traces of **3a**·MeOH.

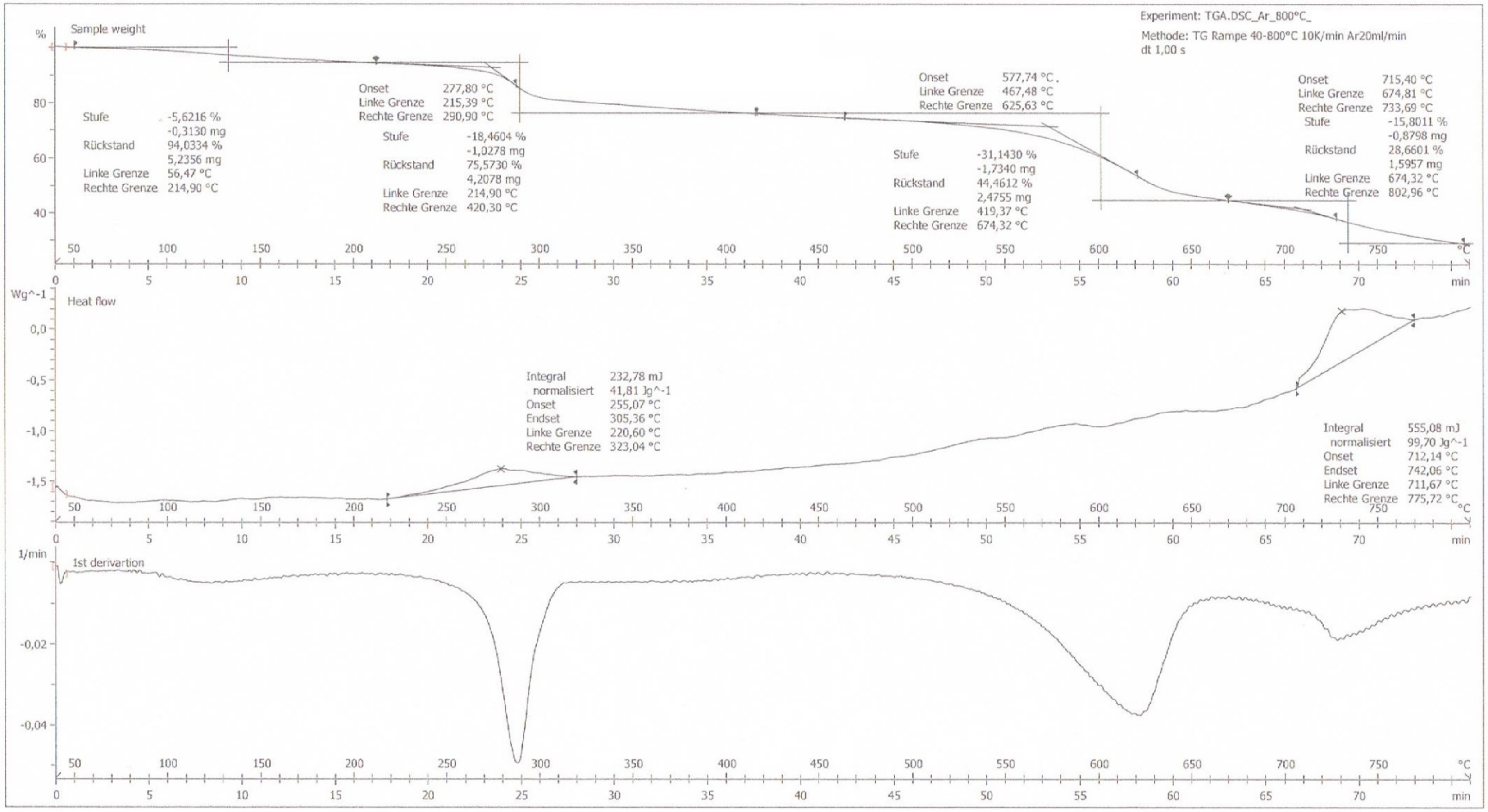

Figure S44. TGA (top), DSC (middle) and TGA´ (below) traces of **3b**.

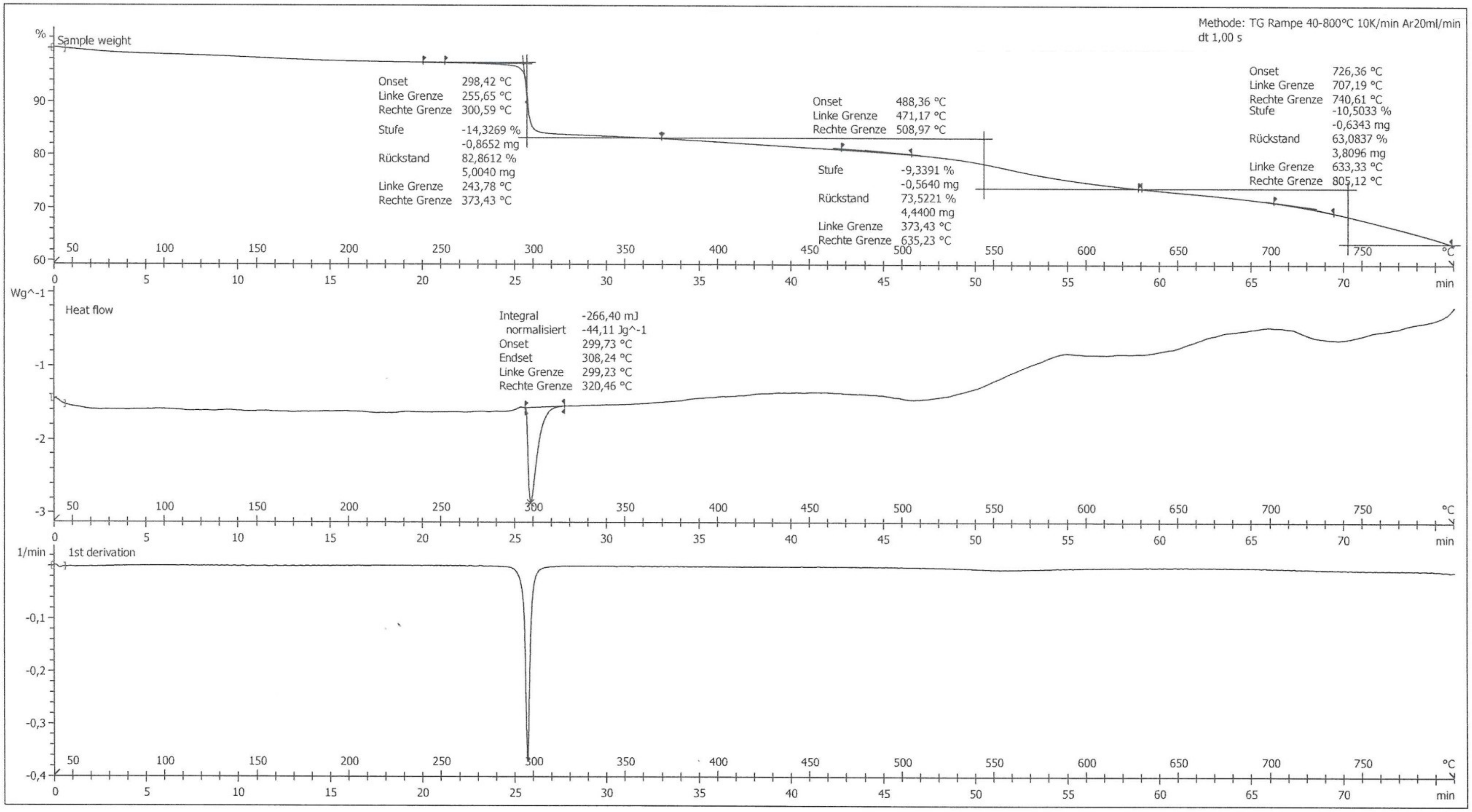

Figure S45. TGA (top), DSC (middle) and TGA´ (below) traces of **3c**.

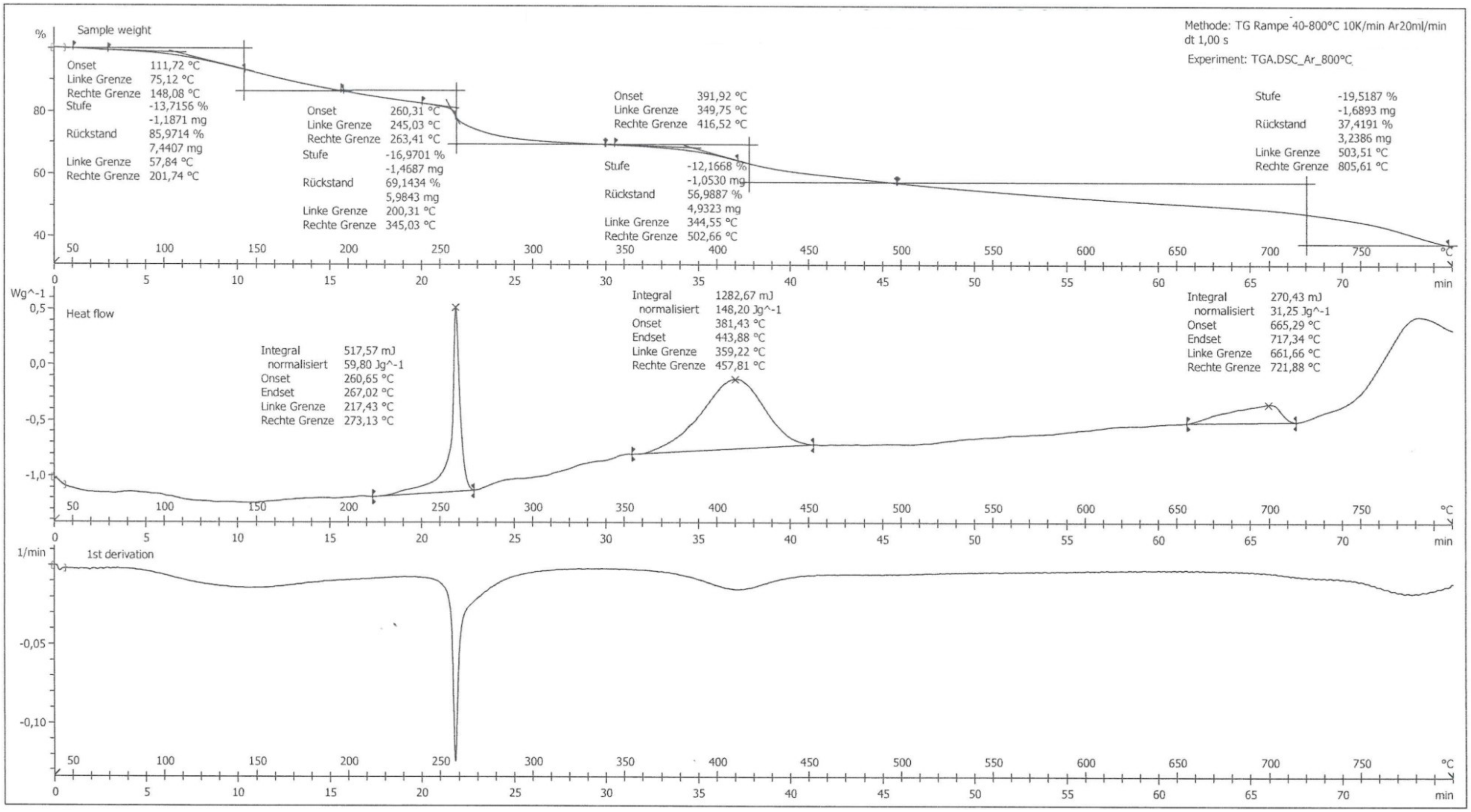

Figure S46. TGA (top), DSC (middle) and TGA´ (below) traces of **3d**.

Table S3. Thermal Stabilities of **3a–d** complexes.

Compound	Temperature range (onset temp.) °C	Assignments
3a	65-150 (123) 174-205 (190)	Loss of packing and coordinating dmf and HCl molecules
	306-407 (335, 396)	Loss of helm group ($C_8H_4N_3$)
	552-617 (586)	Decomposition of formed **CoPc**
3b	57-215 (unidentified)	Loss of packing and coordinating dmf molecule
	215-291 (278)	Loss of helm group ($C_8H_2Cl_2N_3$)
	468-626 (578)	Decomposition of formed **CoPcCl$_8$**
	675-734 (715)	Decomposition of formed **CoPcCl$_8$**
3c	256-301 (298)	Loss of helm group ($C_{10}H_8N_3$)
	471-509 (488)	Decomposition of formed **CoPcMe$_8$**
	707-741 (726)	Decomposition of formed **CoPcMe$_8$**
3d	75-148 (112)	Loss of dmf molecule and MeOH molecule
	245-263 (260)	Loss of helm group ($C_{10}H_8N_3O_2$)
	350-417 (392)	Decomposition of formed **CoPcOMe$_8$**
	504-806 (unidentified)	Decomposition of formed **CoPcOMe$_8$**

4.3 UV/Vis absorption spectra of 3a, 3b and 3d

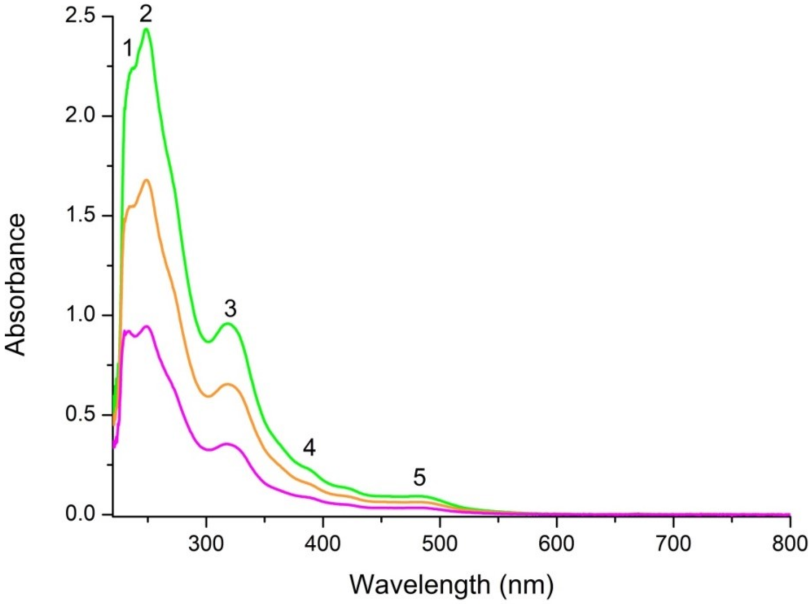

Figure S47. Concentration dependant UV/Vis spectrum of **3a** measured in CH_2Cl_2, recorded at room temperature.

Table S4. UV/Vis data of **3a** measured in CH_2Cl_2.

	Absorption λ_{max} [nm] log (ε [$M^{-1}cm^{-1}$])				
	1	2	3	4	5
C1 = 2.2665.10^{-5}	234.5 (4.99)	248.5 (5.03)	318.5 (4.56)	388 (3.91)	472 (3.54)
C2 = 1.6999.10^{-5}	234.5 (4.96)	248.5 (5.00)	318.5 (4.54)	388 (3.89)	472 (3.53)
C3 = 1.1333.10^{-5}	234.5 (4.91)	248.5 (5.00)	318.5 (4.54)	388 (3.89)	472 (3.53)

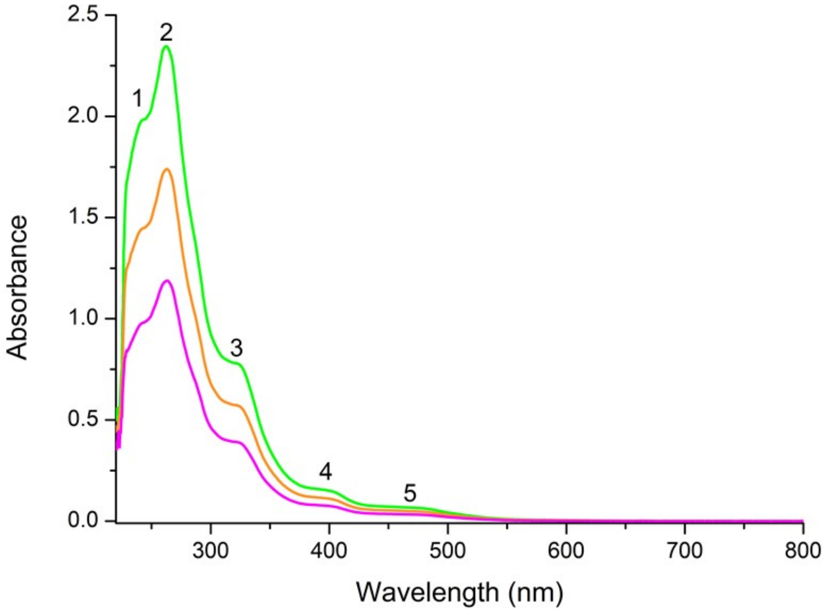

Figure S48. concentration dependent UV/Vis spectrum of **3b** measured in CH_2Cl_2, recorded at room temperature.

Table S5. UV/Vis data of **3b** measured in CH_2Cl_2.

	Absorption λ_{max} [nm] log (ε [$M^{-1}cm^{-1}$])				
	1	2	3	4	5
C1 = $2.2102.10^{-5}$	243 (4.95)	262 (5.03)	318 (4.55)	398 (3.84)	475 (3.47)
C2 = $1.6576.10^{-5}$	243 (4.94)	262 (5.02)	318 (4.54)	398 (3.83)	475 (3.46)
C3 = $1.1051.10^{-5}$	243 (4.95)	262 (5.03)	318 (4.55)	398 (3.84)	475 (3.46)

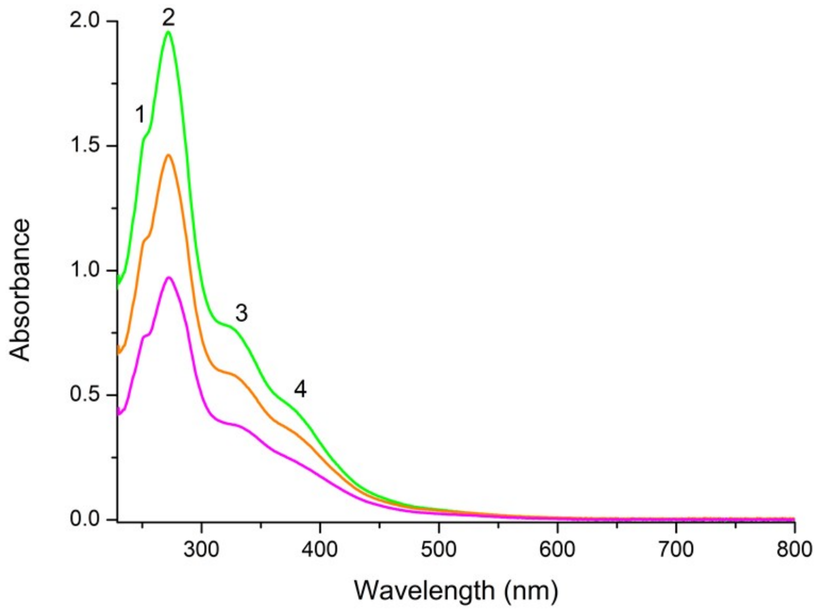

Figure S49. concentration dependant UV/Vis spectrum of **3d** measured in CH_2Cl_2, recorded at room temperature.

Table S6. UV/Vis data of **3d** measured in CH_2Cl_2.

	Absorption λ_{max} [nm] log (ε [$M^{-1}cm^{-1}$])			
	1	2	3	4
C1 = $2.8563.10^{-5}$	251 (4.73)	272 (4.84)	323 (4.43)	384 (4.16)
C2 = $2.1422.10^{-5}$	251 (4.72)	272 (4.83)	323 (4.43)	384 (4.18)
C3 = $1.4282.10^{-5}$	251 (4.72)	272 (4.83)	323 (4.43)	384 (4.19)

5. Heating experiment

The heating experiment of **3a** and **3b** was carried out in a “CARBOLITE Laboratory Horizontal Tube Furnace - MAX Temp 1200 ^{o}C” under an argon atmosphere (Figure S46).

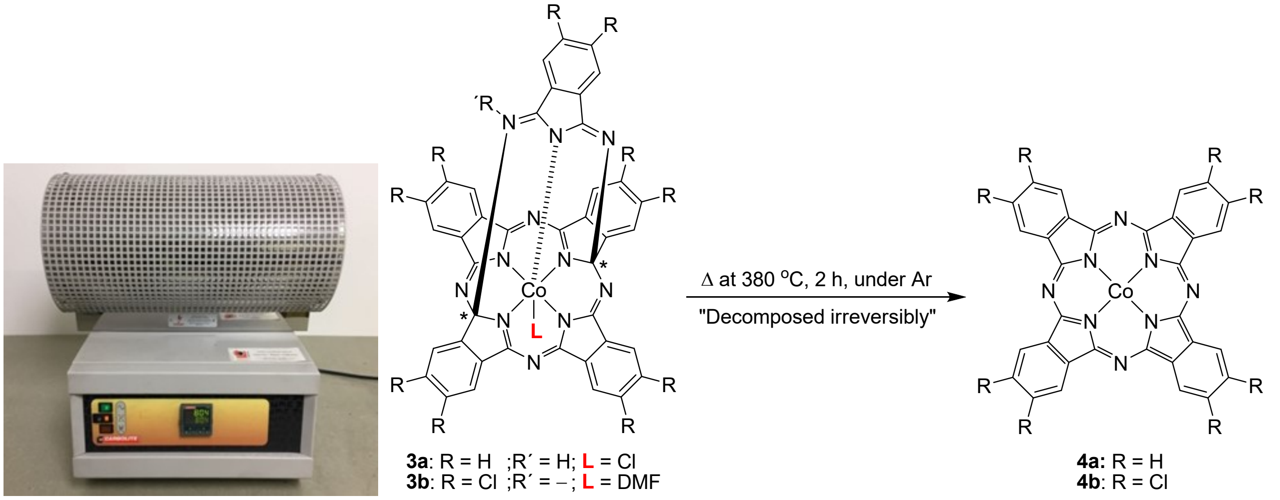

3a: R = H ;R´ = H; **L** = Cl
3b: R = Cl ;R´ = –; **L** = DMF

4a: R = H
4b: R = Cl

Figure S50. Left: “CARBOLITE Laboratory Horizontal Tube Furnace - MAX Temp 1200 ^{o}C”. Right: Formal equation of the conversion of **3a,b** to **4a,b** by heating.

5.1 Detailed description

An amount of each 200 mg of **3a** or **3b** were transferred into alumina ceramic crucible and afterwards the heating was started from ambient temperature to 380 ^{o}C (10 K/min), then the furnace was maintained at that temperature for 2 h and subsequently cooled down to ambient temperature. First observation after heating is color change. The residues obtained were identified as cobalt(II)phthalocyanine (**4a**) and 2,3,9,10,16,17,23,24-octachlorocobalt(II)phthalocyanine (**4b**) respectively.

4a: Purple powder; Yield: 138 mg (91%). **FT-IR** (KBr): 3049 (w), 2923 (w), 2854 (w), 2587 (w), 1743 (w), 1608 (w), 1520 (m), 1467 (w), 1424 (m), 1370 (w), 1330 (s),1288 (m), 1199 (w), 1163 (m), 1120 (s), 1090 (s), 999 (w), 945 (w), 911 (w), 865 (w), 822 (w), 774 (w), 755 (w), 726 (s), 665 (w), 643 (w), 570 (w), 516 (w) cm^{-1}.

4b: Blue powder; Yield: 142 mg (94%). **FT-IR** (KBr): 3087 (w), 2924 (w), 1744 (w), 1607 (w), 1523 (m), 1467 (w), 1417 (s), 1389 (m), 1342 (w), 1291 (w), 1200 (w), 1136 (w), 1089 (s), 1074 (s), 1039 (w), 965 (m), 888 (m), 785 (m), 751 (m), 707 (w), 660 (w), 504 (w) cm^{-1}.

5.2 IR spectra of 4a and 4b obtained out of the thermal treatment of 3a and 3b

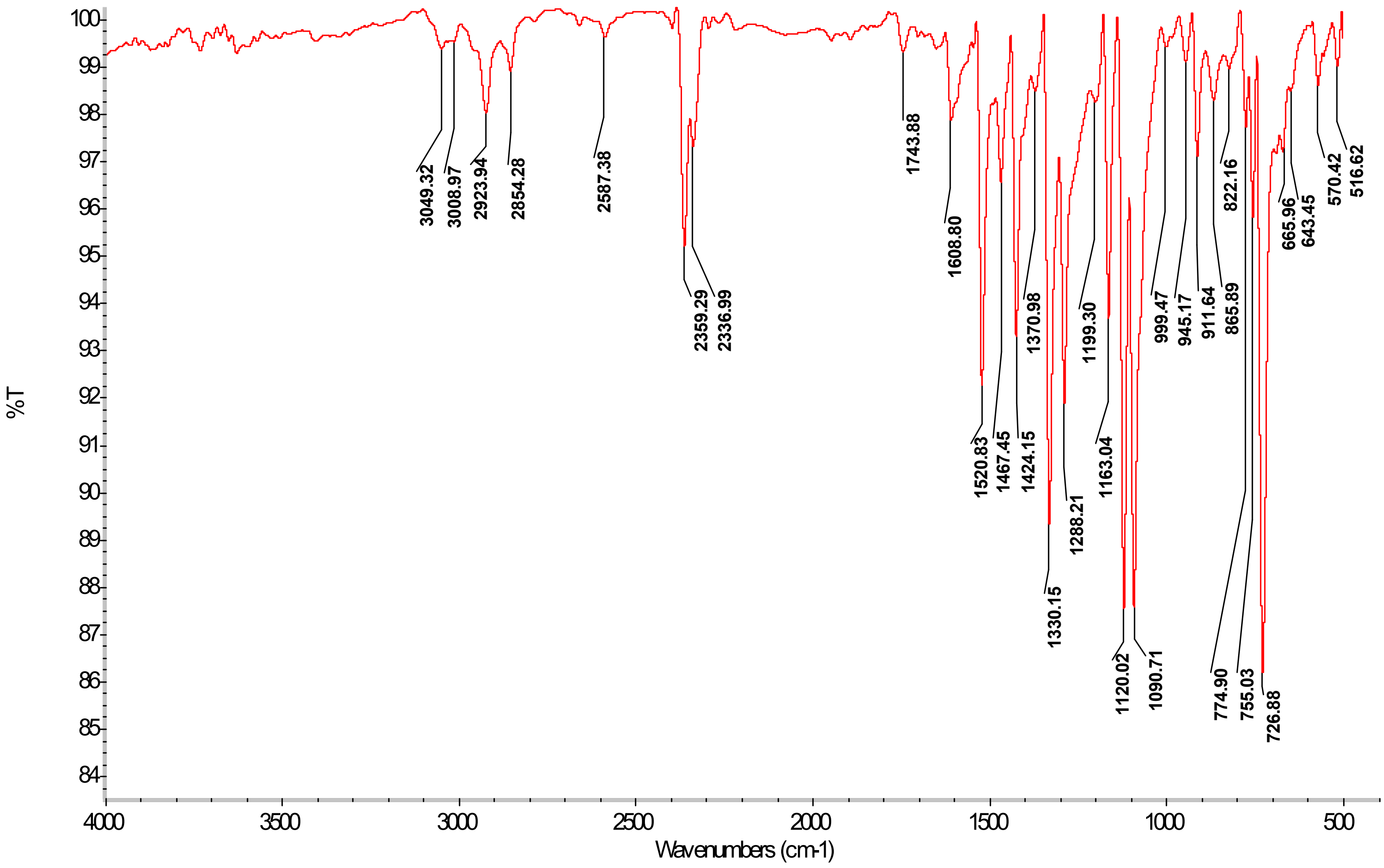

Figure S51. FT-IR spectrum (KBr) of **4a** obtained out of the thermal treatment of **3a**.

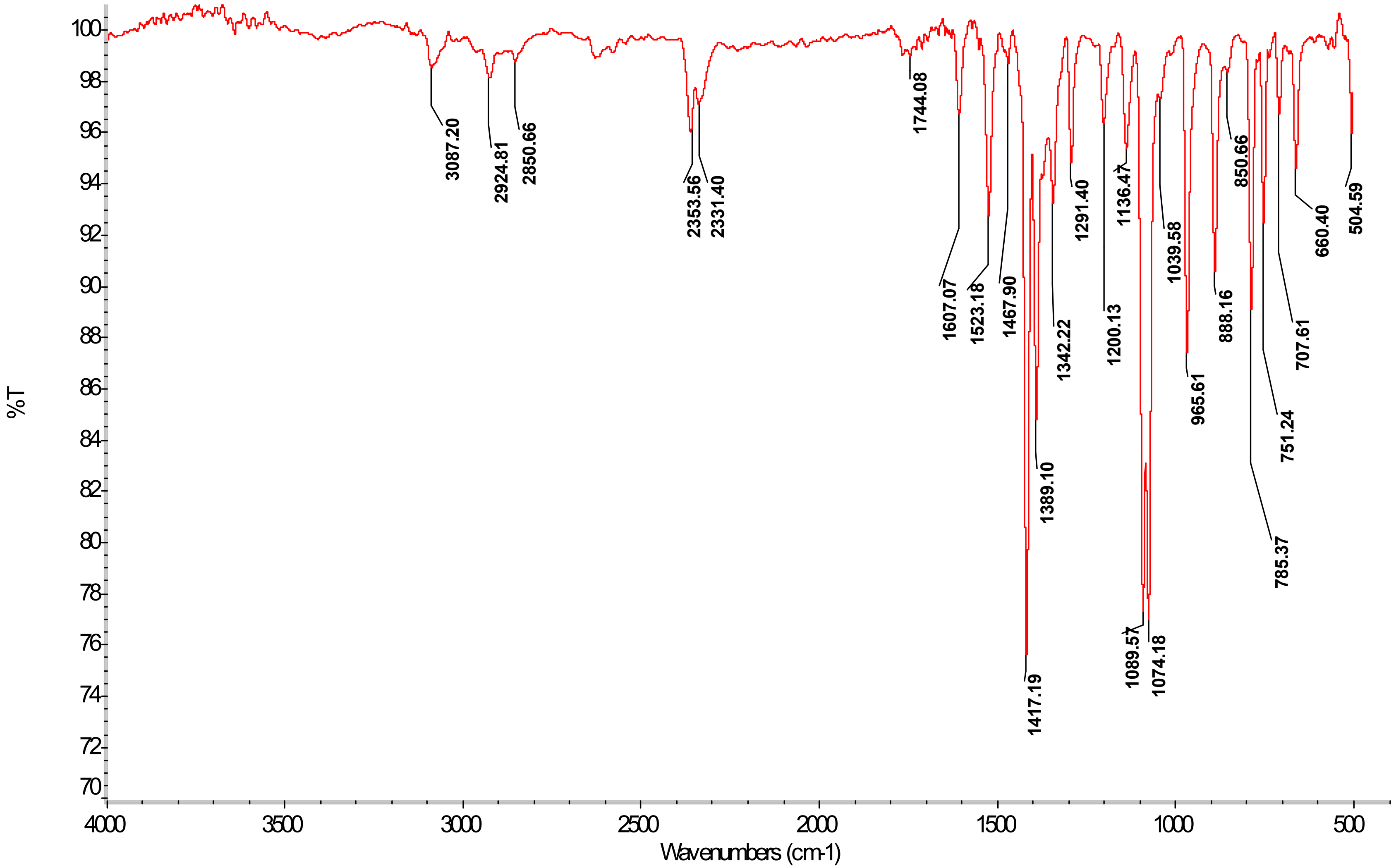

Figure S52. FT-IR spectrum (KBr) of **4b** obtained out of the thermal treatment of **3b**.

5.3 Thermogravimetric analysis (TGA) measurements of 4a and 4b obtained out of the thermal treatment of 3a and 3b

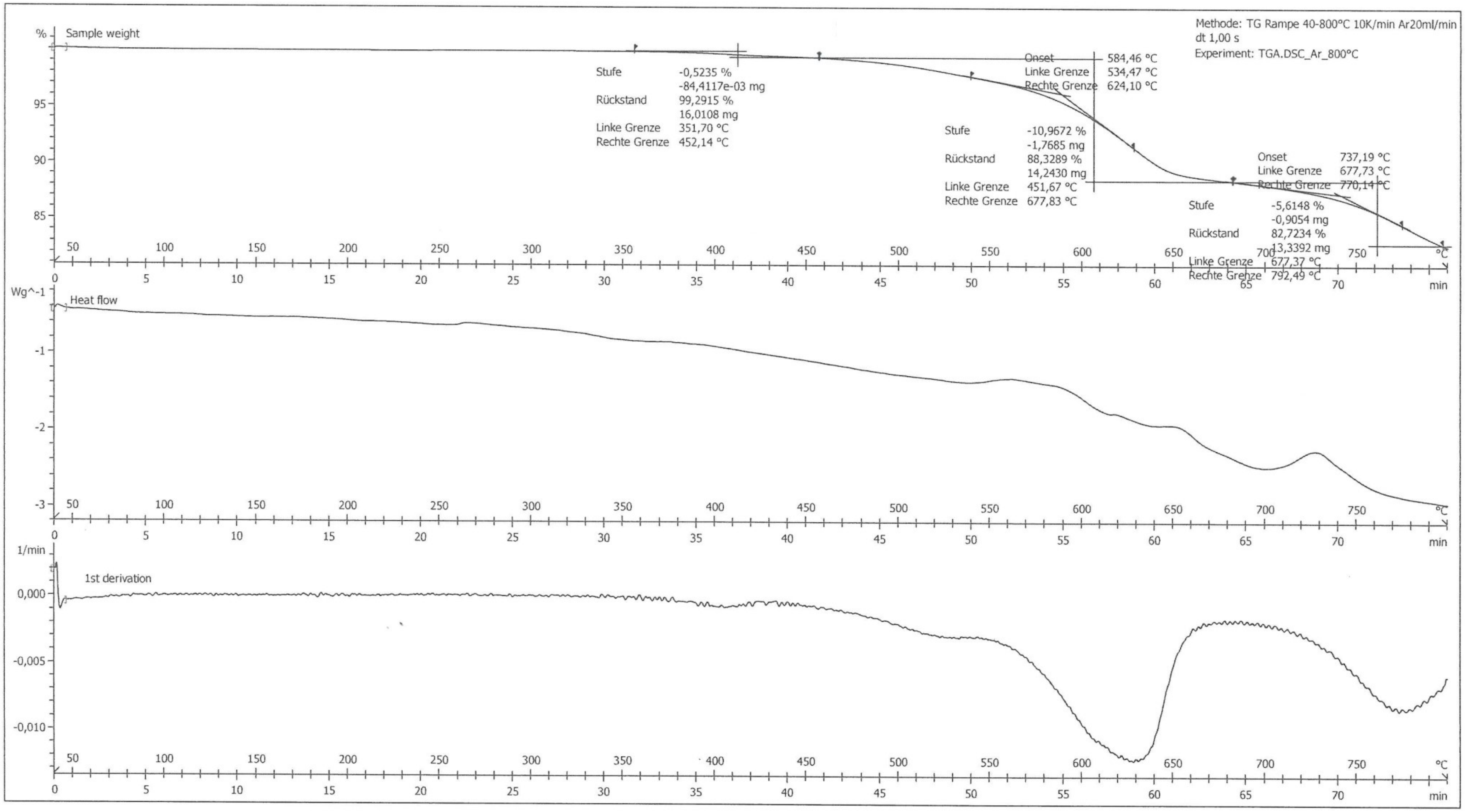

Figure S53. TGA (top), DSC (middle) and TGA´ (below) traces of **4a** obtained out of the thermal treatment of **3a**.

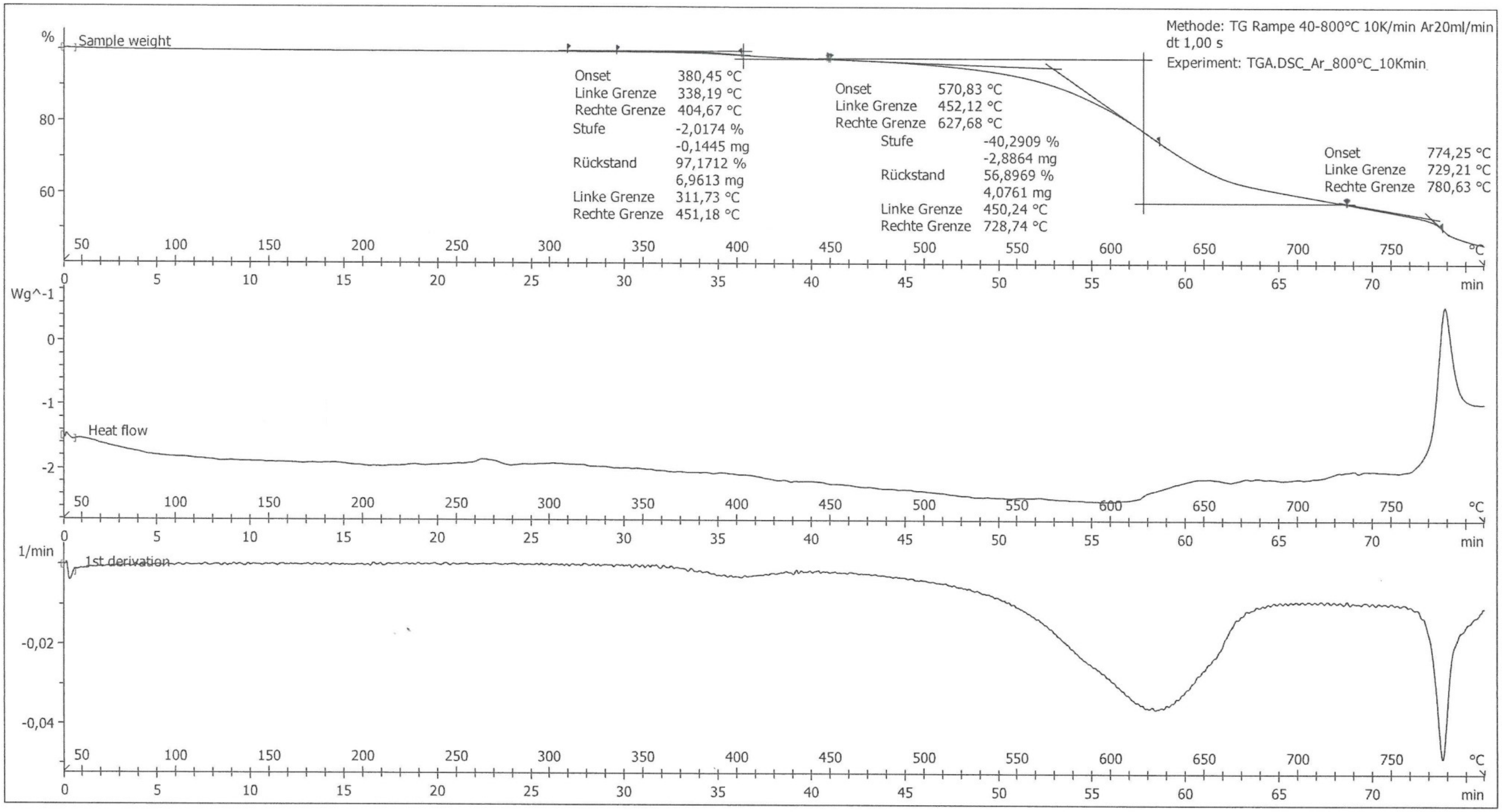

Figure S54. TGA (top), DSC (middle) and TGA´ (below) traces of **4b** obtained out of the thermal treatment of **3b.**

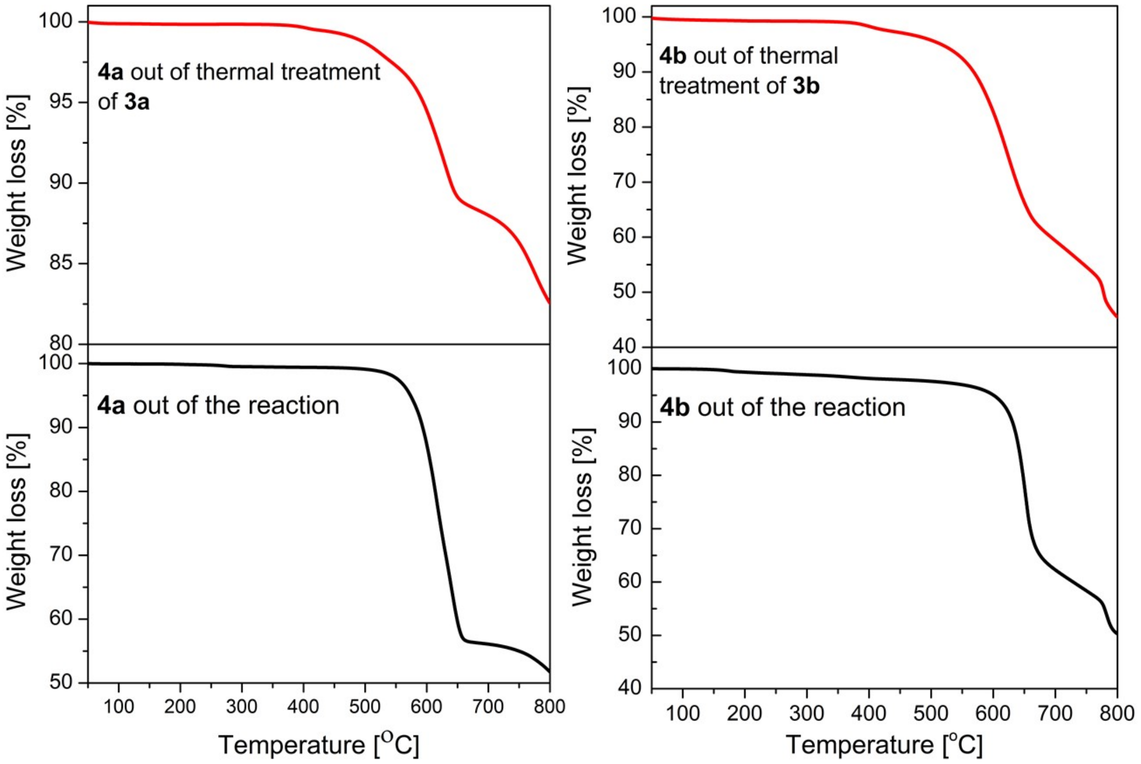

Figure S55. Comparison between; left: TG traces of **4a** obtained out of thermal treatment of **3a** and **4a** obtained out of the reaction, and right: between **4b** obtained out of thermal treatment of **3b** and **4b** obtained out of the reaction, (measured under argon, 40-800 ^oC, heating rate: 10 K/min, Ar gas flow: 20ml/min).

6. Detailed descriptions for the synthesis and characterization of 4a–d out of the reaction

As described above, the Co(II)-containing Phthalocyanins **4a–d** were obtained in course of the reaction used to synthesize the Co(III)-helmet compounds **3a–d**, cf. Scheme S1. A simple DMF treatment of the filter cakes allowed to separate between the two different types of porphyrinoids. It must be noted here that the obtained **4a–d** were further purified once by using the pyridine method which was described earlier by our working group.[7] Next, the results of the IR and UV/vis spectroscopic measurements (**4a–d** and **4c–d**, respectively), the CHN combustion analysis (**4a–d**) and TG analysis (**4a–d**) are shown. These results are summarized in brief at the end of this chapter.

Cobalt(II)phthalocyanine 4a

Purple powder; Yield: 0.9013 g (46%, based on $CoCl_2 \cdot 6H_2O$). **FT-IR** (KBr): 1608, 1589 (w), 1569 (w),1549 (w), 1522 (m), 1468 (w), 1445 (w), 1425 (m), 1332 (s), 1289 (m), 1201 (w), 1167 (m), 1122 (s), 1088 (s), 1069 (w), 10000 (w), 948 (w), 913 (w), 874 (w), 779 (m), 755 (m), 732 (s), 668 (w), 642 (w), 573 (w), 519 (w) cm^{-1}.

Anal. Calc. for $C_{32}H_{16}CoN_8$ (571.46 g mol^{-1}): C, 67.26; H, 2.82; N, 19.61%. **Found:** C, 66.47; H, 2.79; N, 19.60%.

2,3,9,10,16,17,23,24-Octachloro Cobalt(II)phthalocyanine 4b

Blue powder; Yield: 0.8167 g (41%, based on $CoCl_2{\cdot}6H_2O$). **FT-IR** (KBr): 3081 (w), 3015 (w), 2974 (w), 2885 (w), 2834 (w), 1767 (w), 1604 (w), 1525 (m), 1418 (s), 1390 (m), 1369 (w), 1342 (w), 1320 (w), 1293 (w), 1139 (w), 1089 (s), 1074 (s), 1040 (w), 966 (s), 888 (s), 848 (w), 784 (s), 751 (m), 729 (w), 709 (w), 661 (w), 552 (w), 505 (w) cm^{-1}. **Anal. Calc.** for $C_{40}H_8Cl_8CoN_8$ (847.02 g mol^{-1}): C, 45.38; H, 0.95; N, 13.23%. **Found:** C, 44.39; H, 0.94; N, 13.48%.

2,3,9,10,16,17,23,24-Octamethyl Cobalt(II) phthalocyanine 4c

Blue-purple powder; Yield: 1.0267 g (65%, based on $CoCl_2{\cdot}6H_2O$). **FT-IR** (KBr): 3087 (w), 2924 (w), 1744 (w), 1607 (w), 1523 (m), 1467 (w), 1417 (s), 1389 (m), 1342 (w), 1291 (w), 1200 (w), 1136 (w), 1089 (s), 1074 (s), 1039 (w), 965 (m), 888 (m), 785 (m), 751 (m), 707 (w), 660 (w), 504 (w) cm^{-1}. **Anal. Calc.** for $C_{40}H_{32}CoN_8$ (683.67 g mol^{-1}): C, 70.27; H, 4.72; N, 16.39%. **Found:** C, 68.80; H, 4.62; N, 16.45%. **UV/Vis** (H_2SO_4 (conc), 25 °C): λ_{max} (nm): 230, 261, 295, 444, 719, 813.

2,3,9,10,16,17,23,24-Octamethoxy cobalt(II)phthalocyanine 4d

Blue-purple powder; Yield: 0.4992 g (25 %, based on $CoCl_2{\cdot}6H_2O$). **FT-IR** (KBr): 3084 (w), 3003 (w), 2940 (w), 2830 (w), 1774 (w), 1749 (w), 1723 (w), 1603 (m), 1523 (w), 1497 (w), 1481 (s), 1424 (w), 1406 (m), 1363 (m), 1338 (w), 1278 (s), 1227 (w), 1207 (s), 1147 (w), 1104 (s), 1064 (s), 1033 (m), 996 (w), 886 (m), 847 (m), 821 (m), 747 (m), 664 (w), 642 (w), 574 (w), 513 (w) cm^{-1}. **Anal. Calc.** for $C_{40}H_{32}CoN_8O_8$ (811.66 g mol^{-1}): C, 59.19; H, 3.97; N, 13.81%. **Found:** C, 58.87; H, 4.04; N, 11.50%. **UV/Vis** (H_2SO_4 (conc), 25 °C): λ_{max} (nm): 213.5. 248.5, 262, 306, 438, 797.5.

6.1 IR spectra of 4a–d out of the reaction

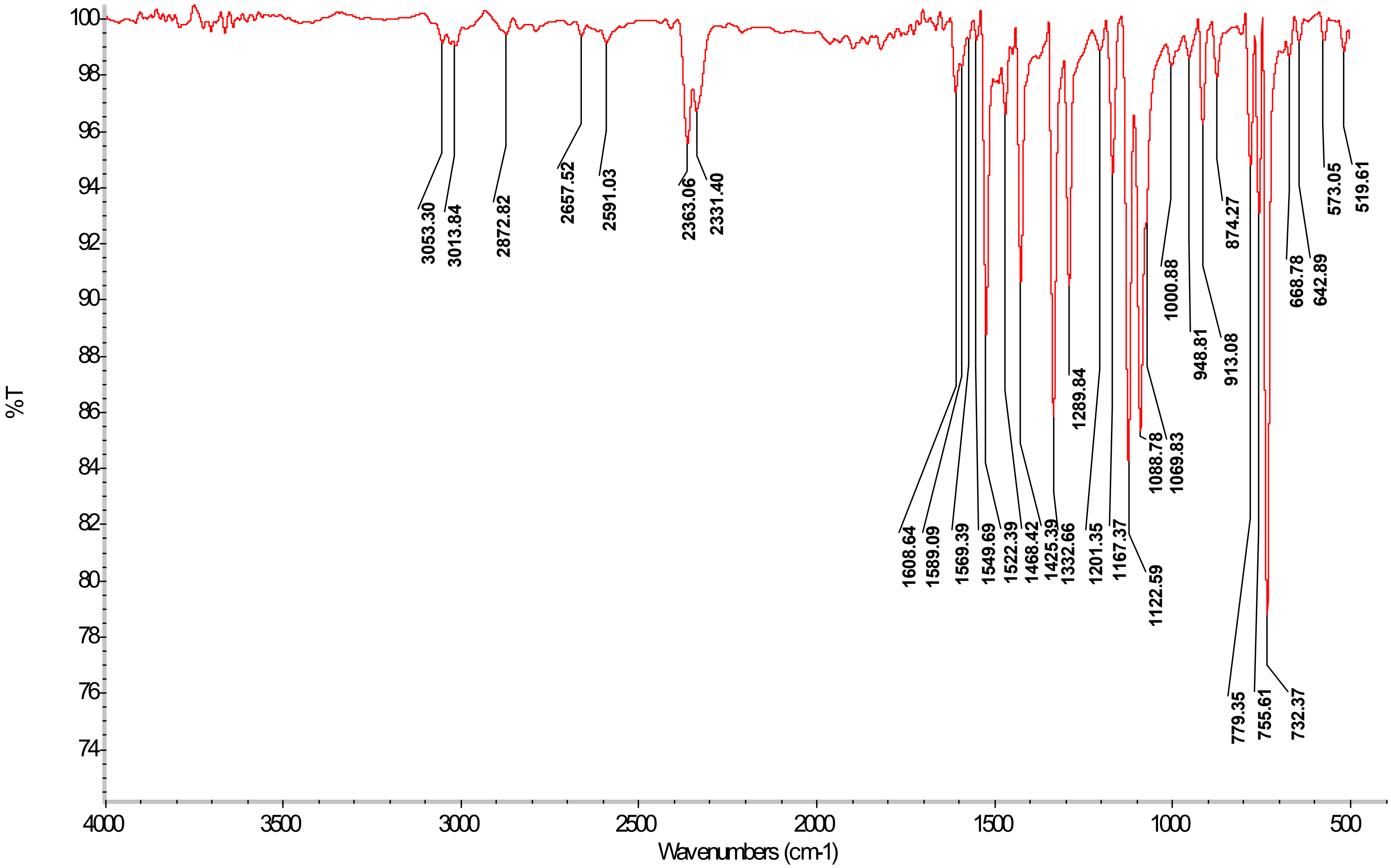

Figure S56. FT-IR spectrum (KBr) of **4a**.

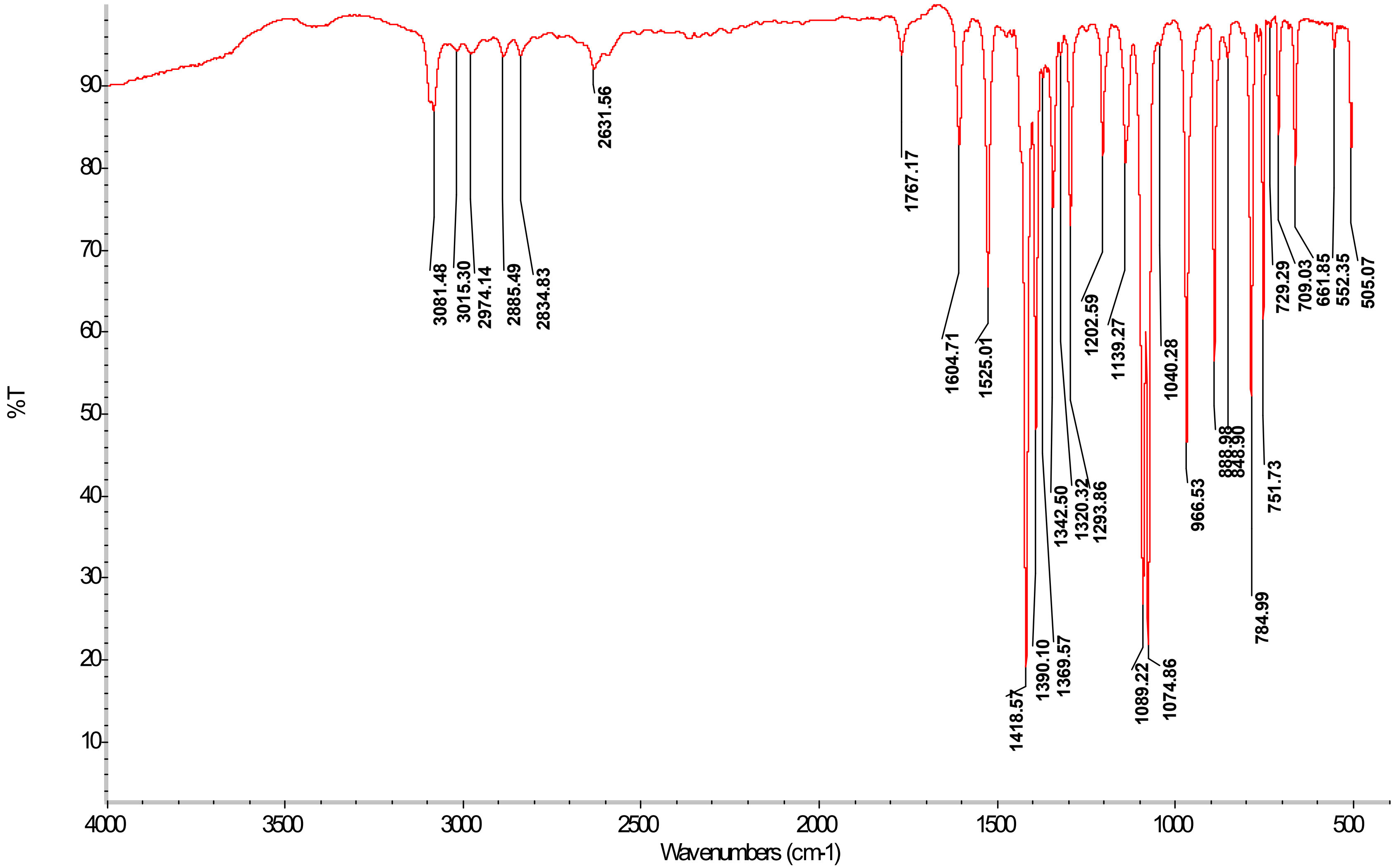

Figure S57. FT-IR spectrum (KBr) of **4b**.

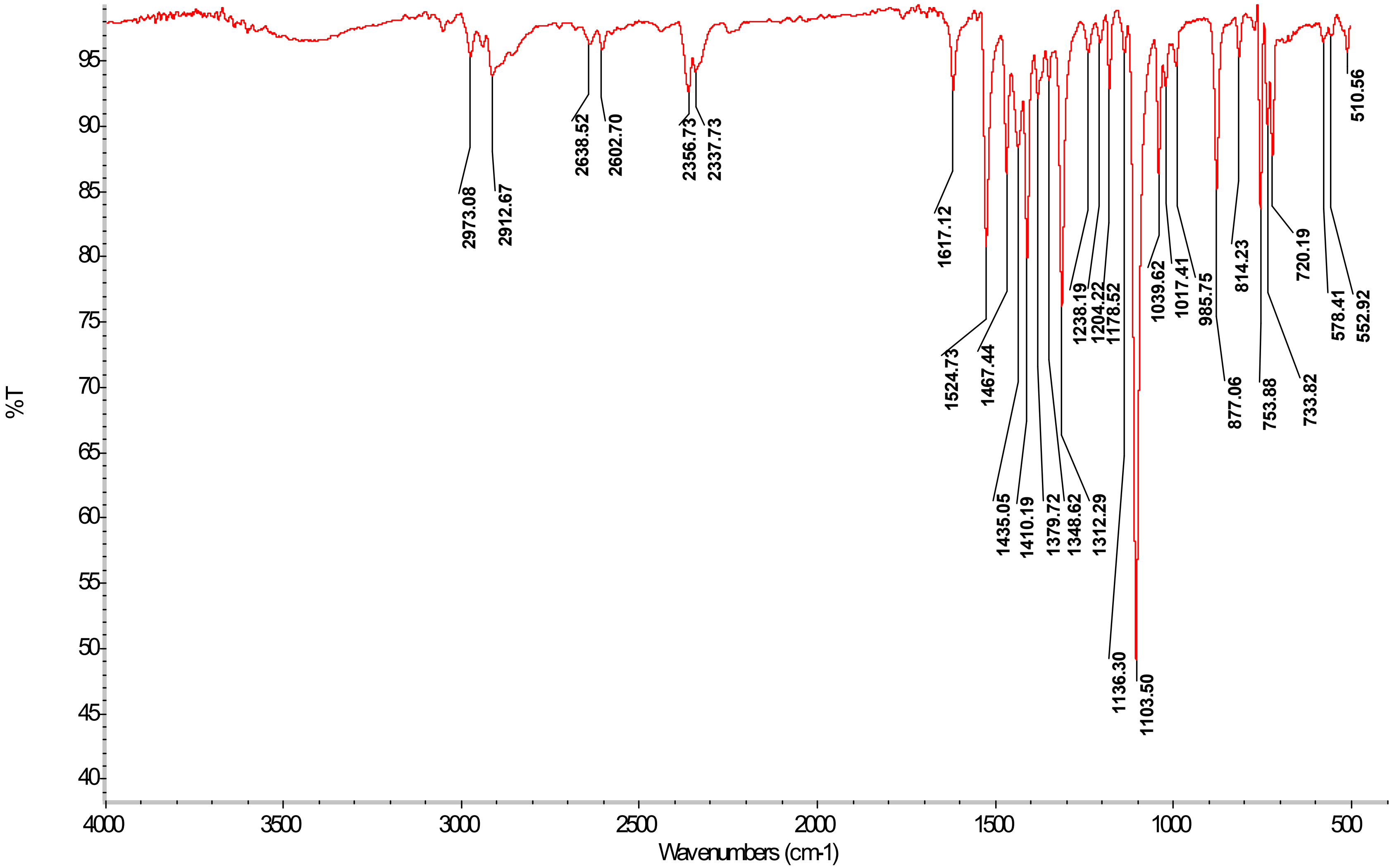

Figure S58. FT-IR spectrum (KBr) of **4c**.

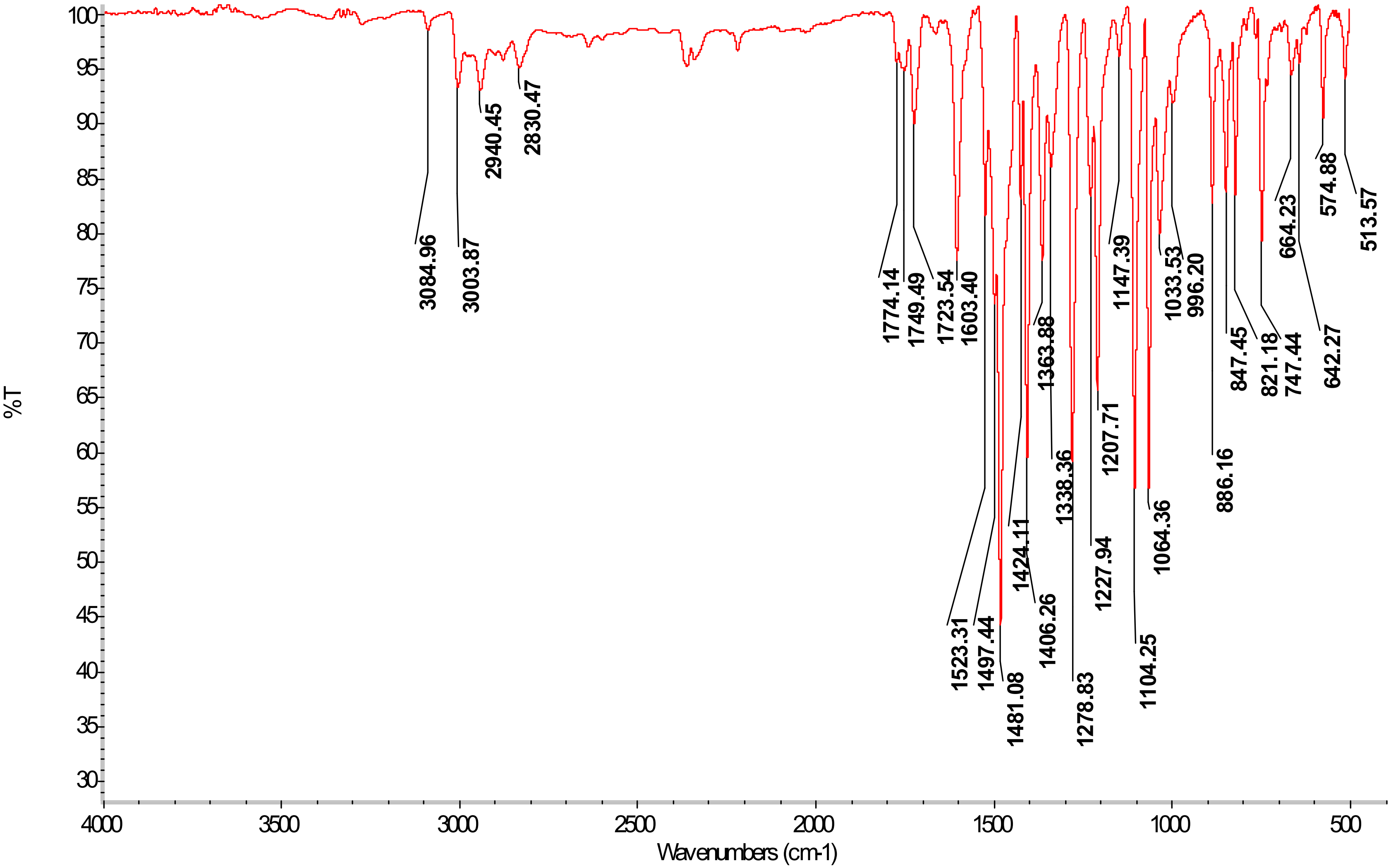

Figure S59. FT-IR spectrum (KBr) of **4d**.

6.2 Thermogravimetric analysis (TGA) measurements of 4a–d out of the reaction

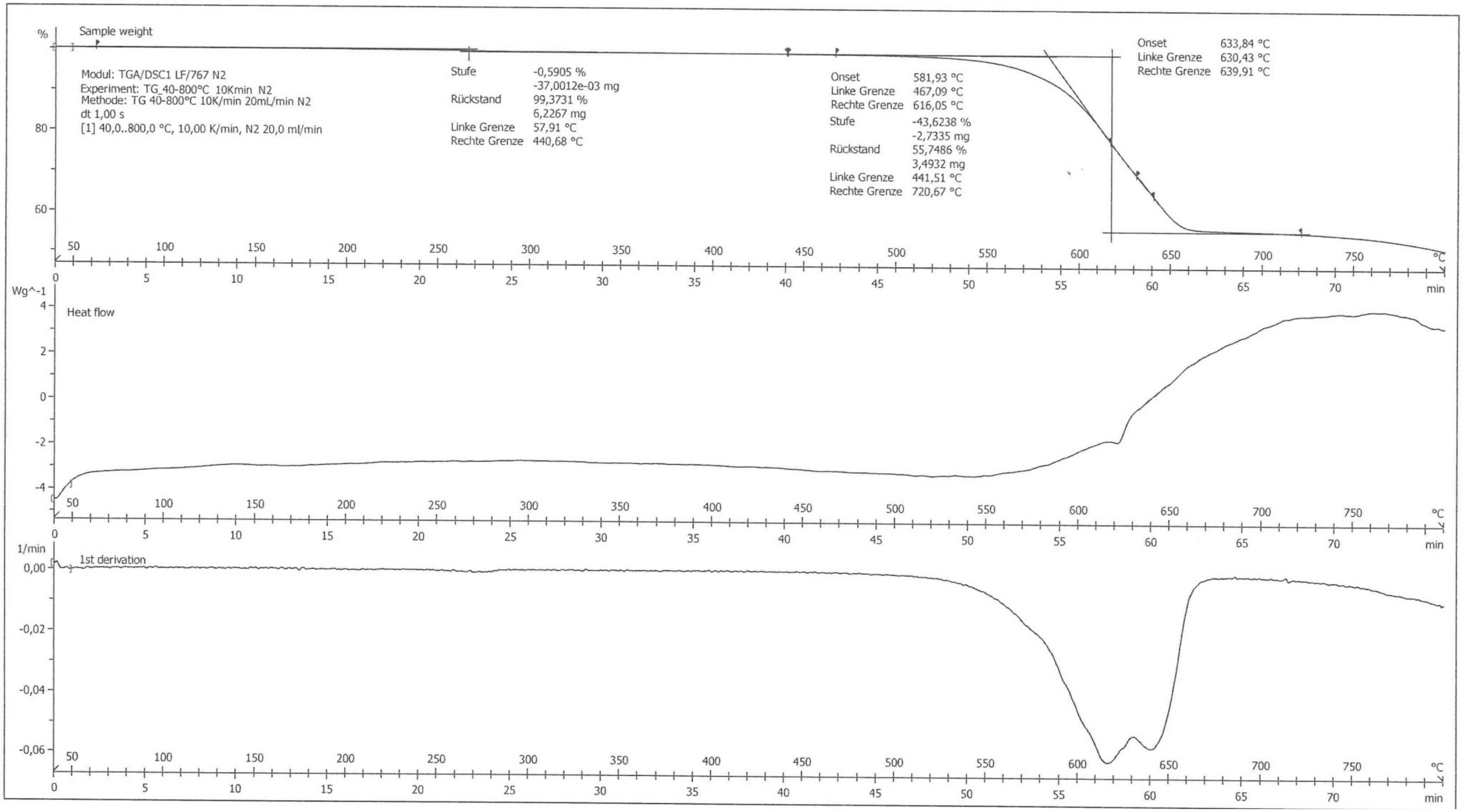

Figure S60. TGA (top), DSC (middle) and TGA´ (below) traces of **4a**.

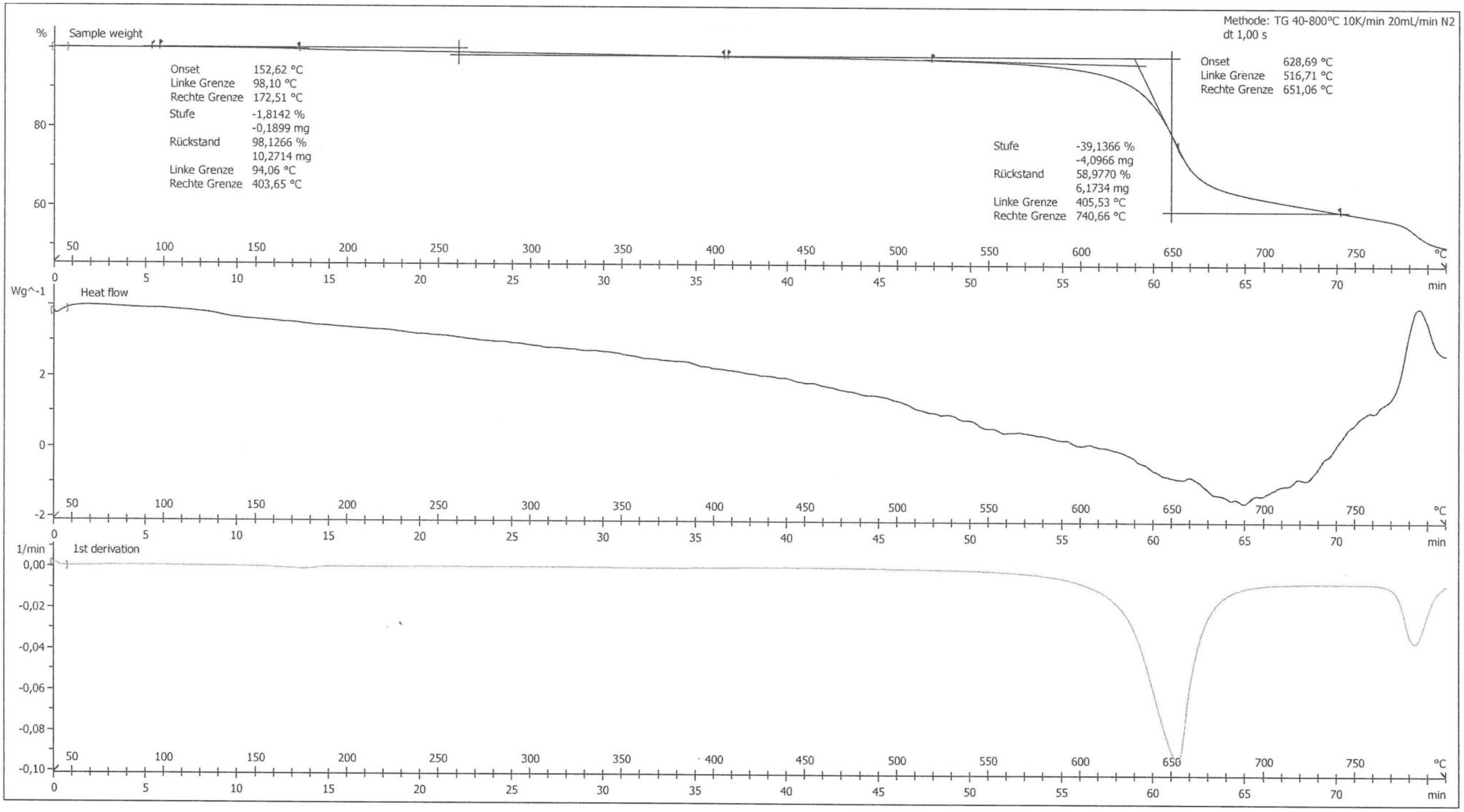

Figure S61. TGA (top), DSC (middle) and TGA´ (below) traces of **4b**.

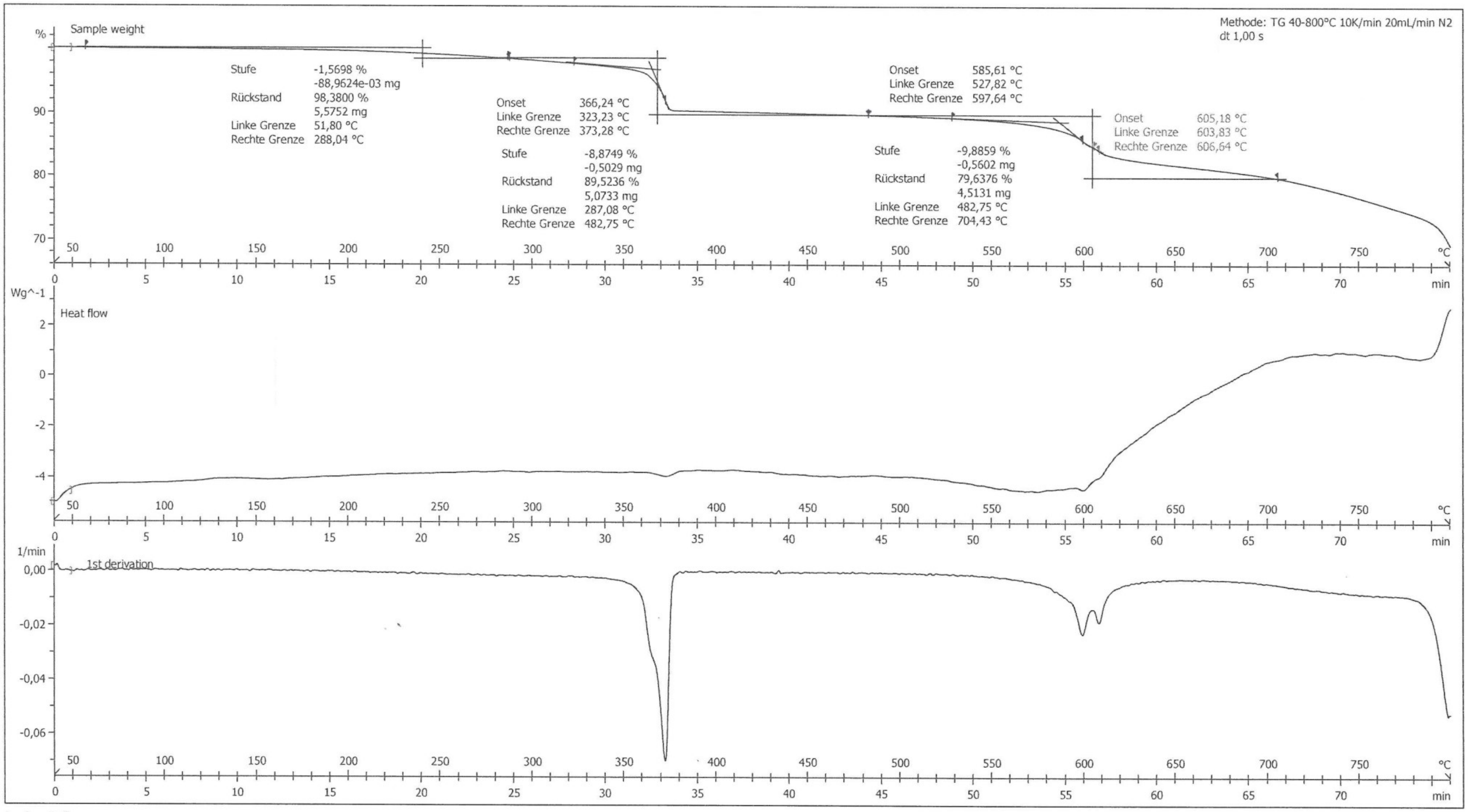

Figure S62. TGA (top), DSC (middle) and TGA´ (below) traces of **4c**.

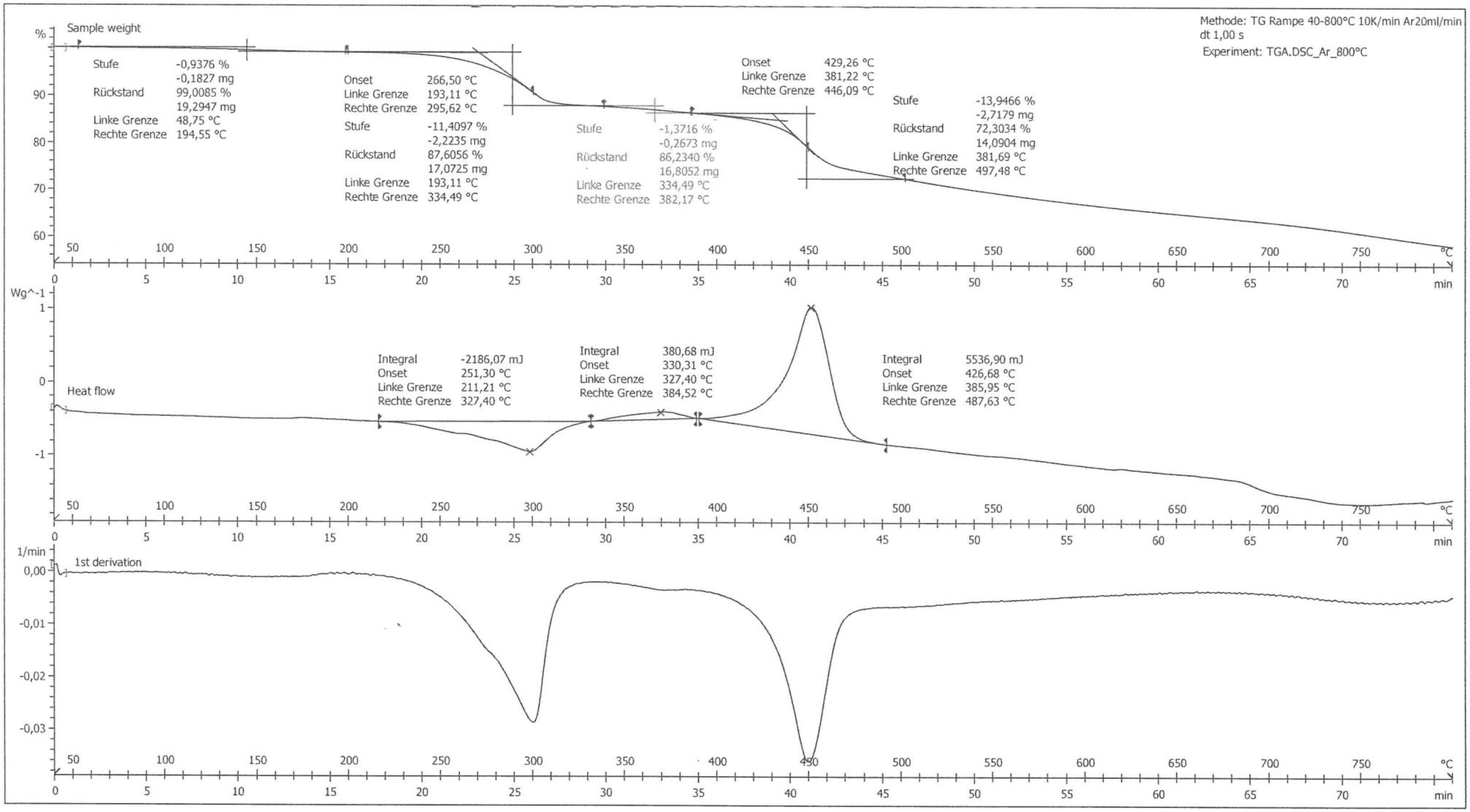

Figure S63. TGA (top), DSC (middle) and TGA´ (below) traces of **4d**.

6.3 UV/Vis absorption spectra of 4c and 4d

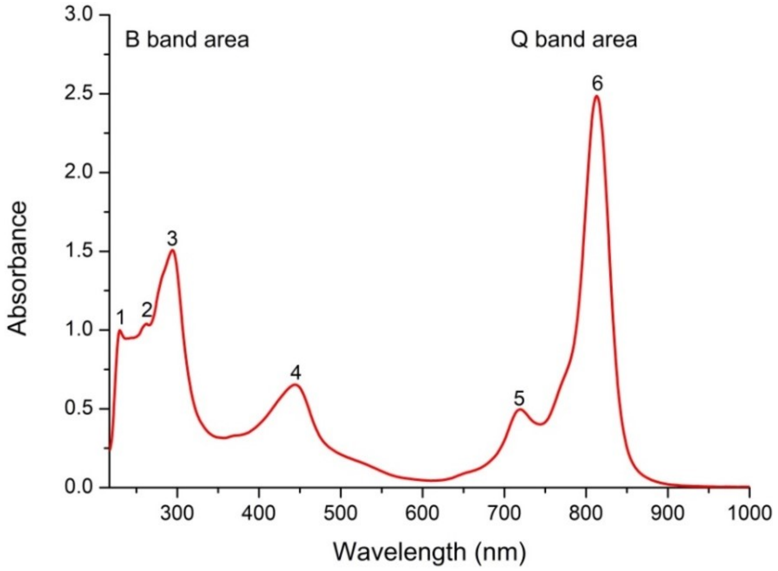

Figure S64. UV/Vis spectrum of **4c** measured in H_2SO_4 (conc), recorded at room temperature.

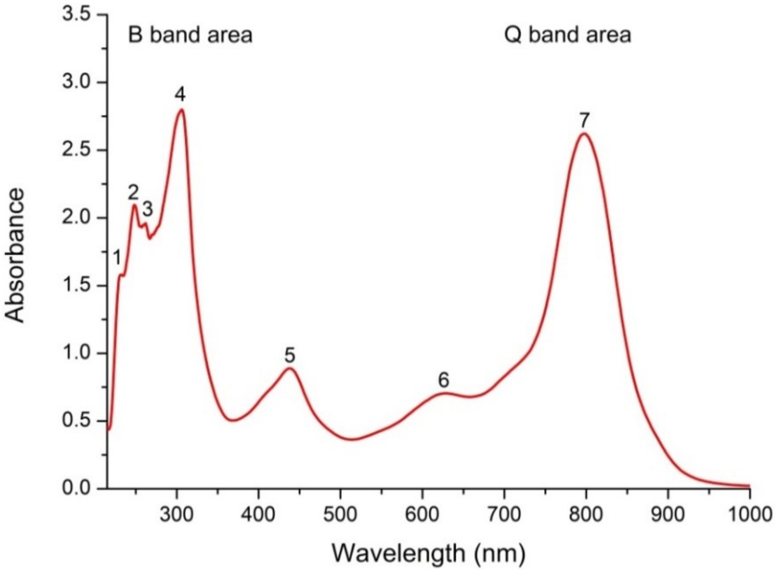

Figure S65. UV/Vis spectrum of **4d** measured in H_2SO_4 (conc), recorded at room temperature.

Table S7. UV/Vis data of **4c** and **4d** measured in H_2SO_4 (conc).

	Absorption λ_{max} [nm]						
	1	**2**	**3**	**4**	**5**	**6**	**7**
CoPcMe$_8$ (4c) **C = 1.4625.10^{-5}**	230 (4.83)	262 (4.86)	295 (5.01)	444 (4.65)	719 (4.53)	813 (5.23)	-
CoPcOMe$_8$ (4d) **C = 1.2321.10^{-5}**	231.5 (5.10)	248.5 (5.23)	262 (5.20)	306 (5.36)	438 (4.85)	628.5 (4.75)	797.5 (5.33)

6.4 Summary of the characterization of 4a–d

As described by us earlier, the characterization of metallophthalocyanines is puzzling.[7] The formation of the here reported Co(II)-phthalocyanines could be deduced, for example, by the color of the materials.

Notice: All four compounds were subjected prior to analysis to the pyridine purification.[7] Some amount of material obtained thereof were dried in addition in a heater at 110 °C overnight, and used next for IR and UV/Vis spectroscopic studies as well as CHN combustion analysis. For TG measurements the non-oven-dried materials were used.

Characterization via broadly used CHN combustion analysis is–and here especially for metallophthalocyanines – hampered by the often observed incomplete combustion of C to CO_2 (even not at temperatures up to 1800 °C, see reference [7]), while at such high temperature H and N usually fully converts to H_2O and N_2.

For the CHN combustion analysis we used here a ThermoFlash EA 1112 Series Analyzer with a tube temperature of 950 °C and 5 sec O_2-ignition time. The results reported here seem to fit the calculated values well. Higher than calculated N-contents should be attributable to remaining pyridine of the pyridine purification procedure.[7]

IR spectroscopy is from our point of view well-suited to allow to identify the formation of **4a–d**, especially as the IR spectra of **4a**[1] and **4b** (cf. reference [7]) match precisely to those reported independently. As we didn't found IR spectra of **4c,d** for KBr discs (in the full spectral range) we cannot identify unambiguously their formation. For that reason we measured for these two compounds the UV/vis in H_2SO_{4conc} – and found the basic features (B and Q band area absorptions) as well-fitting in comparison with those of **4b** (cf. reference [7]) which allows to conclude that Co(II)-phthalocyanines are formed.

The results of the TG measurement of **4b** are in full agreement with the ones reported earlier for independently obtained **4b**.[7] The TGA of **4a** is given here to verify that also this compound can be regarded as being pure (purity > 99%, cf. reference [7]). The results obtained for **4c,d** are somewhat surprising. In both cases some mass loss at lower temperatures is observed: **4c** = 372 °C (10.5 %); **4d** = 305 °C (11.4 %).[2] These mass losses do not correspond to the cleaving of the "helm" of the related "helmet" compounds, which occurs at different temperatures and different mass loss: **3c** = 295 °C (14.3 %); **3d** = 258 °C (17 %). We attribute these mass losses to the formation of adducts **4c·pyridine** and **4d·pyridine**, which loses pyridine when heated. The theoretic mass losses for the latter compounds would amount to 10.4 % (**4c·pyridine**) and 11.2 % (**4b·pyridine**). Certainly the question is for which reason **4c,d** form pyridine adducts, while **4a,b** do not? This is attributed tentatively to the electron-

---

[1] The IR spectra of CoPc (**4a**) can be found in the online freely available Spectral Database for Organic Compounds (SDBS) either under the CAS or SDBS numbers via the link http://sdbs.db.aist.go.jp/sdbs/cgi-bin/cre_index.cgi. SDBS number: CoPc (24499).

[2] The temperatures were taken from Figures S51,52 from the 1st maxima of the 1st derivatization of the mass loss curves.

donating properties of the –CH_3 (**4c**) and –OCH_3 (**4d**) substituents, while **4b** possess electron-withdrawing Cl-substituents. To answer this question was, however, beyond the focus of this work; but we will report about it in a forthcoming report together with accompanying quantum chemical calculation.

7. Remark I: Trial to synthesize 3a in 1-hexanol

In another experiment we examined the possibility of synthesizing **3a** by carrying out the reaction of 1,3-diiminoisoindoline **2a** with $CoCl_2·6H_2O$ in 1-hexanol instead of 1,2,4-trichlorobenzene. Only conventional CoPc was formed in a high purity and good yield.

Detailed description of the experiment:

To a 500 mL one-neck (ground glass joint, NSH 29) round bottom flask containing a solution of 1,3-diiminoisoindoline **2a** (2.00 g, 13.8 mmol, 5 equiv) in 1-hexanol (150 mL), $CoCl_2·6H_2O$ (0.6556 g, 2.76 mmol, 1 equiv) was added in one portion at ambient temperature. Afterwards, a ca. 30 cm long reflux condenser (NSK 29) was mounted, and the reaction mixture temperature was raised slowly to 80 ^{o}C (within 1 h) under permanent stirring. Then the reaction mixture was heated gradually up to reflux (ca. up to 170 ^{o}C; in the rate of 20 ^{o}C/2 h). Noteworthy, by reaching ca. 80-90 ^{o}C the gas development, identified as NH_3, was observed. The mixture was then heated as long as NH_3 development was noticed (heating take up to 5 days). After the NH_3 gas development had stopped, the reaction mixture was allowed to cool down to ambient temperature, filtrated and washed with CH_2Cl_2 (40 mL). The intense purple-violet filter cake was next transferred into a 100 mL one-neck round bottom flask containing 50 mL DMF, and the resulting mixture was sonicated for 15 min and next refluxed for 2 h. After cooling down to ambient temperature the suspension was filtered off, and the volume of the light green DMF filtrate was reduced and diethyl ether was allowed to condensate inside very slowly. Out of these trials we never observed the formation of any solid material out of the DMF filtrates. On the other hand the violet filter cake was washed first with DMF (5 × 30 mL) and next with freshly distilled THF (4 × 50 mL) and finally dried on air. The violet material was determined to be analytically pure CoPc (**4a**).[7] Yield: 1.2216 g (78%, based on $CoCl_2·6H_2O$).

Remark II: By using the synthetic procedure described above and by replacing 1-hexanol by 1,2,4-trichlorobenzene and of $CoCl_2·6H_2O$ with $CuCl_2·2H_2O$ and $NiCl_2·6H_2O$, respectively, or by working in the absence of any transition metal salt we observed the formation of CuPc (87%), NiPc (67%) or H_2Pc (5%). When working in 1-hexanol instead of 1,2,4-trichlorobenzene the yields of the analytically pure materials were even higher. We abstain from giving here further characterisation of the isolated compounds but like to emphasize that in all cases no formation of “helmet-type” Cu(II)- or Ni(II)-compounds was observed, as well as of the metal-free representative. Furthermore, by using Fe(II)- and Mn(II)-salts we could never isolate FePc and MnPc, respectively.

8. Electrochemical measurements of 3a

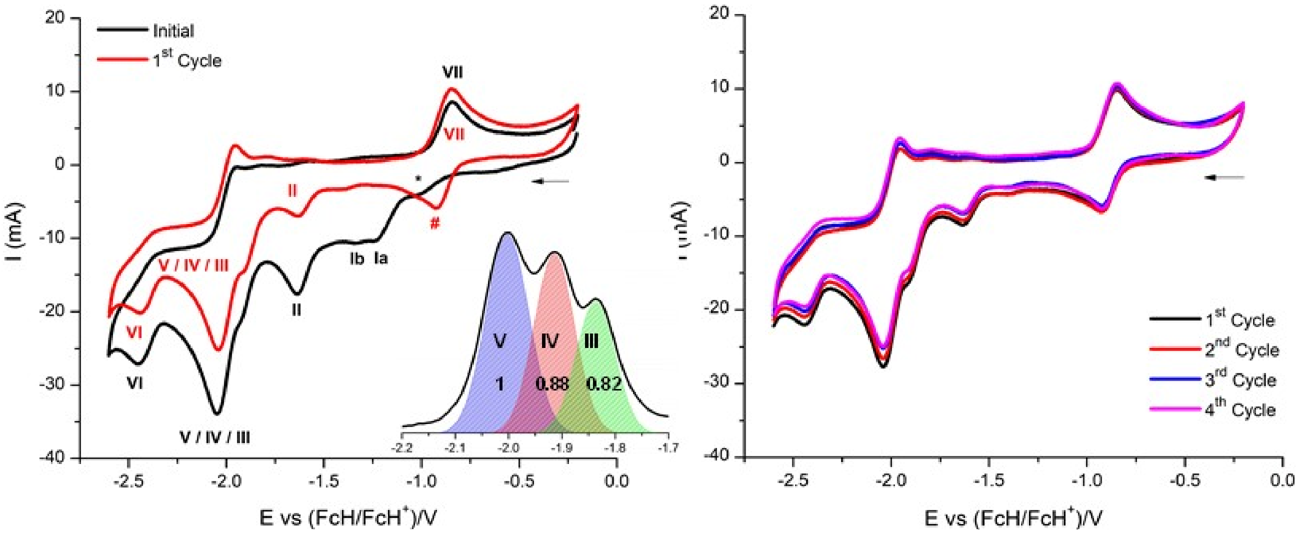

Figure S66. Left: Cyclic voltammograms of **3a**; inset: the square-wave voltammogram of **3a** (duration 5 s, amplitude 5 mV, pulse 25 mV); right: set of cyclic voltammograms of **3a**. Scan rate: 100 mV s^{-1}; in DMF solutions (1.0 mmol L^{-1}) at 25 °C, supporting electrolyte 0.1 mol L^{-1} of $[N(n\mathrm{Bu})_4][B(C_6F_5)_4]$, working electrode: glassy carbon electrode. . Hint: Roman numbers; **in black**: correspond to processes in initial cycle, while **in red**: correspond to processes in 1st cycle

Table S8. Cyclic voltammetry data of **3a**. All potentials are given in [mV].

Couple	$E^{o\prime}$ [mV][a]	ΔE_p[mV][b]
Ia	-1228[c]	-
Ib	- 1330	-
II	-1634[c]	-
III	-1837[d]	-
IV	-1913[d]	-
V	-2000[d]	-
VI	-2407	85
VII	-883	74

[a] $E^{o\prime}$ = Formal potential = $((E_{pa} + E_{pc})/2)$. [b] $\Delta E_p = (E_{pa} - E_{pc})$. [c] E_{pc} = cathodic peak potential of the irreversible process. [d] Values taken from the square-wave voltammogram.

9. Crystallography

Table S9. Selected ccrystal and structural refinement data of **2b**, **2c, [3a(HCl)(dmf)]·2dmf, [3b(dmf)]·2dmf and 4a (CoPc)**.

	2b	**2c**	**[3a(HCl)/dmf)]·2dmf**	**[3b(dmf)]·2dmf**	**4a (CoPc)**
Chemical formula	$C_8H_5Cl_2N_2$	$C_{10}H_{11}N_3$	$C_{49}H_{42}ClCoN_{14}O_3$	$C_{49}H_{42}ClCoN_{14}O_3$	$C_{32}H_{16}CoN_8$
Formula weight (gmol^{-1})	214.05	173.22	969.34	1277.31	571.46
Crystal system	monoclinic	monoclinic	orthorhombic	triclinic	monoclinic
Space group	$P2_1/c$	$P2_1/c$	$Pna2_1$	P-1	$P2_1/n$
a (Å)	7.4877(7)	7.4806(7)	24.9709(2)	14.1394(11)	14.5319(9)
b (Å)	8.2215(6)	8.2712(10)	13.3223(1)	14.6764(7)	17.1718(9)
c (Å)	14.1340(12)	14.3479(14)	13.1876(1)	14.8076(10)	21.9279(14)
α (°)	90.0	90	90.0	76.749(5)	90.0
β (°)	100.951(9)	96.512(6)	90.0	64.267(7)	105.818(6)
γ (°)	90.0	90	90.0	74.741(5)	90.0
Volume (Å^3)	854.25(13)	882.03(16)	4387.12(6)	2647.0(3)	1146.38(12)
Z	4	4	4	2	2
Temperature (K)	120	100	120	115	120
Radiation source	Cu Kα	Cu Kα	Cu Kα	Mo Kα	Cu Kα
Wavelength (A)	1.54184	1.54178	1.54184	0.71073	1.54184
D_{calcd} (gcm^{-3})	1.664	1.304	1.468	1.603	1.656
μ (mm^{-1})	6.425	0.646	4.140	0.887	6.223
F(000)	432	358	2008	1288	582
Reflections collected	2596	14034	32458	23271	4539
Reflections unique/R_{int} $^{a)}$	1454, 0.0188	1561, 0.1436	6654, 0.0306	9790, 0.0323	1977, 0.0403
Index ranges	$-5 \leq h \leq 8$, $-9 \leq h \leq 9$, $-16 \leq h \leq 13$	$-8 \leq h \leq 8$, $-9 \leq k \leq 9$, $-17 \leq h \leq 17$	$-28 \leq h \leq 29$, $-15 \leq k \leq 15$, $-14 \leq h \leq 15$	$-17 \leq h \leq 17$, $-17 \leq k \leq 17$, $-17 \leq h \leq 17$	$-17 \leq h \leq 15$, $-5 \leq k \leq 5$, $-15 \leq l \leq 20$
θ data collection range (°)	6.020 - 65.970	5.953 - 66.913	3.540 - 65.986	2.955 - 25.499	3.541 - 666.352
Data / Restrains / Parameters	1454 / 0 / 130	1561 / 0 / 133	6654 / 18 / 613	9790 / 98 / 735	1977 / 0 / 187
Goodness-of-fit on F^2 $^{b)}$	1.067	1.168	1.029	1.053	1.020
Final R indices [$I > 2\sigma(I)$]$^{c)}$	$R_1 = 0.0369$, $wR_2 = 0.1014$	$R_1 = 0.0824$, $wR_2 = 0.1564$	$R_1 = 0.0364$, $wR_2 = 0.0997$	$R_1 = 0.0647$, $wR_2 = 0.1521$	$R_1 = 0.0420$, $wR_2 = 0.1069$
R indices (all data)$^{c)}$	$R_1 = 0.0420$, $wR_2 = 0.1059$	$R_1 = 0.1130$, $wR_2 = 0.1684$	$R_1 = 0.0389$, $wR_2 = 0.1015$	$R_1 = 0.0949$ $wR_2 = 0.1642$	$R_1 = 0.0499$, $wR_2 = 0.1145$
Largest diff. peak/hole (eÅ^{-3})	0.354/–0.269	0.238/–0.245	0.320/–0.397	1.000/–0.582	0.395 and –0.366

[a] $R_{\mathrm{int}} = \Sigma | F_o^2 - F_o^2(\mathrm{mean}) | / \Sigma F_o^2$, where $F_o^2(\mathrm{mean})$ is the average intensity of symmetry equivalent diffractions. [b] $S = [\sum w(F_o^2 - F_c^2)^2]/(n - p)^{1/2}$, where n = number of reflections, p = number of parameters. [c] $R = [\sum(||F_o| - |F_c|)/\sum|F_o|)$; $wR = [\sum(w(F_o^2 - F_c^2)^2)/\sum(wF_o^4)]^{1/2}$.

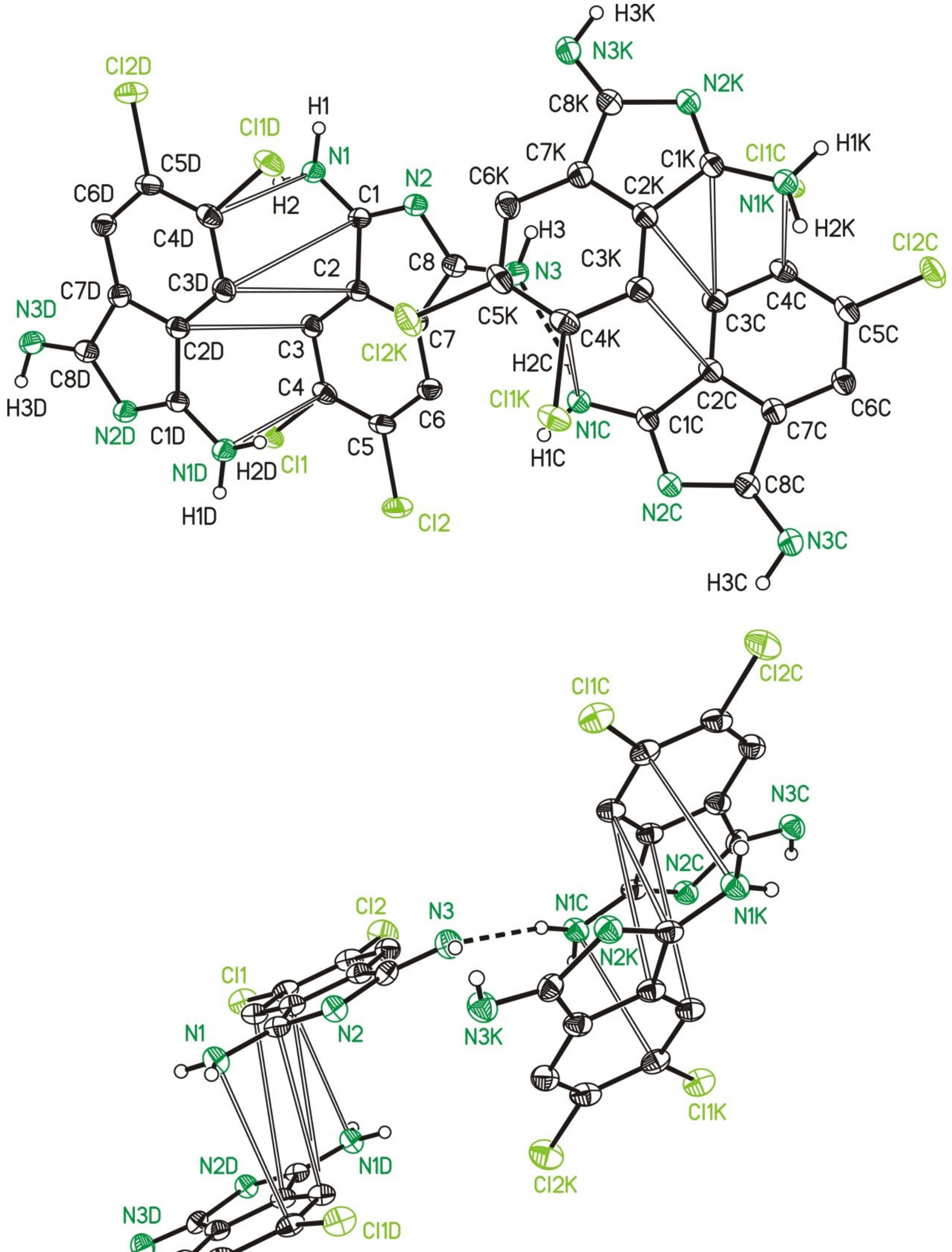

Figure S67. ORTEP (50 % probability ellipsoids) of four molecules of **2b** involved in formation of layer I in two different perspective views. Dotted lines refer to intermolecular hydrogen bonds. Hollow bonds indicate π-interactions with intermolecular distances < 3.6 Å (N1–C4D = 3.356 Å. C1–C3D = 3.570 Å. C3–C2D = 3.581 Å. C3–C1D = 3.570 Å). Symmetry codes: "C" = *x*, ½ – *y*, *z* + ½. "D" = –*x*, 1 – *y*, –*z*. "K" = –*x*, –½ + *y*, –*z* + ½.

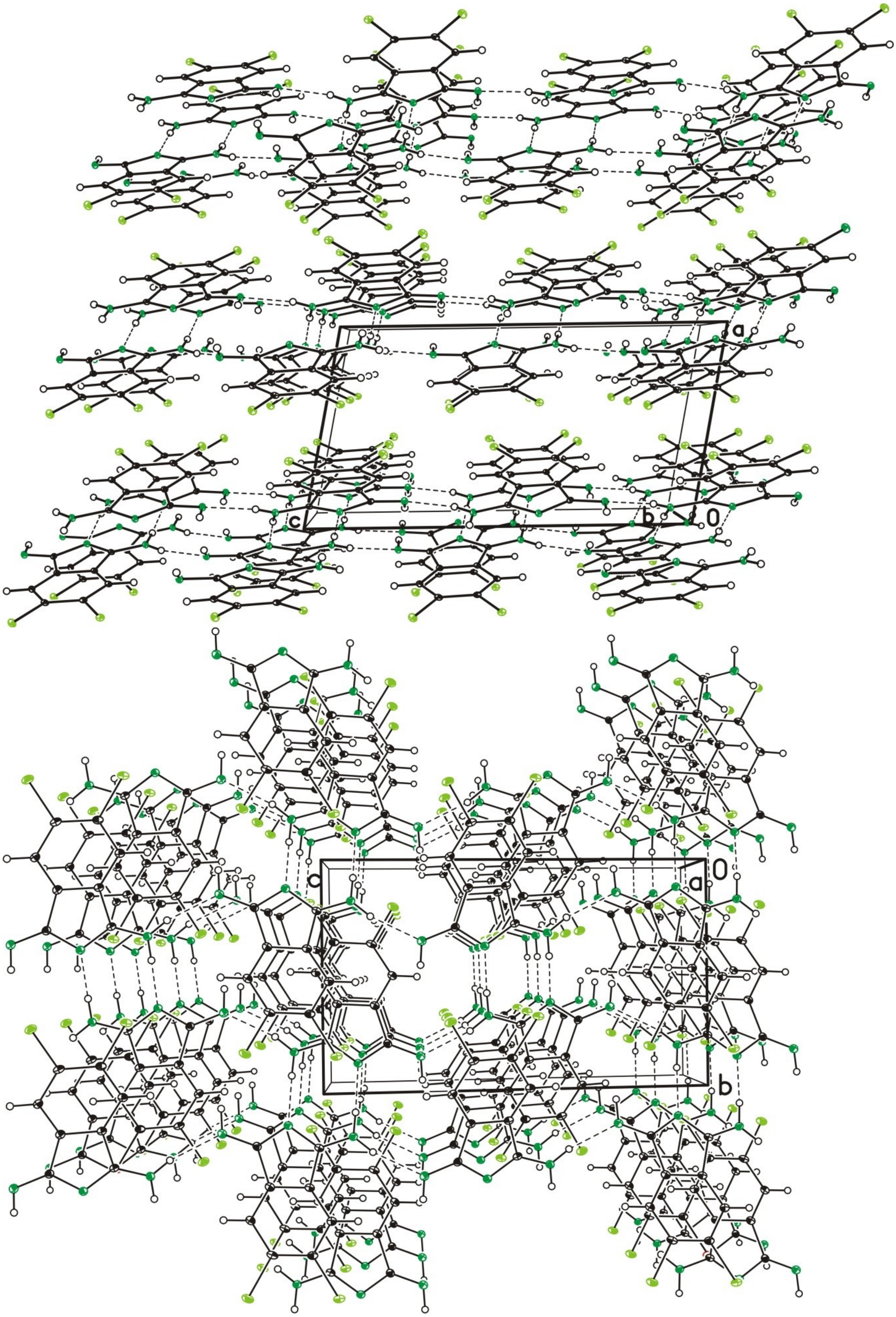

Figure S68. Top views along the crystallographic *b* (above) and *a* axes (below) on selected parts of three adjacent layers formed by **2b** by hydrogen bonds. Notice: Top view along the *a* axes (below) indicates superpositions of **2b** and band formation. Dotted lines refer to intermolecular hydrogen bonds, intermolecular π-interactions are not displayed.

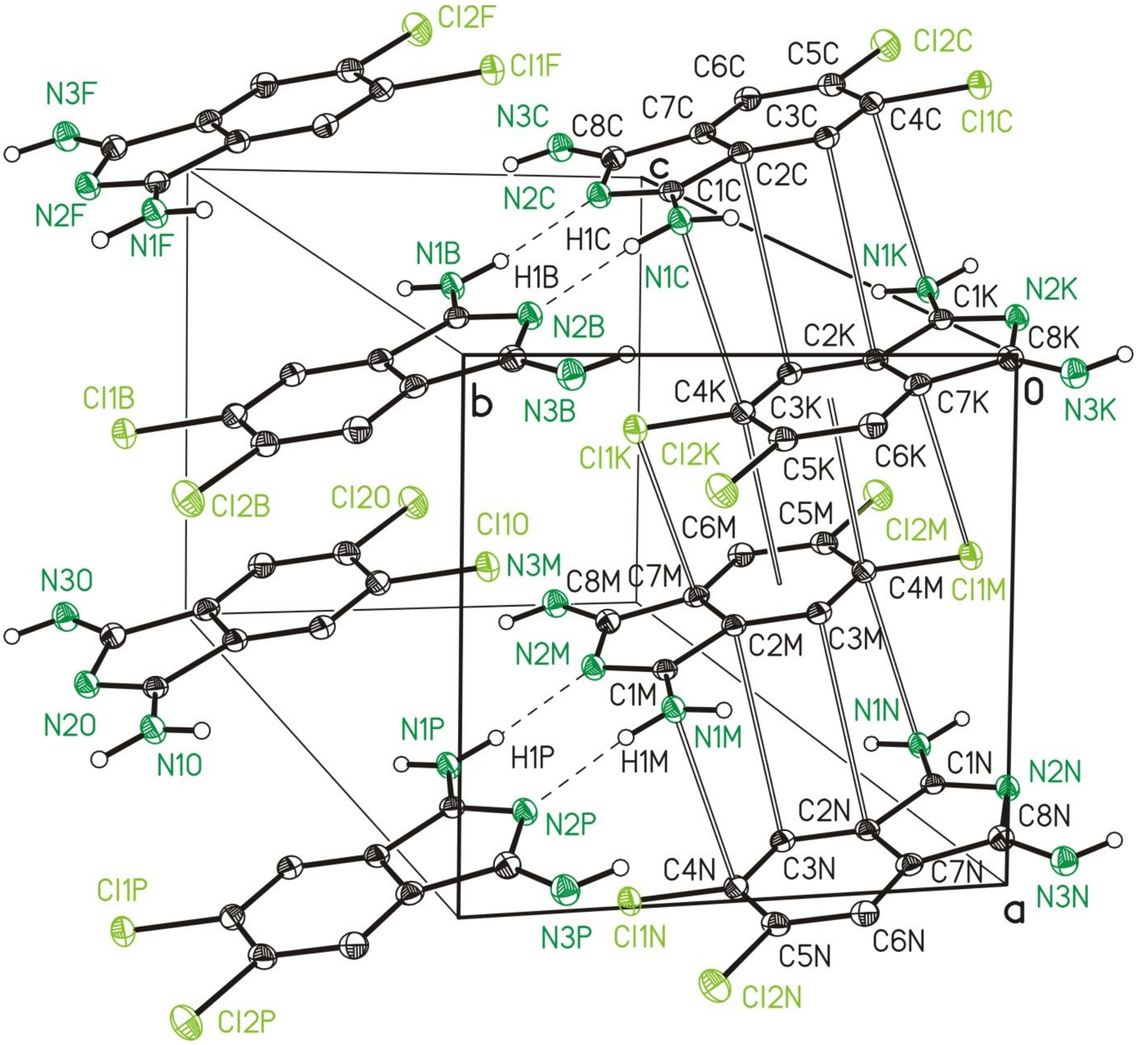

Figure S69. Selected part of the 3D network of **2b** indicating formation of intermolecular hydrogen bonds (dotted lines) and perpendicular formation of intermolecular π-interactions (hollow bonds) along the *a* axes. Intermolecular distances < 3.6 Å: Cl1M–C7K/C7M–Cl1K = 3.455 Å. C4M–D1/C4K–D2 = 3.435 Å. C5M–C3K/C3M–C5K = 3.424 Å. D1/D2 = geometrical centroids of C2K-C7K/C2M-C7M. Symmetry codes: “B” = –*x*, *y* + ½, –*z* + ½. “C” = *x*, ½ – *y*, *z* + ½. “F” = –*x*, $^{3}/_{2}$ – *y*, *z* + ½. “K” = –*x*, –½ + *y*, –*z* + ½. “M” = *x* +1, ½ – *y*, *z* + ½. “N” = –*x* +1, –½ + *y*, –*z* + ½. “O” = *x* +1, $^{3}/_{2}$ – *y*, *z* + ½. “P” = –*x* +1, ½ + *y*, –*z* + ½.

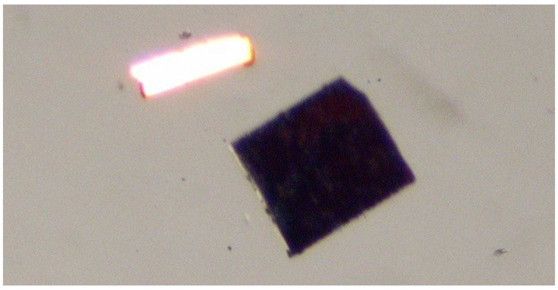

Figure S70. Optical photograph of two single crystals of **CoPc**. Above: shiny, ca. 0.5 × 0.1 × 0.02 mm. Below: dark, ca. 0.6 × 0.6 × 0.03 mm.

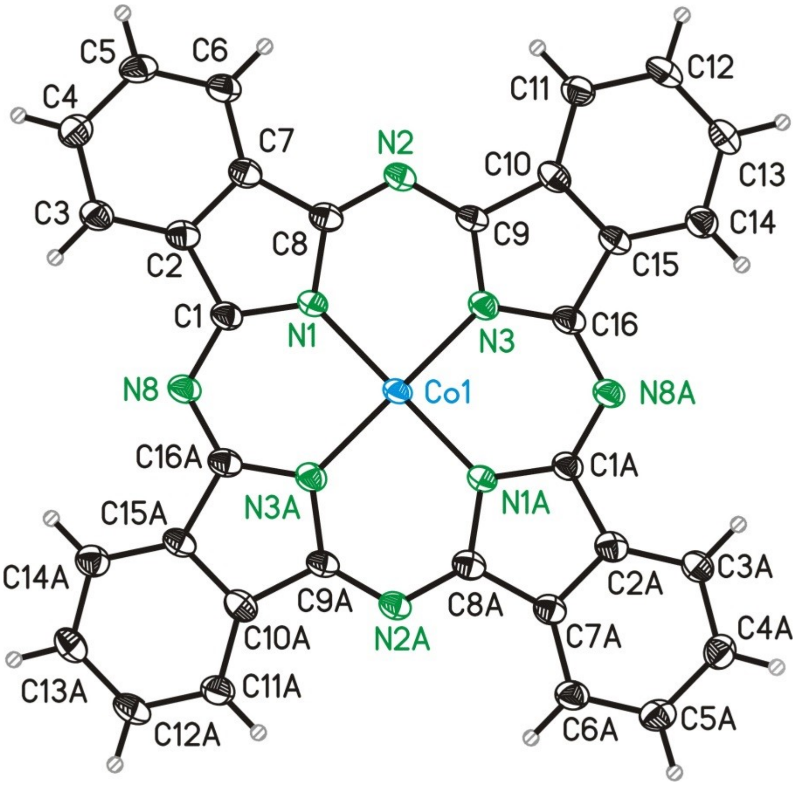

Figure S71. ORTEP diagram (50 % probability ellipsoids) of the molecular structure of CoPc. Symmetry code “A”: –*x*, –*y*, –*z*.

Table S10. CoPc reported in the Cambridge Structural Database in the β-polymorphic form.

Chemical formula	Unit cell	Refcode	Crystal grow technique	Reference
CoPc in P21/c @293 K	$a = 14.495(5)$ $b = 4.742(4)$ $c = 19.107(5)$ $\beta = 120.76(2)$	COPTCY01	"… crystals of CoPc … were grown, with difficulty, by … vacuum sublimation …"	8
CoPc in P21/n @not given/	$a = 14.567$ $b = 4.784$ $c = 17.305$ $\beta = 105.53$	COPTCY04	most likely PVD	9
CoPc in P21/c @115 K	$a = 14.542(4)$ $b = 4.790(1)$ $c = 19.215(5)$ $\beta = 120.74(2)$	COPTCY05	Not described/given	10
CoPc in P21/c @ 115 K	$a = 14.489(9)$ $b = 4.763(4)$ $c = 19.156(16)$ $\beta = 120.76(4)$	COPTCY06	sublimation	11
CoPc in P21/c @ 295 K	$a = 14.5982(9)$ $b = 4.7937(3)$ $c = 19.4348(11)$ $\beta = 120.782(3)$	COPTCY08	sublimation	12
CoPc in $P2_1/c$ @ 295 K	$a = 14.542(2)$ $b = 4.7731(5)$ $c = 19.352(2)$ $\beta = 120.824(7)$	COPTCY10	sublimation	13
CoPc in $P2_1/n$ @298 K	$a = 14.594(2)$ $b = 4.7928(6)$ $c = 17.304(3)$ $\beta = 105.607(6)$	CoPTCY11	sublimation	14

Table S11. Selected bond lengths (A) and bond and torsion angles (°) of **CoPc (4a)**.

Bond length							
Co1–N1	1.924(2)	Co1–N3	1.922(2)	C1–N1	1.367(4)	C1–C2	1.450(4)
C1–N8	1.922(2)	N8–C16A	1.323(4)	N1–C8	1.379(4)	C7–C8	1.454(4)
N2–C8	1.329(4)	N2–C9	1.316(4)	C9–N3	1.383(3)	C9–C10	1.453(4)
N3–C16	1.369(4)	C15–C16	1.453(4)				

Bond angles					
N1–Co1–N3	89.24(9)	N1–Co1–N1A	180.0	N3–Co1–N3A	180.0
N8–C1–N1	128.1(3)	N8–C1–C2	121.7(3)	N1–C1–C2	110.2(2)
N1–C8–N2	127.4(3)	N1–C8–C7	110.0(2)	N2–C8–C7	122.6(2)
N2–C9–C10	122.9(2)	N2–C9–N3	127.7(2)	N3–C9–C10	109.4(2)
N3–C16–C15	110.1(2)	N3–C16–N8A	128.3(3)	N8A–C16–C15	121.6(3)

Torsion angles			
N3–C9–C10–C11	–177.8(3)	N2–C9–C10–C11	2.6(5)

10. References

1. A. V. Ivanov, K. V. Kabanova, M. O. Breusova, I. V. Zhukov, L. G. Tomilova and N. S. Zefirov, *Russian Chemical Bulletin,* 2008, **57**, 1665–1670.
2. Z. Iqbal, A. Lyubimtsev and M. Hanack, *Synlett*, 2008, **15**, 2287–2290.
3. L. Babel, T. N. Y Hoang, L. Guenee, C. Besnard, T. A. Wesolowski, M. Humbert-Droz and C. Piguet, *Chem. Eur. J.*, 2016, **22**, 8113–8123.
4. R. B. Cole, *Electrospray ionization mass spectrometry: fundamentals, instrumentation, and applications*; John Wiley & Sons, Inc., New York, USA, 1997.
5. B. O. Keller, J. Sui, A. B. Young and R. M. Whittal, *Analytica Chimica Acta*, 2008, **627**, 71–81.
6. L. Wang, L. Lin, G. Zhang, K. Kodama, M. Yasutake and T. Hirose, *Chem. Commun.*, 2014, **50**, 14813–14816.
7. T. Rüffer, D. Nurpeisova, Z. Jakupova, A. Tashenov, N. Uhlig, A. Khalladi, L. Mertens, A. Gonser, M. Mehring and H. Lang, *Z. Naturforsch.*, 2017, **72**, 589–601.
8. G. A. Williams, B. N. Figgins, R. Mason, S. A. Mason, P. E. Fielding, *J. Chem. Soc., Dalton Trans.* 1980, 1688–1692.
9. L. Ruiz-Ramirez, A. Martinez, J. J.Sosa, J. L.Brianso, E. Estop, X. Alcobe, J. S. Chinchon, Afinidad, *Revista de quimica teorica y aplicada*, 1986, **43**, 337–340. Not available online.
10. B. N. Figgis, E. S. Kucharksi, P. A. Reynolds; *J. Am. Chem. Soc.* **1989**, *111*, 1683-1692.
11. P. A. Reynolds, B. N. Figgis, E. S. Kucharski, S. A. Mason, *Acta Cryst, Sect. B: Struct. Science*, 1991, 47, 899.
12. P. Ballirano, R. Caminiti, C. Ercolani, A. Maras, M. A. Orru, *J. Am. Chem. Soc.*, 1998, 120, 12798.
13. R. Mason, G. A. Williams, P. E. Fielding, *J. Chem. Soc., Dalton Trans.*, 1979, 676.
14. H. Jiang, P. Hu, J. Ye, R. Ganguly, Y. Li, Y. Long, D. Fichou, W. Hu, C. Kloc, *Ang. Chem. Int. Edt.*, 2018, **57**, 10112.